

Kinetic Resolution of Alcohols by Catalytic Enantioselective Sulfonylation and Silylation

Author: Hekla Alite

Persistent link: <http://hdl.handle.net/2345/2585>

This work is posted on [eScholarship@BC](#),
Boston College University Libraries.

Boston College Electronic Thesis or Dissertation, 2012

Copyright is held by the author, with all rights reserved, unless otherwise noted.

Boston College

The Graduate School of Arts and Sciences

Chemistry Department

KINETIC RESOLUTION OF ALCOHOLS BY CATALYTIC ENANTIOSELECTIVE
SULFONYLATION AND SILYLATION

a thesis

by

HEKLA ALITE

submitted in partial fulfillment of the requirements

for the degree of

Master of Science

May 2012

© copyright by HEKLA ALITE

2012

Kinetic Resolution of Alcohols by Catalytic Enantioselective Sulfonylation and Silylation

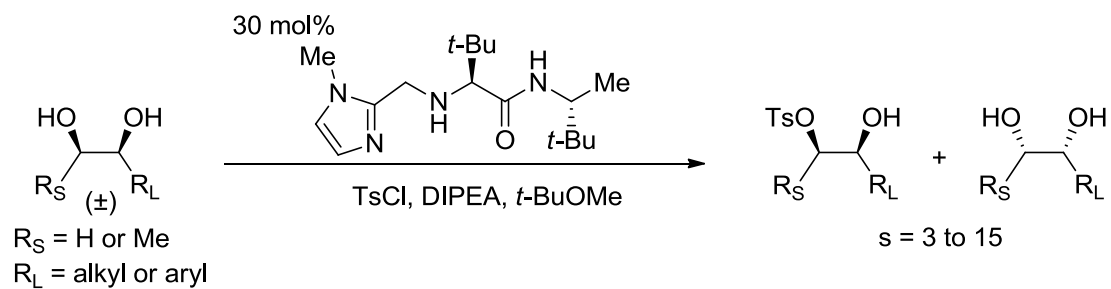
Hekla Alite

Thesis Advisor: Professor Marc L. Snapper

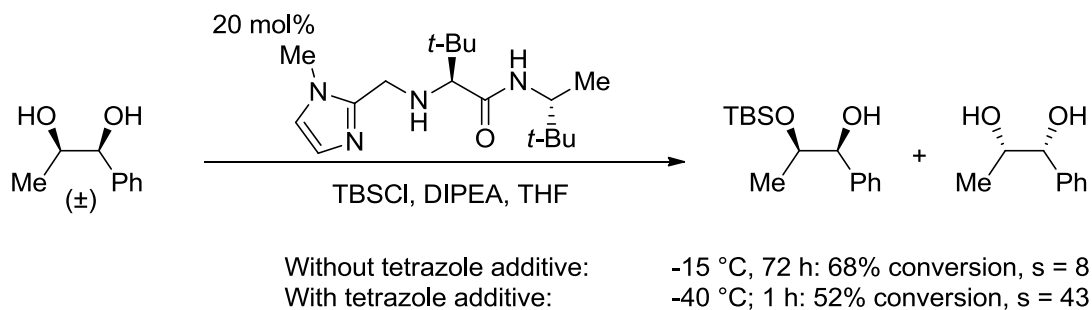
ABSTRACT

Chapter 1: Brief overview of the catalytic enantioselective functionalization and kinetic resolution of alcohols

Chapter 2: Kinetic resolution of *syn*-diols by catalytic enantioselective sulfonylation



Chapter 3: Significant improvement on catalytic enantioselective silylation of *syn*-diols and triols through the use of a tetrazole additive



ACKNOWLEDGMENTS

My experience in the Boston College chemistry department has been the most humbling and challenging experience of my entire life. I came to B.C. with the intention of exploring, discovering, and pushing the boundaries of organic chemistry. What I didn't expect was how much I would learn about myself, my abilities, and my career/life goals. After nearly three years of devoting myself to organic chemistry and problem solving, I leave B.C. wiser, more mature, but still devoted. I know that my time at B.C. will serve me well in the future and I wouldn't change a moment of it.

I cannot emphasize enough how large of an impact the people at B.C. have had on me. My advisor, Professor Marc L. Snapper, is a wealth of knowledge whose philosophy on graduate school pushed me to work as hard as I did. My other advisor, Professor Amir H. Hoveyda, is simultaneously caring, strict, and superbly funny. He also has the ability to make the least scientifically inclined person fall in love with organic chemistry. Professor T. Ross Kelly taught me the importance of being on time and reminded me that science is wildly exciting. Professor Lynne A. O'Connell's tireless meticulousness is a quality I aspire to. Every undergraduate student who learned something from me or taught me something made my experience as a graduate student highly fulfilling.

I absolutely adore my class: Kevin (my quarterback), Julie (my stalker), Omar (my Italian), Nathan (my lab buddy), Brian, Mike, Zach, Jess, Hao, Jin, Zhiyong, Yue, Yani, and Tyler. We started off as a team and we had a lot of fun together. As soon as I joined the Snapper lab, I fell in love with it: Jing (the quiet, hilarious one), Lu (the quiet, passionate one), Youn Hee (my swimming student with a heart of gold), Jason G. (the loud, hilarious one), Jason M. (always helpful), Kurtis (my favorite Trident Layers-loving lab member), Roberto (the Spanish one), and Fengqi (what can I say about my unique mentor, maybe I'll write a book one day). Later on, there was Alisa (my good friend) and Val (the dancer). I also had the honor of working with many wonderful undergraduate students: Steve (the genius), Doug (the hard worker), Lisa and Pat (both invaluable to the peptide project), Aaron (thank you for cheering me up when I needed it), and Matt (manganese, just manganese).

To the many people whose names I haven't mentioned, thank you for making me laugh or smile, or setting a good example, or teaching me something, or just plain saying "hello". I will remember each one of you.

To my family, thank you for making me what I am today and for continually supporting me.

To Tyler, thank you for being my support system during the hardest time of my life. I am forever grateful to you.

TABLE OF CONTENTS

1. Brief overview of the catalytic enantioselective functionalization and kinetic resolution of alcohols.....	1
1.1. Introduction to the catalytic enantioselective functionalization of alcohols.....	1
1.2. Catalytic enantioselective silylation of alcohols.....	2
1.2.1. Hoveyda-Snapper amino-acid-derived catalyst.....	2
1.2.2. Tan's scaffolding catalyst.....	4
1.3. Catalytic enantioselective sulfonylation of alcohols.....	6
1.3.1. Importance of alcohol activation in synthesis.....	6
1.3.2. Miller's tetrapeptide catalyst.....	6
1.3.3. Onomura's copper complex.....	8
1.4. Kinetic resolution of alcohols.....	9
1.4.1. Overview of kinetic resolution.....	9
1.4.2. Examples of kinetic resolution of alcohols.....	10
2. Kinetic resolution of <i>syn</i> -diols by catalytic enantioselective sulfonylation.....	20
2.1. Catalytic enantioselective sulfonylation of <i>syn</i> -diols and triols using amino-acid-derived catalyst.....	20
2.1.1. Initial screenings.....	20
2.1.2. Substrate scope.....	22
2.2. Kinetic resolution of <i>syn</i> -diols by catalytic enantioselective sulfonylation using amino-acid-derived catalyst.....	25
2.2.1. Time screening.....	26

2.2.2. Solvent screening.....	27
2.2.3. Sulfonylation reagent screening.....	28
2.2.4. Substrate scope.....	29
2.3. Experimental and Supporting information.....	36
3. Significant improvement on catalytic enantioselective silylation of <i>syn</i> -diols and triols through the use of a tetrazole additive.....	77
3.1. Catalytic enantioselective silylation of <i>syn</i> -diols and triols using amino-acid-derived catalyst.....	77
3.1.1. Previously proposed transition state.....	77
3.1.2. Additive study and discovery of rate enhancement.....	80
3.1.3. Newly proposed transition state.....	84
3.2. Rate enhancement for previously successful substrates.....	85
3.2.1. <i>meso</i> -diols and triols.....	85
3.2.2. Kinetic resolution substrates.....	87
3.3. Previously unsuccessful substrates.....	89
3.4. Rate enhancement for catalytic enantioselective sulfonylation?.....	92
3.5. Catalyst modification.....	93
3.6. Conclusion and future outlook.....	94
3.7. Experimental and Supporting Information.....	95

CHAPTER 1:

BRIEF OVERVIEW OF THE CATALYTIC ENANTIOSELECTIVE FUNCTIONALIZATION AND KINETIC RESOLUTION OF ALCOHOLS

1.1 Introduction to the catalytic enantioselective functionalization of alcohols

The functionalization of alcohols using a protecting group or an activating group is a transformation commonly used in organic chemistry synthesis.¹ Although the ideal synthesis² requires no protecting group modifications, in most realistic syntheses, protecting groups are unavoidable.³ Nonetheless, there are ways to reduce the number of functional group interconversions in syntheses, and enantioselective functionalization of alcohols is one of these ways. Whenever a protecting group is added to a molecule in a stereospecific fashion, the step builds complexity, as well as prevents unwanted reactions in the next step(s); in other words, one enantioselective functionalization step serves two important roles in synthesis.

An example of a synthetic route that was significantly improved by the discovery of an enantioselective functionalization reaction is shown in Scheme 1.1.⁴ (R)-(+)-4-tert-butyltrimethylsilyloxy-2-cyclopenten-1-one (**1.8**) is a precursor to various biologically active molecules, such as prostaglandins, nucleosides, thromboxane, etc., and, therefore, has been enantioselectively synthesized a number of times.⁴ Prior to 2006, one of the most efficient ways to synthesize **1.8** from a commercially available starting material required seven steps, most of which were functional group interconversions. With the

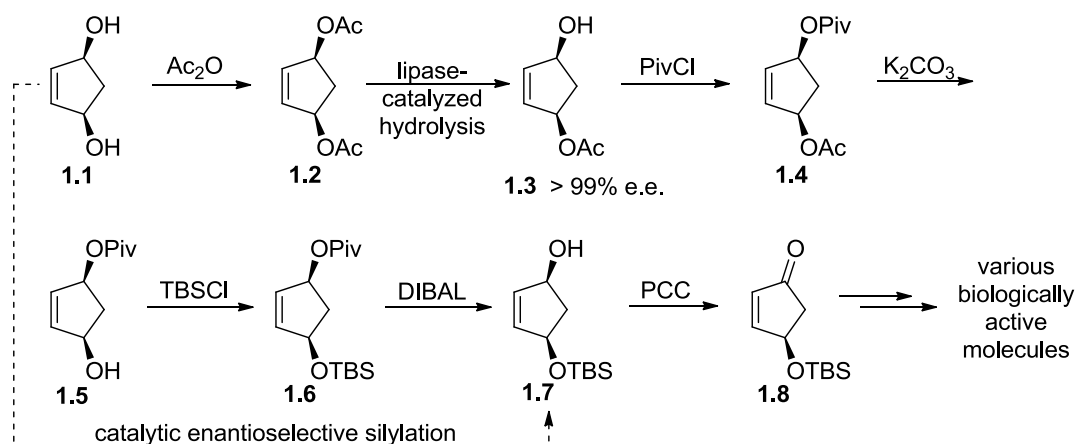
¹ Kocienski, P. J. *Protecting Groups*, 3rd ed.; Thieme: New York, 2005.

² Wender, P. A. "Introduction: frontiers in organic synthesis." *Chem. Rev.* **1996**, *96*, 1-2.

³ Baran, P.S.; Young, I. S. *Nature Chemistry*. **2009**, *1*, 193-205.

⁴ Myers, A. G.; Hammond, M.; Wu, Y. *Tetrahedron Lett.* **1996**, *37*, 3083-3086.

discovery of catalytic enantioselective silylation, however, *meso*-diol **1.1** could be desymmetrized to produce enantioenriched mono-silylated diol **1.7** in one step, reducing the total number of steps in the synthetic route (towards **1.8**) from seven steps to two steps.⁵



Scheme 1.1 Enantioselective functionalization of alcohols can reduce the number of functional group interconversions.

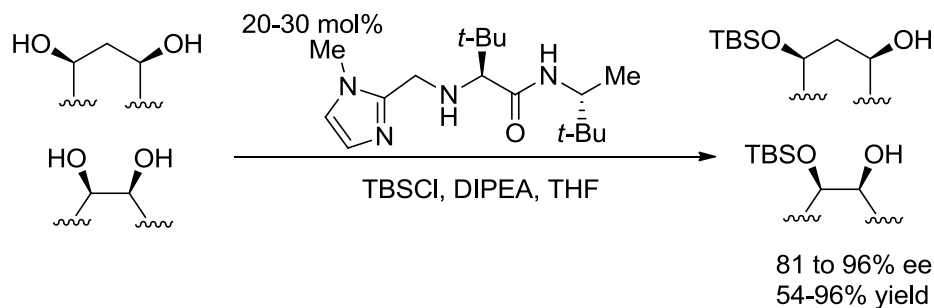
1.2 Catalytic enantioselective silylation of alcohols

1.2.1 Hoveyda-Snapper amino-acid-derived catalyst

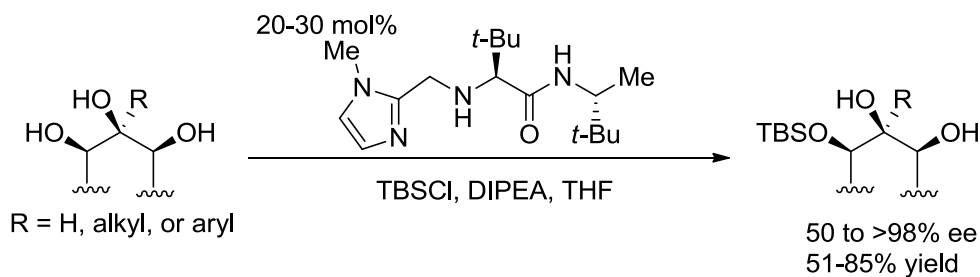
The first method of catalytic enantioselective silylation of alcohols was developed in our lab and it uses a small amino-acid-derived catalyst (Figure 1.1).⁵ This catalyst can successfully catalyze the enantioselective silylation of cyclic and acyclic *meso*-1,2- and *meso*-1,3-diols with 54-96% yields and 81 to 96% ee's when using *tert*-butyldimethylsilyl chloride (TBSCl), which is the most common silylation reagent (Scheme 1.2).⁵ The chiral silylation catalyst can also desymmetrize cyclic and acyclic *meso*-1,2,3-triols with 51-85% yields and 50 to >98% ee's (Scheme 1.3).⁶

⁵ Zhao, Y.; Rodrigo, J.; Hoveyda, A. H.; Snapper, M. L. *Nature*. **2006**, *443*, 67-70.

⁶ You, Z.; Hoveyda, A. H.; Snapper, M. L. *Angew. Chem. Int. Ed.* **2009**, *48*, 547-550.



Scheme 1.2 Desymmetrization of *meso*-diols by catalytic enantioselective silylation using the Hoveyda-Snapper amino-acid-derived catalyst



Scheme 1.3 Desymmetrization of *meso*-triols by catalytic enantioselective silylation using the Hoveyda-Snapper amino-acid-derived catalyst

The Hoveyda-Snapper desymmetrization catalyst is made up of three simple, effective components: (1) Lewis base, (2) chiral amine, and (3) amino acid (Figure 1.1).

The N-methylimidazole moiety acts as a Lewis base to activate the silicon electrophile.⁷ The chiral amine moiety provides steric hindrance so that the substrate approaches the catalyst only from one enantiotopic face. The amino acid moiety provides additional steric hindrance; it

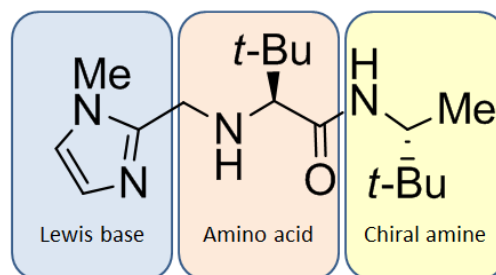


Figure 1.1 Hoveyda-Snapper desymmetrization catalyst

⁷ Denmark, S. E.; Beutner, G. L. *Angew. Chem. Int. Ed.* **2008**, *47*, 1560-1638.

also forms hydrogen-bonds with the substrate and, thus, secures it in position for catalysis to occur. Finally, the secondary amine of the amino acid acts as a Bronsted base to deprotonate the silylated diol.

There are several advantages to the Hoveyda-Snapper desymmetrization catalyst. The catalyst is commercially available or it can be prepared in three easy steps; the reagents and solvents do not require further purification from commercially available sources, and the catalyst itself can be easily purified. Second, the catalyst is relatively stable to air and moisture; thus, it does not require an inert atmosphere in order to function properly. Moreover, the catalyst can be recovered quantitatively without loss in efficiency or selectivity. However, when using the Hoveyda-Snapper desymmetrization catalyst, relatively high catalyst loadings and long reaction times are needed. Successful attempts from our lab to eliminate these shortcomings will be discussed in Chapter 3.

1.2.2 Tan's scaffolding catalyst

The second method of catalytic enantioselective silylation of alcohols uses a scaffolding catalyst, which was recently developed in the Tan lab (Figure 1.2).⁸ Tan's scaffolding catalyst can desymmetrize cyclic and acyclic *meso*-1,2-diols with 78-

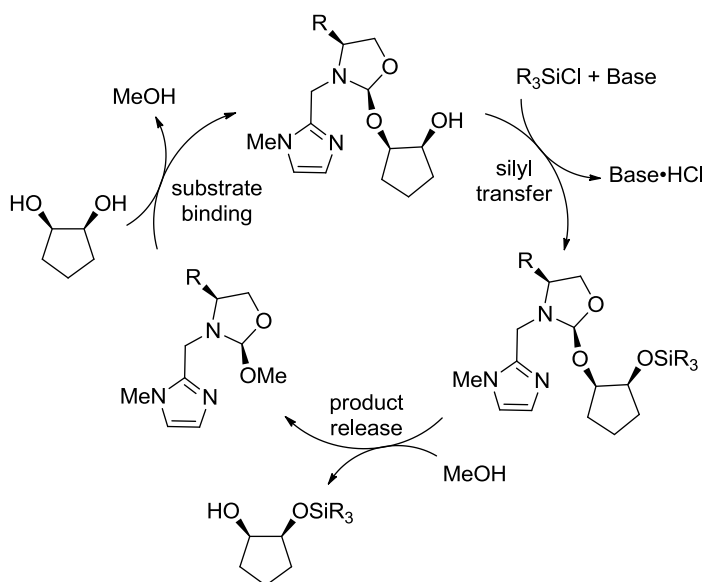
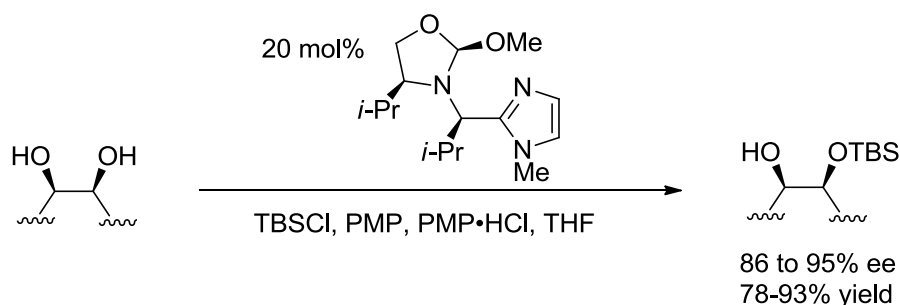


Figure 1.2 Proposed catalytic cycle of Tan's scaffolding catalyst

⁸ Tan, K. L.; Sun, X.; Worthy, A. D. *Angew. Chem. Int. Ed.* **2011**, *50*, 8167-8171.

93% yields and 86 to 95% ee's (Scheme 1.4).⁸ The principle behind this scaffolding catalysis is that the substrate can form a reversible covalent bond with the catalyst. The covalent bond is formed as the methoxy group of the catalyst rapidly exchanges with one of the hydroxyl groups of the substrate. The N-methylimidazole moiety of the catalyst activates the silicon electrophile, which results in silyl group transfer to the free hydroxyl group of the substrate. After deprotonation, there is another alcohol exchange process that releases the product and continues the catalytic cycle. The intramolecular nature of the silyl group transfer or the deprotonation step gives the reaction an entropic advantage. The enantioselectivity of the reaction originates from the functionalization step. Tan's scaffolding catalyst is easy to prepare from inexpensive commercially available starting materials, it is relatively stable to air, and it is effective towards a range of *meso*-1,2-diols. However, the catalyst is limited to 1,2-diols; also, acyclic substrates that are sterically hindered require small silyl electrophiles.



Scheme 1.4 Desymmetrization of *meso*-diols by catalytic enantioselective silylation using Tan's scaffolding catalyst

Tan's scaffolding catalyst was reported in 2011, while the Hoveyda-Snapper desymmetrization catalyst was reported in 2006. To date, these are the only two methods that can afford synthetically useful, enantioenriched products through catalytic

enantioselective silylation of diols. While there are many other catalytic enantioselective protections⁹ (e.g. acylations, benzoylations, carbamoylations) of diols in the literature, few catalytic enantioselective activations (e.g. sulfonylations) have been reported.

1.3 Catalytic enantioselective sulfonylation of alcohols

1.3.1 Importance of alcohol activation in synthesis

The hydroxyl group can be transformed into a good leaving group, or become activated, by the addition of a sulfonyl group. The sulfonate product of an alcohol can be used in bimolecular nucleophilic substitution (S_N2) reactions to form new C-C, C-N, and C-O bonds. Since S_N2 reactions proceed with inversion of configuration at the nucleophile, an enantioselective sulfonylation of an alcohol followed by an S_N2 reaction can lead to a variety of substituted products with controlled stereochemistry. Therefore, the concept of catalytic enantioselective sulfonylation of alcohols is attractive towards synthesis and has been explored on more than one occasion.

1.3.2 Miller's tetrapeptide catalyst

In 2009, Miller's lab reported enantioselective sulfonylation reactions catalyzed by a tetrapeptide catalyst.¹⁰ Miller followed a

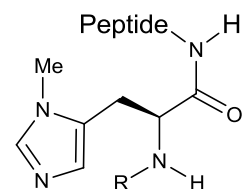
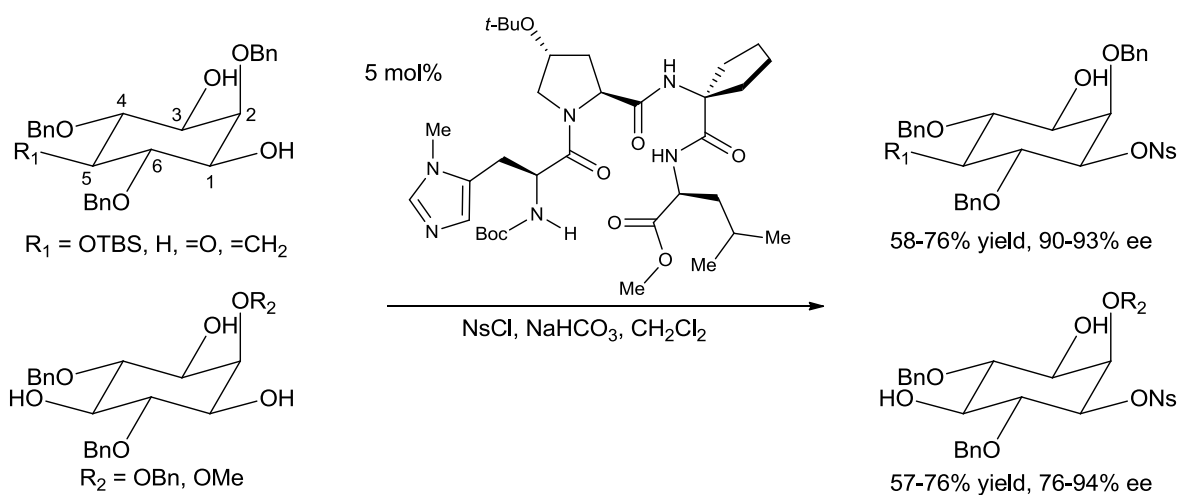


Figure 1.3 Miller's catalyst platform

⁹(a) Mukaiyama, T.; Tomioka, I.; Shimizu, M. *Chem. Lett.* **1984**, 49-52. (b) Mukaiyama, T.; Ichikawa, J.; Asami, M. *Chem. Lett.* **1984**, 949-1952. (c) Yamamoto, H.; Ishihara, K.; Kubota, M. *Synlett.* **1994**, 611-614. (d) Vedejs, E.; Daugulis, O.; Diver, S. T. *J. Org. Chem.* **1996**, *61*, 430-431. (e) Oriyama, T.; Imai, K.; Hosoya, T.; Sano, T. *Tetrahedron Lett.* **1998**, *39*, 397-400. (f) Oriyama, T.; Imai, K.; Hosoya, T.; Sano, T. *Tetrahedron Lett.* **1998**, *39*, 3529-3532. (g) Fujimoto, T.; Mizuta, S.; Sadamori, M.; Yamamoto, I. *Angew. Chem. Int. Ed.* **2003**, *42*, 3383-3385. (h) Trost, B. M.; Mino, T. *J. Am. Chem. Soc.* **2003**, *125*, 2410-2411. (i) Matsumura, Y.; Maki, T.; Murakami, S.; Onomura, O. *J. Am. Chem. Soc.* **2003**, *125*, 2052-2053. (j) Kawabata, T., et al. *Tetrahedron Lett.* **2003**, *44*, 1545-1548. (k) Vedejs, E.; Daugulis, O.; Tuttle, N. *J. Org. Chem.* **2004**, *69*, 1389-1392. (l) Pfaltz, A.; Mazet, C.; Kohler, V. *Angew. Chem. Int. Ed.* **2005**, *44*, 4888-4891. (m) Yamada, S., et al. *J. Org. Chem.* **2006**, *71*, 6872-6880. (n) Matsumura, Y., et al. *Tetrahedron Lett.* **2006**, *47*, 8453-8456. (o) Shirai, R.; Nakamura, D.; Kakiuchi, K.; Koga, K. *Org. Lett.* **2006**, *8*, 6139-6142.

¹⁰ Miller, S. J.; Fiori, K. W., Puchlopek, A. L. A. *Nature Chemistry.* **2009**, *1*, 630-634.

biomimetic approach to develop peptide catalysts that can mediate a variety of group transfer reactions of alcohols. Similar to the Hoveyda-Snapper desymmetrization catalyst, Miller's catalyst platform contains an N-methylimidazole moiety, which can activate the electrophile (Figure 1.3). It is thought that the reactions go through an N-methylimidazolium intermediate, which is formed upon nucleophilic attack of the N-methylimidazole on the electrophile. The peptide chain of the catalyst is thought to hold the substrate in place, and variations on the peptide chain can improve the catalyst's effectiveness.



Scheme 1.5 Desymmetrization of *meso*-diols and triols by catalytic enantioselective sulfonylation using Miller's tetrapeptide catalyst

Scheme 1.5 shows alcohol desymmetrizations by sulfonylation with one of Miller's peptide catalysts. The substrate scope is made up of *myo*-inositol derivatives (2,4,6-tribenzyl-*myo*-inositol with different R groups on C5 and C2) and the sulfonylation reagent is *p*-nitrobenzenesulfonyl chloride (NsCl). Although the catalyst's selectivity in the reactions presented ranges from 76-94% ee, the substrate scope is narrow and NsCl is the only sulfonylation reagent that doesn't produce low yields. When the more simplified substrate *meso*-1,3-cyclohexanediol is used in the reaction, the yield is low and there is

no enantioselectivity. Miller's tetrapeptide catalyst is advantageous in that it is relatively stable to air, and it is effective towards a range of *myo*-inositol derivatives. However, the catalyst is limited in substrate scope and in sulfonylation reagent.

1.3.3 Onomura's copper complex

In 2007, Onomura and coworkers developed an enantioselective sulfonylation reaction catalyzed by a copper complex.¹¹ The copper complex can desymmetrize cyclic and acyclic *meso*-1,2-diols with 71-99% yields and 93 to >98% ee's when using *p*-toluenesulfonyl chloride (TsCl), which is the most common sulfonylation reagent (Scheme

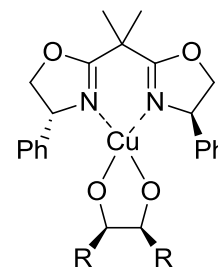


Figure 1.4 Intermediate in the desymmetrization of *meso*-diols by catalytic enantioselective sulfonylation using a copper (II) complex

1.6). The catalyst precursors are copper (II) triflate and (*R,R*)-Ph-BOX ligand. The BOX ligand is a chiral bidentate ligand, which coordinates to copper. The triflate ligands exchange for the diol substrate, which, in turn, acts as a bidentate ligand. This chiral intermediate (Figure 1.4) undergoes tosyl group transfer to the hydroxyl group that is not blocked by an R group from the substrate or a phenyl group from the BOX ligand. Once the *meso*-diol is

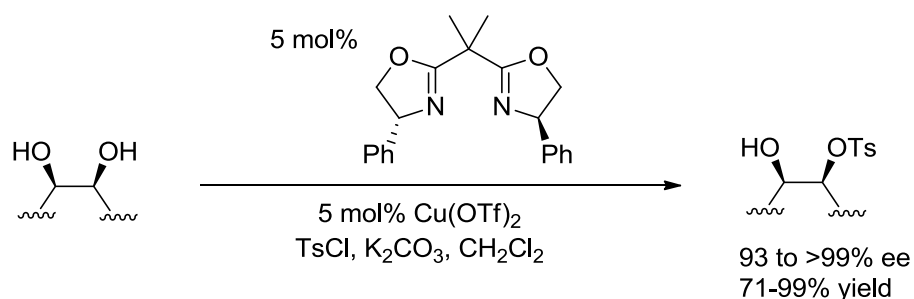
desymmetrized,

the tosylated

product is

released, and the

copper complex



Scheme 1.6 Desymmetrization of *meso*-diols by catalytic enantioselective sulfonylation using a copper (II) complex

¹¹ Onomura, O.; Demizu, Y.; Matsumoto, K.; Matsumura, Y. *Tetrahedron Lett.* **2007**, 48, 7605-7609.

continues the catalytic cycle.

The copper complex is easy to prepare from commercially available starting materials, it is effective towards a range of *meso*-1,2-diols, and it can tolerate sulfonylation reagents other than TsCl (benzenesulfonyl chloride, *p*-nitrobenzenesulfonyl chloride, *p*-chlorobenzenesulfonyl chloride, and *p*-methoxybenzenesulfonyl chloride all work well). In terms of disadvantages, the catalyst requires an inert atmosphere in order to function properly as it is relatively unstable to air and moisture, and it is limited to 1,2-diols.

1.4 Kinetic resolution of alcohols

1.4.1 Overview of kinetic resolution

When catalytic enantioselective functionalization is extended from *meso*-diols to *anti*-diols or simply mono-alcohols, the result is a kinetic resolution reaction. Kinetic resolution occurs when one enantiomer of a racemic mixture reacts faster with a chiral catalyst or reagent than the other enantiomer. In the case of a perfect kinetic resolution, at 50% conversion, all of one enantiomer is converted into product, and all of the other enantiomer remains unreacted. Therefore, the maximum yield of a kinetic resolution is 50%, which is a disadvantage when compared to an enantioselective transformation. However, the interesting advantage of kinetic resolution is that the enantiopurity of the product and the starting material depends on the conversion; it is not limited by the selectivity of the catalyst. This concept is best described by Sharpless in the following passage:

The enantiometric excess realized in an asymmetric synthesis is simply a consequence of the energy difference between two diastereomeric transition

states; the only way to improve the % ee is to increase that energy difference. Kinetic resolution too depends on there being an energy difference between diastereomeric transition states, but the manner in which that energy difference is expressed is unique to kinetic resolutions. The energy difference, manifested as a relative rate difference, represents a constant and unrelenting differential pressure upon the two enantiomers. This winnowing should continue until the last molecule of the more reactive enantiomer is swept away, and one is left with a substance possessed of absolute enantiomeric purity.¹²

Despite its drawback, there are numerous practical considerations that can render kinetic resolution the reaction of choice in a synthesis. For example, if the racemate is inexpensive or there are no other ways to make the product enantioselectively, then kinetic resolution can be invaluable. If the catalyst is highly selective and effective at low loadings, if the catalyst is inexpensive or it can be recovered efficiently, and if the product and starting material are separable, then kinetic resolution can be practical. Also, a kinetic resolution reaction can be utilized when it is more cost-effective and safer than an enantioselective transformation reaction. In the ideal kinetic resolution, however, both the product and starting material are desired and can be recovered in highly enantioenriched form.

1.4.2 Examples of kinetic resolution of alcohols

With the development of “planar-chiral” DMAP derivatives, Fu and coworkers have strongly contributed the field of kinetic resolution of alcohols. In 1996, Fu introduced

chiral metal complexes based on ferrocene for use as catalysts in enantioselective synthesis. While DMAP is a flat molecule and has no chirality, one of Fu’s chiral DMAP

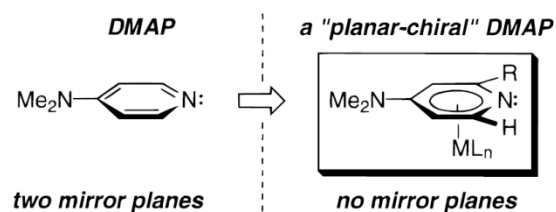
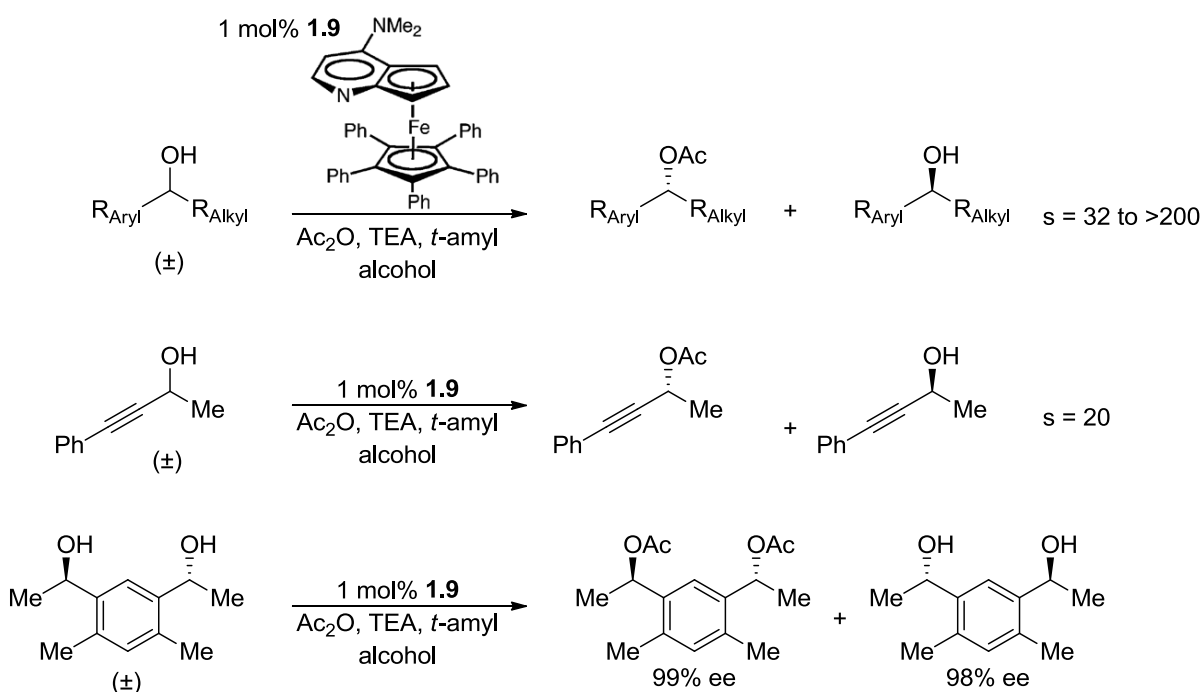


Figure 1.5 DMAP versus “planar-chiral” DMAP

¹² Sharpless, K. B., et al. *J. Am. Chem. Soc.* **1981**, *103*, 6237-6240.

catalysts has planar chirality that stems from the metal complex blocking one face of the molecule (Figure 1.5). These chiral DMAP catalysts can provide nucleophilic activation in an enantioselective fashion, thus desymmetrizing achiral molecules whilst performing a group transfer reaction. When complex **1.9** is used in conjunction with acetic anhydride, in the presence of triethylamine as general base and *t*-amyl alcohol as solvent, mono-alcohols and *anti*-diols can be resolved with selectivities (*s*) of up to >200 (Scheme 1.7).¹³

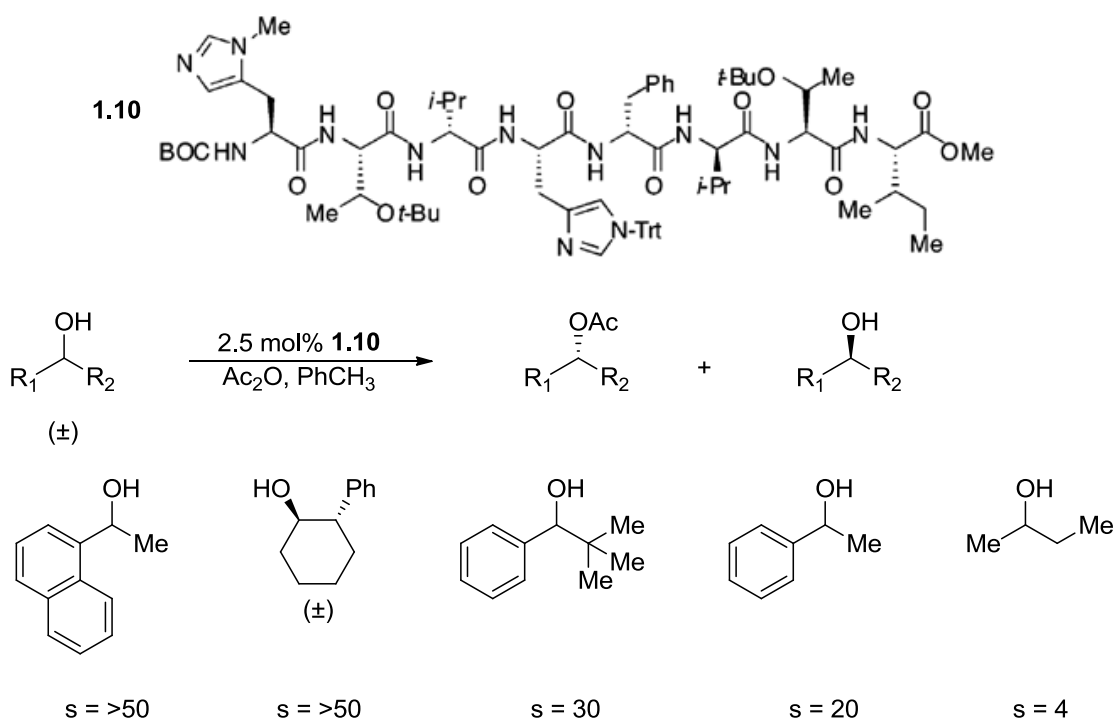


Scheme 1.7 Kinetic resolution of mono-alcohols and *dl*-diols by catalytic acylation using Fu's "planar-chiral" catalyst

Miller's peptide catalysts are effective not only towards *meso*-diols, but also towards functionalized and unfunctionalized mono-alcohols. In 2001, Miller reported the impressive kinetic resolution of unfunctionalized mono-alcohols by catalytic acylation

¹³ (a) Fu, G. C. *Acc. Chem. Res.* **2000**, 33, 412-420. (b) France, S.; Guerin, D. J.; Miller, S. J.; Lectka, T. *Chem. Rev.* **2003**, 103, 2985-3012.

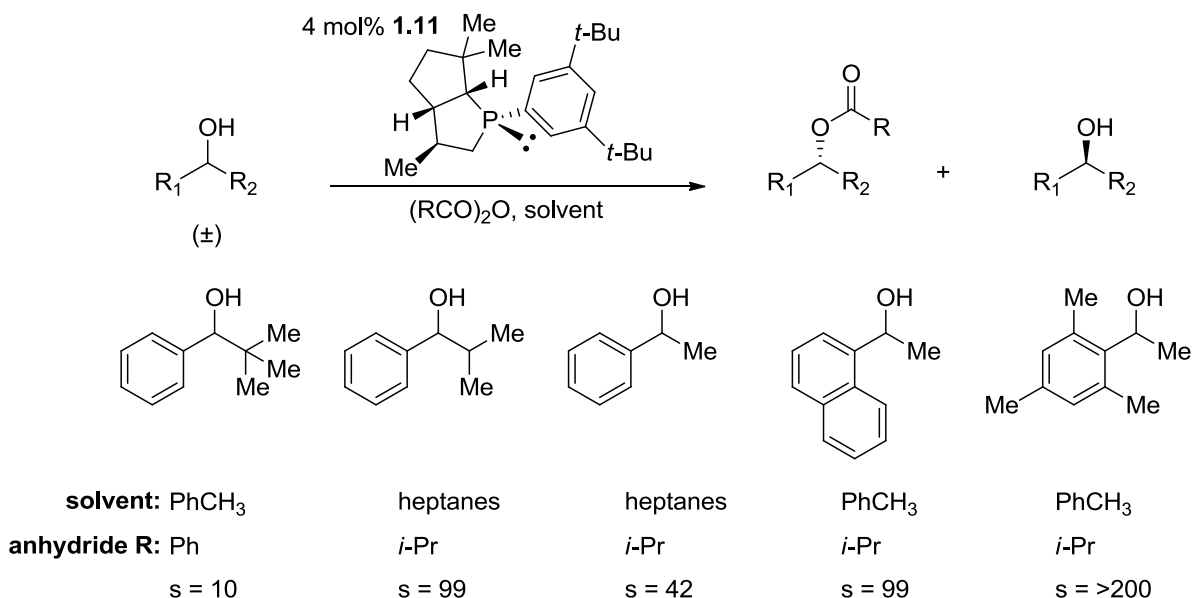
using peptide catalyst **1.10**, which was discovered through rigorous screening (Scheme 1.8).¹⁴ As previously mentioned, Miller's catalyst platform contains an N-methylimidazole moiety, which can activate the electrophile. The peptide chain of catalyst **1.10** contains eight amino acids, making the catalyst highly selective. In the case of 2-butanol, the catalyst has to differentiate between a methyl group and a methylene unit. Although the selectivity for 2-butanol is poor ($s = 4$), the fact that this alcohol can be resolved is proof of the effectiveness of Miller's peptide catalyst. However, despite the practicality and ease of peptide coupling reactions, synthesis of catalyst **1.10** requires an undesirably large number of steps, which, along with the large size of the catalyst, are disadvantages of using Miller's kinetic resolution method.



Scheme 1.8 Kinetic resolution of mono-alcohols by catalytic acylation using Miller's peptide catalyst

¹⁴ Miller, S. J. *Acc. Chem. Res.* **2004**, 37, 601-610.

In 1996, Vedejs's lab reported the first chiral phosphine catalyst that can kinetically resolve mono-alcohols by chlorobenzoylation.¹⁵ However, the selectivities were moderate ($s = 13-15$) and the reactions were slow, which prompted further catalyst optimization. In 2003, Vedejs reported a highly selective phosphabicyclooctane catalyst that can kinetically resolve benzylic alcohols by benzoylation or *iso*-butyroylation (Scheme 1.9).¹⁶ The kinetic resolution selectivities for benzylic alcohols using catalyst



Scheme 1.9 Kinetic resolution of mono-alcohols by catalytic benzoylation or *iso*-butyroylation using Vedejs's phosphabicyclooctane catalyst

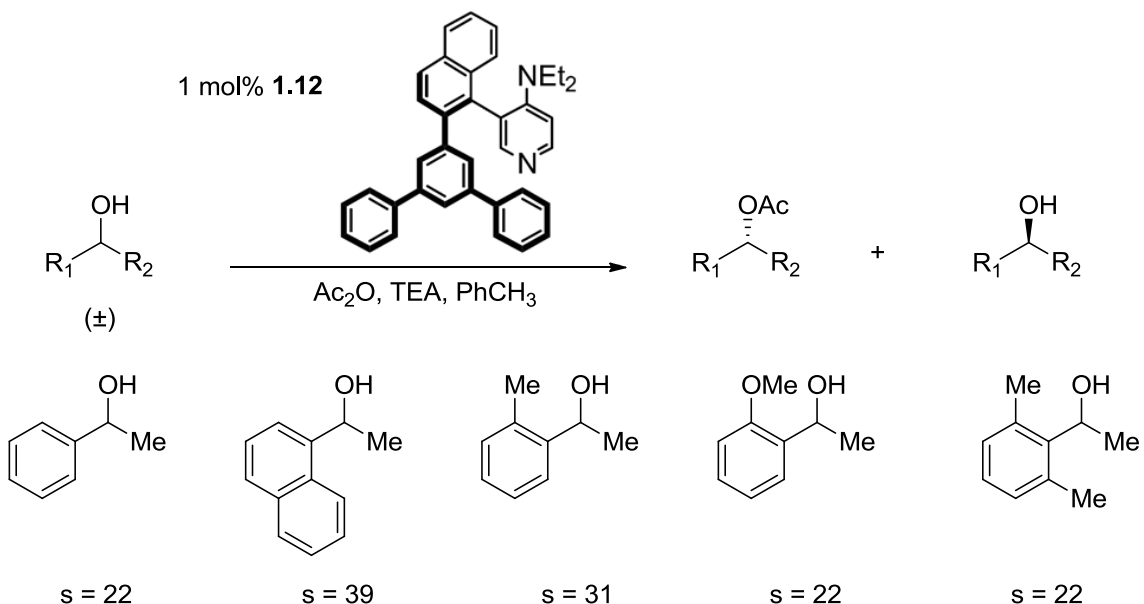
1.11 can go up to >200 . It is thought that phosphine catalyzed kinetic resolutions involve a "P-acylphosphonium carboxylate intermediate and a tightly ion paired transition state." Given that the phosphine is chiral, the active intermediate is also chiral and it prefers to react with one enantiomer of the benzylic alcohol. Despite Vedejs's advances in chiral phosphine synthesis, synthesis of catalyst **1.11** requires a number of sensitive steps and

¹⁵ Vedejs, E.; Daugulis, O.; Diver, S. T. *J. Org. Chem.* **1996**, *61*, 430-431.

¹⁶ Vedejs, E.; Daugulis, O. *J. Am. Chem. Soc.* **2003**, *125*, 4166-4173.

includes the formation of diastereomers during more than one step. The difficulties in catalyst synthesis and the limitation of the substrate scope to benzylic alcohols are drawbacks to Vedejs's phosphine catalyzed kinetic resolutions.

In 2006, Spivey and coworkers reported an axially chiral 4-aminopyridine catalyst that can successfully resolve benzylic alcohols by acylation (Scheme 1.10).¹⁷ When catalyst **1.12** is used in conjunction with acetic anhydride, in the presence of triethylamine as general base and toluene as solvent, mono-alcohols can be resolved with selectivities of up to 39. The axially chiral 4-aminopyridine catalyst can provide Lewis basic nucleophilic activation in an enantioselective fashion, similar to Fu's "planar-chiral" DMAP catalysts. However, unlike Fu's DMAP catalysts, Spivey's catalyst is limited to the kinetic resolution of benzylic alcohols.



Scheme 1.10 Kinetic resolution of mono-alcohols by catalytic acylation using Spivey's axially chiral 4-aminopyridine catalyst

¹⁷ Spivey, A. C., et al. *Tetrahedron*. **2006**, *62*, 295-301.

As previously stated, mono-alcohols are not the only alcohols that can undergo kinetic resolution; primary-secondary diols and secondary-secondary *anti*-diols are two other examples from literature that have been resolved kinetically. A few selected methods will be discussed in the remainder of this chapter.

In 1999, Matsumura and coworkers reported an organotin catalyst for the purpose of kinetically resolving primary-secondary diols by benzylation (Scheme 1.11).¹⁸ When catalyst **1.13** is used in conjunction with benzoyl chloride, in the presence of sodium

bicarbonate as general base, water as an additive and tetrahydrofuran as solvent, primary-secondary alcohols can be resolved with poor to good selectivities (*s* = 3-22).

The inorganic base forms an aqueous layer and serves to deprotonate the diol (this process is assisted by water hydrogen-bonding interactions as shown in Figure 1.6¹⁹). In the organic layer, only one enantiomer of the diol can be approached by the catalyst without leading to steric repulsion; when the catalyst comes close enough to this enantiomer, the bromine ligands on the catalyst exchange for the diol. The chiral intermediate that's formed undergoes benzoyl group transfer to the primary (less hindered) hydroxyl group. Then, the benzyolated product is released, and the organotin

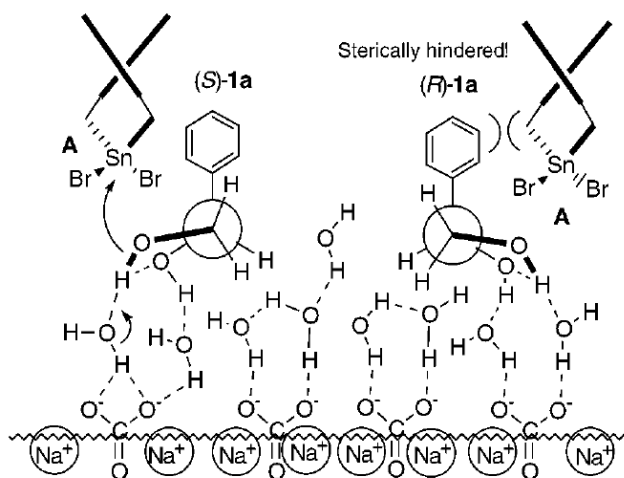
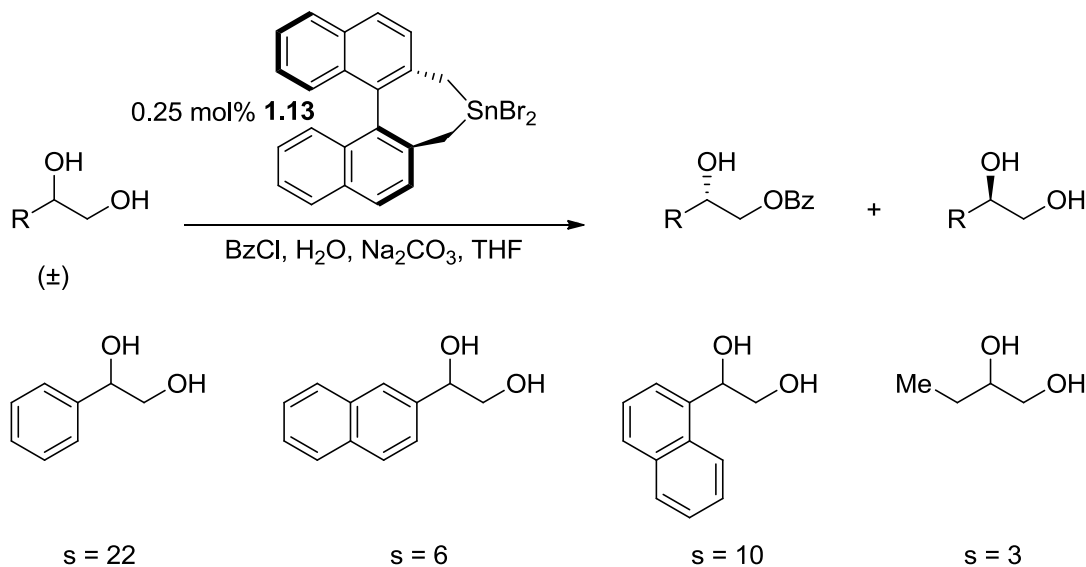


Figure 1.6 Origin of selectivity of Matsumura's organotin catalyst for the kinetic resolution of primary-secondary diols

¹⁸ Matsumura, Y., et al. *Org. Lett.* **1999**, *1*, 969-972.

¹⁹ Figure was copied from Matsumura, Y., et al. *Org. Lett.* **1999**, *1*, 969-972.

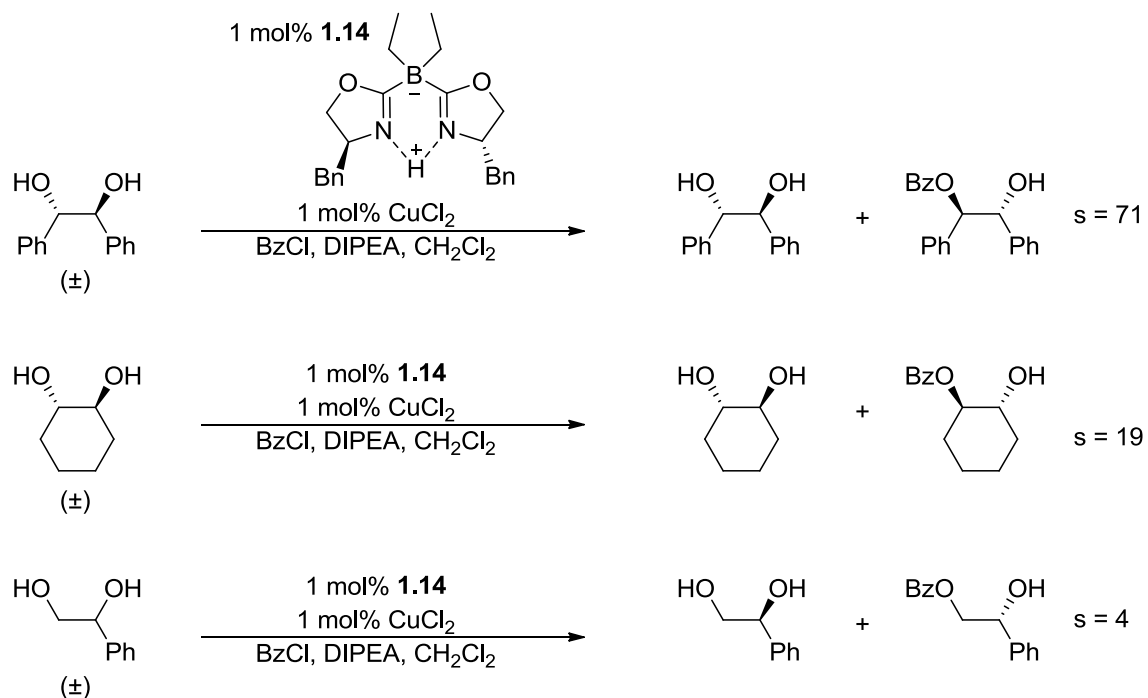
catalyst continues the catalytic cycle. Unfortunately, although Matsamura's catalyst is highly site-selective, it is not as enantioselective as desired.



Scheme 1.11 Kinetic resolution of 1,2-diols by catalytic benzylation using Matsumura's axially chiral organotin catalyst

More recently, in 2006, Pfaltz and coworkers reported that a copper (II) boron-bridged bisoxazoline (borabox) catalyst can kinetically resolve *anti*-1,2-diols better than a copper (II) carbon-bridged BOX catalyst (Scheme 1.12).²⁰ When the borabox catalyst (formed by mixing precursors **1.14** and copper (II) chloride) is used in conjunction with benzoyl chloride, in the presence of diisopropylethylamine as general base and dichloromethane as solvent, *anti*-1,2-diols can be resolved with good to great selectivities ($s = 19$ or 71). The catalyst can also resolve 1-phenyl-1,2-ethanediol with poor selectivity ($s = 4$). The mechanism of this reaction is similar to Matsamura's organotin catalyzed reaction. Also, in both cases, the catalyst is selective for diols versus mono-alcohols; this prevents the undesired formation of bis-benzoylated products.

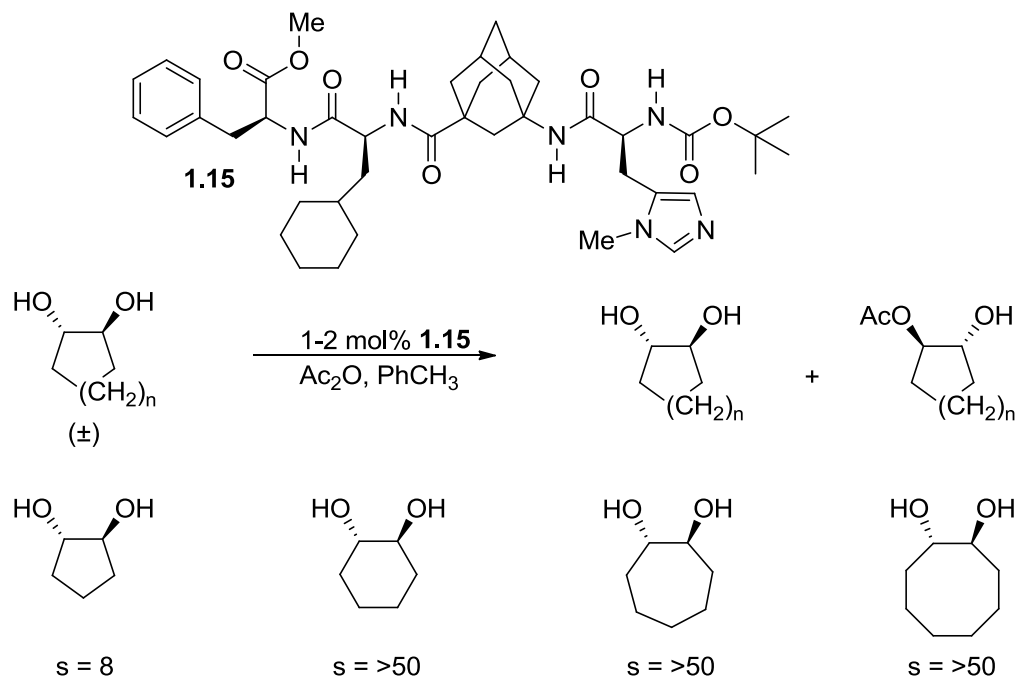
²⁰ Pfaltz, A.; Mazet, C.; Roseblade, S.; Kohler, V. *Org. Lett.* **2006**, *8*, 1879-1882.



Scheme 1.12 Kinetic resolution of 1,2-diols by catalytic benzylation using Pfaltz's copper (II) borabox catalyst

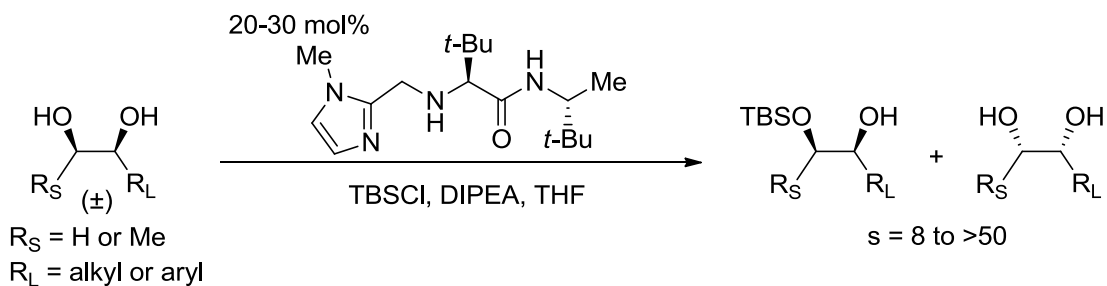
An impressive example of kinetic resolution of *anti*-1,2-diols using a tetrapeptide catalyst was reported in 2008 by Schreiner and coworkers (Scheme 1.13).²¹ Catalyst **1.15** is similar to Miller's peptide catalysts because it also contains an N-methylimidazole moiety and it is made up of natural and unnatural amino acids. The conformation of Schreiner's catalyst, however, is restricted by an adamantane unit. As shown in Scheme 1.13, Schreiner's catalyst can successfully resolve cyclic *anti*-1,2-diols by acylation ($s = 8$ to >50).

²¹ Schreiner, P. R.; Muller, C. E.; Wanka, L.; Jewell, K. *Angew. Chem. Int. Ed.* **2008**, *47*, 6180-6183.



Scheme 1.13 Kinetic resolution of 1,2-diols by catalytic acylation using Schreiner's tetrapeptide catalyst

The last example of kinetic resolution of diols that will be discussed in this chapter comes from our lab. In 2007, the kinetic resolution of primary-secondary and secondary-secondary asymmetric diols by catalytic silylation using the Hoveyda-Snapper desymmetrization catalyst was reported by our lab (Scheme 1.14).²² In addition to being highly enantioselective, the catalyst is highly site-selective towards a variety of



Scheme 1.14 Kinetic resolution of 1,2-diols by catalytic silylation using the Hoveyda-Snapper desymmetrization catalyst

²² Zhao, Y.; Mitra, A. W.; Hoveyda, A. H.; Snapper, M. L. *Angew. Chem. Int. Ed.* **2007**, *46*, 8471-8474.

asymmetric diols, the most impressive of which is *syn*-pentane-2,3-diol, where the catalyst has to differentiate between a methyl group and a methylene unit.

This last discovery prompted us to extend the application of the Hoveyda-Snapper desymmetrization catalyst even further. We thought that we could improve upon the two previous methods of catalytic enantioselective sulfonylation of diols, and that we could develop the first kinetic resolution of diols by catalytic sulfonylation. The results of those studies will be discussed in the following chapter.

CHAPTER 2:

KINETIC RESOLUTION OF *SYN*-DIOLS BY CATALYTIC ENANTIOSELECTIVE SULFONYLATION

2.1 Catalytic enantioselective sulfonylation of *syn*-diols and triols using amino-acid-derived catalyst

Given the success of the Hoveyda-Snapper desymmetrization catalyst with silylation, we hoped to expand the catalyst's scope to more than just enantioselective protection of diols. We were interested in sulfonylation, in particular tosylation, because it is well known that the tosylate product of an alcohol can be used in S_N2 reactions to form new C-C, C-N, and C-O bonds. Therefore, enantioselective activation of an alcohol can lead to a variety of substituted products with controlled stereochemistry.

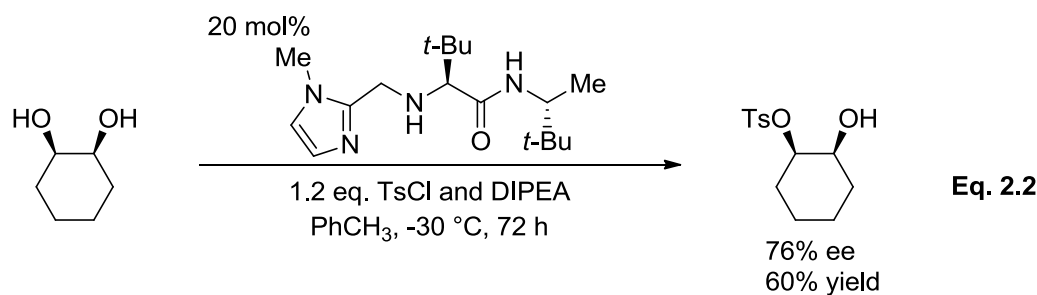
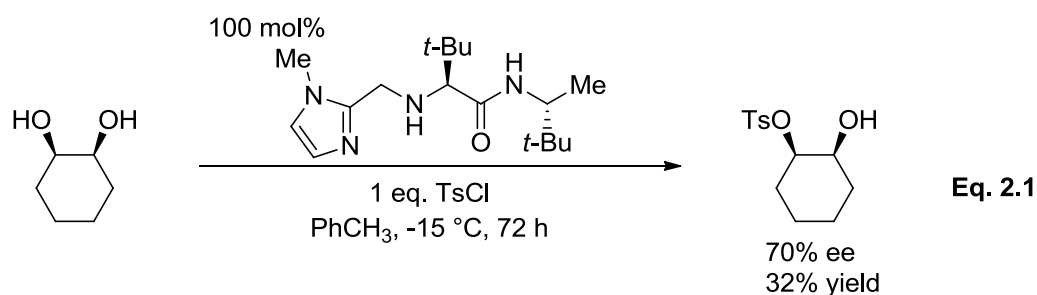
2.1.1 Initial screenings

Fengqi Wen and Dr. Zhen You's soon-to-be published work on the catalytic enantioselective tosylation of *meso*-diols using the Hoveyda-Snapper desymmetrization catalyst demonstrates the effectiveness of this method. The initial investigation by Dr. You tested the catalyst's Lewis basic ability to activate a new electrophile: TsCl. The test substrate (*meso*-1,2-cyclohexanediol) was reacted with 100 mol% catalyst, 1 equivalent of TsCl, in the presence of toluene as solvent (Eq. 2.1).²³ Although the yield for the reaction was low (32%), the enantioselectivity was promising (70% ee). The next steps were to lower the catalyst loading and to add a base (diisopropylethylamine, DIPEA) that could potentially recycle the catalyst. *meso*-1,2-Cyclohexanediol was reacted with 20

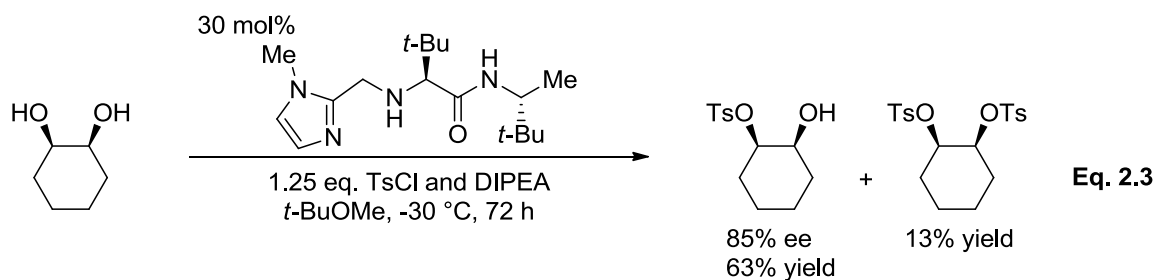
²³ You, Zhen. PhD. Dissertation, Boston College, 2009.

mol% catalyst, 1.2 equivalents of TsCl and DIPEA, in the presence of toluene as solvent.

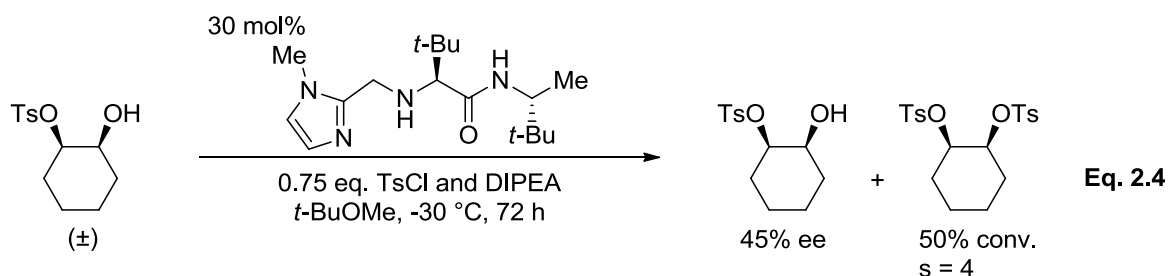
As shown in Eq. 2.2, the results were once again promising (60% yield and 76% ee), proving that DIPEA could recycle the catalyst without interfering with its activity.²³



The next course of action was to optimize and, thus, probe the mechanism of the catalytic enantioselective tosylation reaction by screening different conditions. When evaluating which conditions were the optimal, three factors were considered: the reaction conversion, the ee of the mono-tosylate, and the mono:bis ratio of the products. The optimal reaction conditions were found to include a catalyst loading of 30 mol%, *t*-butyl methyl ether (*t*-BuOMe) as the solvent, a concentration of 0.25 M, a temperature of -30 °C, and DIPEA as the base (Eq. 2.3).²³



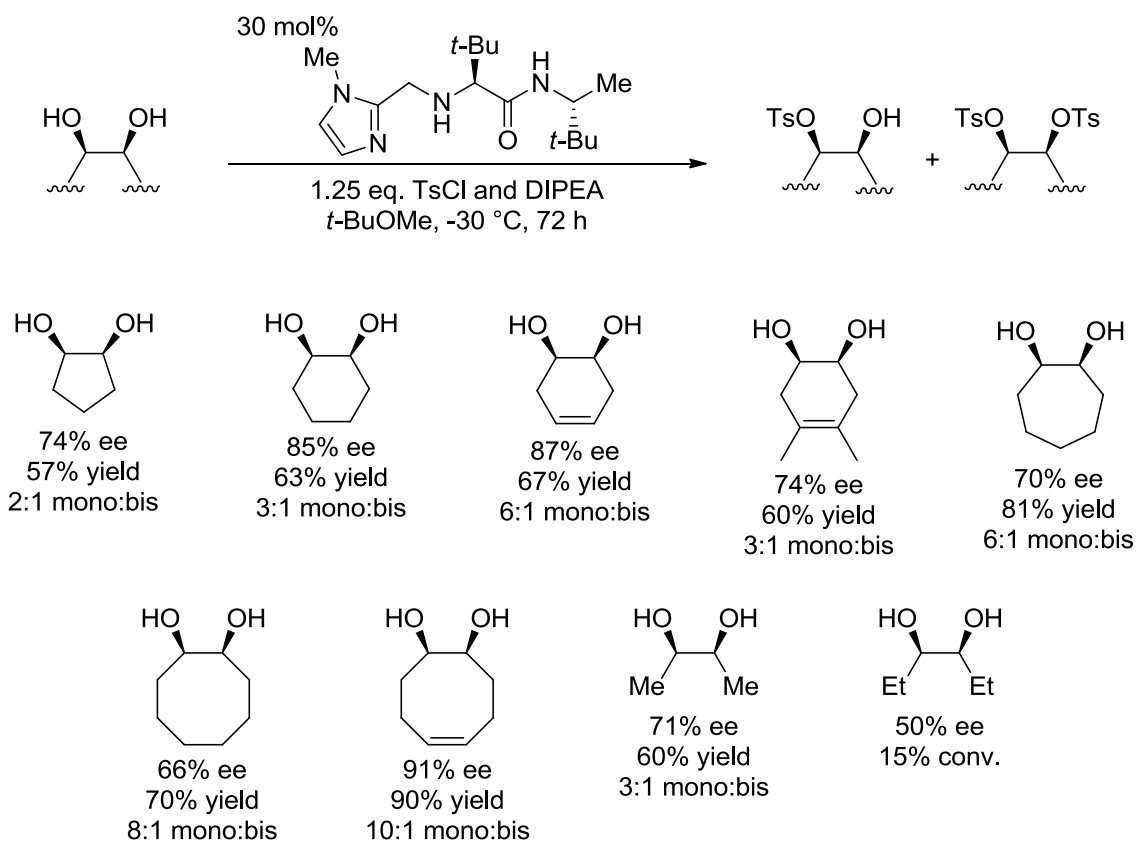
Unfortunately, in the case of tosylation (versus silylation), bis-tosylate formation was a challenge. Interestingly enough, the more bis-tosylate formed, the higher the ee of the mono-tosylate. The hypothesis was that after the first reaction, the minor enantiomer of the product reacts faster than the major enantiomer and produces the bis-tosylate (secondary kinetic resolution). Therefore, the more bis-tosylate formed, the higher the ee of the mono-tosylate. Dr. You tested this hypothesis by subjecting a racemic mixture of the mono-tosylate to the catalytic enantioselective tosylation conditions. As shown in Eq. 2.4, the mono-tosylate was kinetically resolved, albeit with poor selectivity ($s = 4$).²³



After optimizing the reaction conditions, Fengqi Wen and Dr. You attempted to find a more reactive and selective version of the Hoveyda-Snapper desymmetrization catalyst for the enantioselective tosylation reaction. They systematically modified the catalyst one portion at a time (Lewis base, chiral amine, or amino acid) and tested each modified version under the optimized reaction conditions. Ultimately, it was found that the original catalyst was more reactive and selective than each modified version.

2.1.2 Substrate scope

Finally, Fengqi Wen and Dr. You probed the substrate scope of the catalytic enantioselective tosylation reaction. They found that cyclic *meso*-1,2-diols could be desymmetrized with moderate to good yields and moderate to excellent ee's, while acyclic *meso*-1,2-diols proved to be difficult substrates (Scheme 2.1).²⁴ Cyclic and

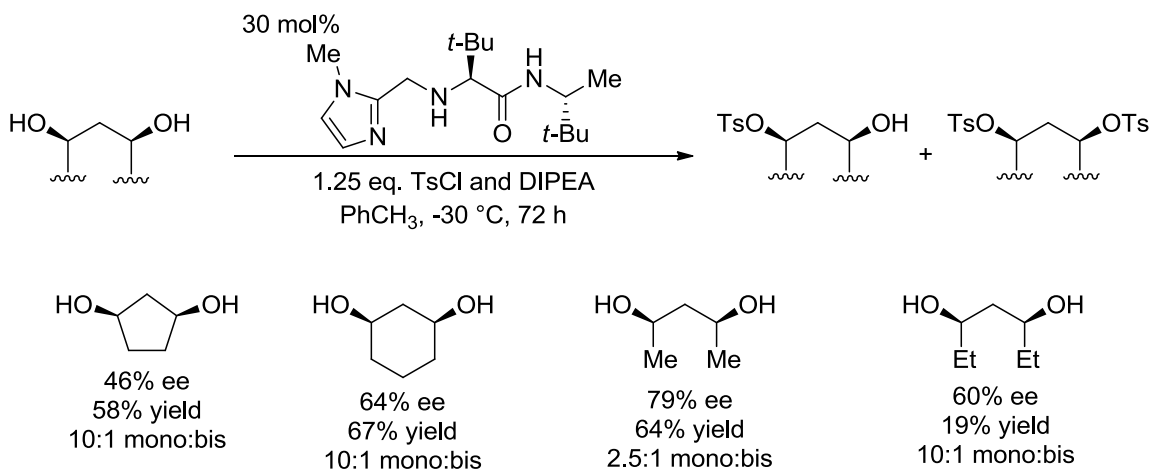


Scheme 2.1 Desymmetrization of *meso*-1,2-diols by catalytic enantioselective tosylation using the Hoveyda-Snapper amino-acid-derived catalyst

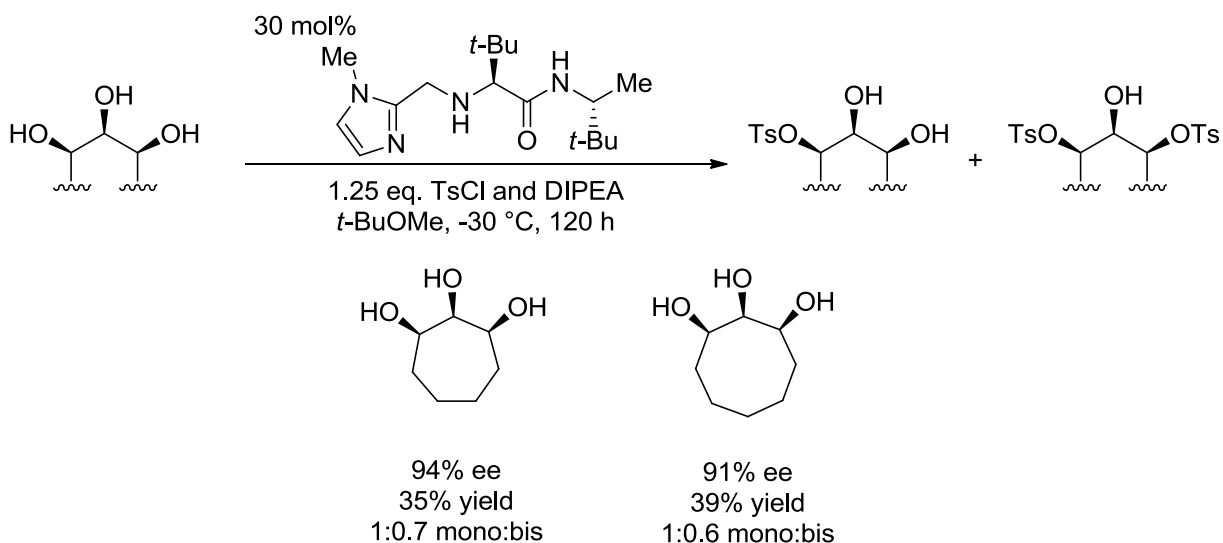
acyclic *meso*-1,3-diols could also be desymmetrized, albeit with moderate yields and ee's (Scheme 2.2).²⁴ Finally, mono-tosylates of cyclic *meso*-1,2,3-triols could be obtained in low yields but high ee's (Scheme 2.3).²⁴ As previously mentioned, due to a secondary kinetic resolution reaction, the more bis-tosylate formed, the higher the ee of the mono-tosylate. Therefore, a mono-tosylate with high yield suffers in ee, and vice versa.

²⁴ Wen, Fengqi. MS. Thesis, Boston College, 2011.

Another disadvantage of this reaction is that some substrates, especially triols, are very insoluble in organic solvents, leading to heterogeneous mixtures and long reaction times.



Scheme 2.2 Desymmetrization of *meso*-1,3-diols by catalytic enantioselective tosylation using the Hoveyda-Snapper amino-acid-derived catalyst



Scheme 2.3 Desymmetrization of *meso*-1,2,3-triols by catalytic enantioselective tosylation using the Hoveyda-Snapper amino-acid-derived catalyst

Overall, the catalytic enantioselective tosylation of *meso*-diols using the Hoveyda-

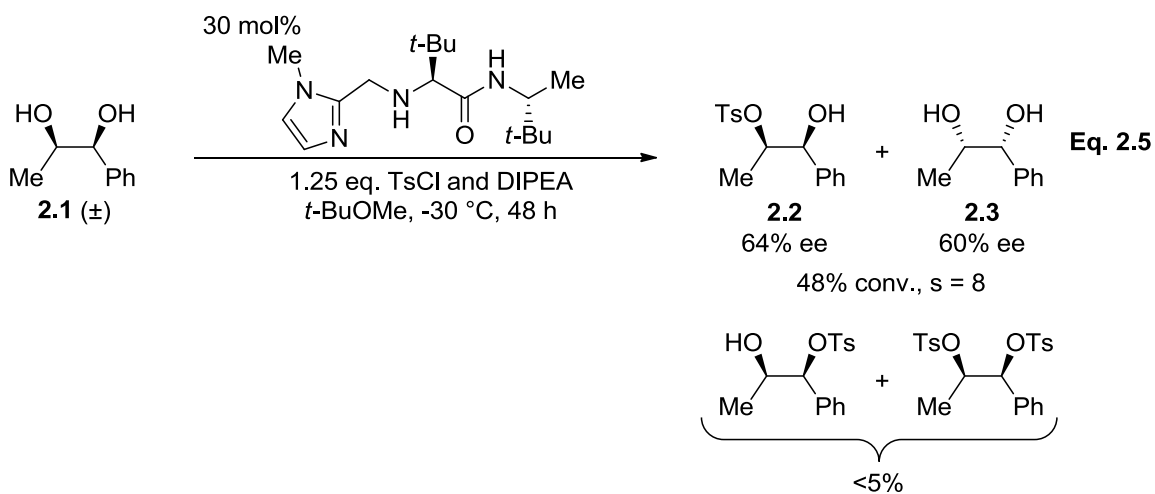
Snapper desymmetrization catalyst can be a useful method in organic synthesis. In terms

of advantages, the reaction is practical due to the relative stability of the catalyst and the breadth of the substrate scope.

2.2 Kinetic resolution of *syn*-diols by catalytic enantioselective sulfonylation using amino-acid-derived catalyst

Once the catalytic enantioselective tosylation reaction using the Hoveyda-Snapper amino-acid-derived catalyst was developed, we decided to explore the possibility of kinetic resolution by catalytic sulfonylation. To date, there is no report of unfunctionalized alcohols being kinetically resolved by sulfonylation. Such a method would be attractive as it would produce enantioenriched alcohols and sulfonates that may be difficult or impossible to synthesize otherwise.

The success of the kinetic resolution of diols by silylation using the Hoveyda-Snapper peptide catalyst gave us hope that we could resolve primary-secondary and secondary-secondary asymmetric diols by sulfonylation as well. We first tested an asymmetric diol under the optimized conditions of the enantioselective tosylation reaction. The test substrate (*syn*-1-phenyl-1,2-propanediol) was reacted with 30 mol%

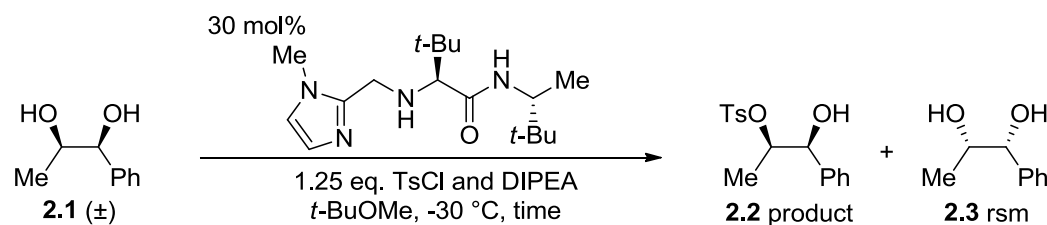


catalyst, 1.25 equivalents of TsCl and DIPEA, in the presence of *t*-BuOMe as solvent (Eq. 2.5). After 48 hours at -30 °C, 48% of diol **2.1** had been converted into mono-tosylate **2.2**. We were pleased to learn that this substrate was resolved with a moderate selectivity ($s = 8$)²⁵ and that the amount of minor mono-tosylate and bis-tosylate formed in the process was negligible (<5%).

2.2.1 Time screening

We then began to study this kinetic resolution reaction by screening different reaction times (Table 2.1). In 37 hours, which was chosen as the optimal time, the reaction proceeded to 42% conversion (the maximum yield is 50%). It is important to note that the selectivity of a kinetic resolution reaction does not change depending on the conversion. Therefore, there were only minor variations in the s values calculated for the different reaction times ($s = 5$ -11).

Table 2.1 Reaction Time Screening



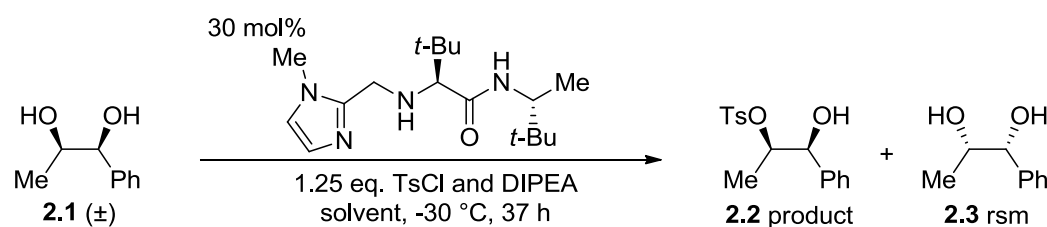
Entry	Time	ee _{rsm}	ee _{product}	Conv.	S
1	15 h	18%	64%	22%	5
2	37 h	54%	74%	42%	11
3	48 h	60%	64%	48%	8
4	62 h	64%	56%	53%	6

²⁵ The equations used to calculate the conversion and s value were taken from: Kagan, H. B.; Fiaud, J. C. *Top. Stereochem.* **1998**, *18*, 249-330.

2.2.2 Solvent screening

We continued to study this new reaction by screening different solvents. Racemic diol **2.1** was reacted with 30 mol% catalyst, 1.25 equivalents of TsCl and DIPEA, in the presence of various solvents at -30 °C for 37 hours (Table 2.2). THF and toluene provided low conversions: 12% and 18%, respectively. Diethyl ether, *t*-BuOMe, and a 1:1 mixture of the two provided comparable high conversions: 39%, 41%, and 44%, respectively. However, the original solvent, *t*-BuOMe, was chosen as the optimal solvent since it exhibited the highest selectivity ($s = 9$).

Table 2.2 Solvent Screening

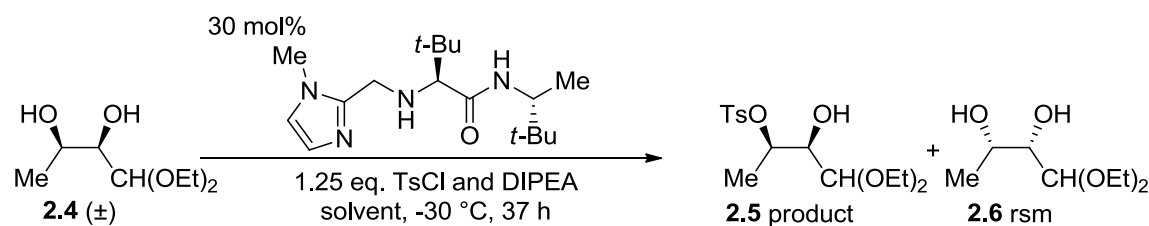


Entry	Solvent	ee _{rsm}	ee _{product}	Conv.	s
1	THF	8%	59%	12%	4
2	PhCH ₃	12%	56%	18%	4
3	diethyl ether	38%	60%	39%	6
4	<i>t</i>-BuOMe	48%	70%	41%	9
5	1:1 diethyl ether: <i>t</i> -BuOMe	44%	55%	44%	5

A new substrate gave us slightly different solvent screening results. Racemic diol **2.4** was reacted with 30 mol% catalyst, 1.25 equivalents of TsCl and DIPEA, in the presence of various solvents at -30 °C for 60 hours (Table 2.3). THF provided the lowest conversion and selectivity: 8% and $s = 6$. Toluene and the acyclic ethers (diethyl ether, *t*-BuOMe, and a 1:1 mixture of the two), all provided similar conversions and

selectivities: 49-54% and $s = 15$ -19. Therefore, we decided to keep *t*-BuOMe as the optimal solvent.

Table 2.3 Solvent Screening with a New Substrate



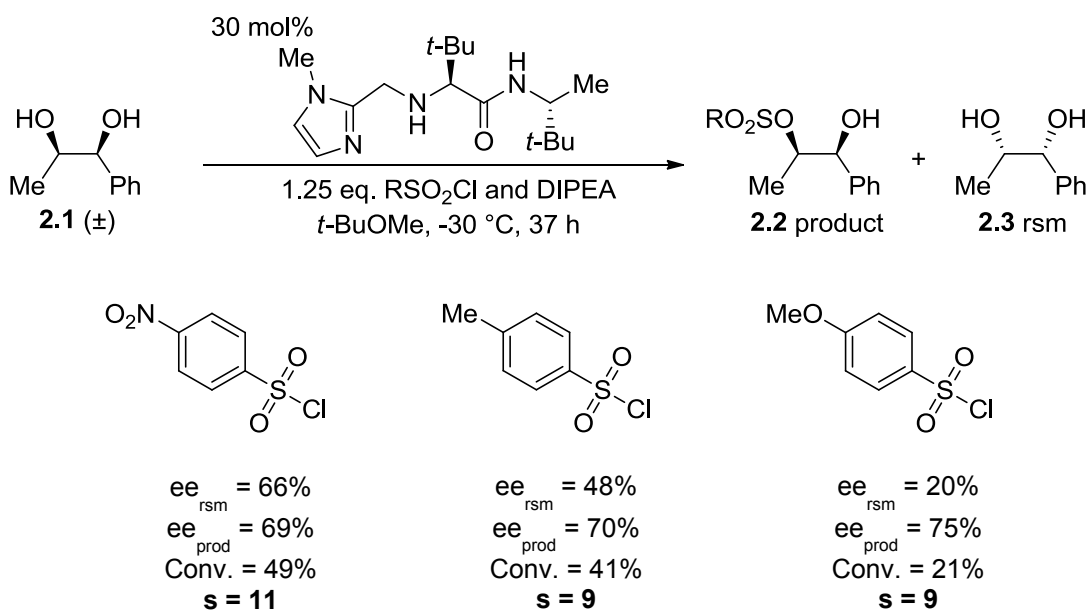
Entry	Solvent	ee _{rsm}	ee _{product}	Conv.	S
1	THF	6%	70%	8%	6
2	PhCH ₃	76%	74%	51%	15
3	diethyl ether	84%	76%	53%	19
4	<i>t</i> -BuOMe	74%	76%	49%	16
5	1:1 diethyl ether: <i>t</i> -BuOMe	86%	73%	54%	17

2.2.3 Sulfonylation reagent screening

Although the kinetic resolution of asymmetric diols by tosylation is already a valuable synthetic method, we didn't want this reaction to be limited to one type of sulfonylation. Previously, Fengqi Wen and Dr. You had shown that the Hoveyda-Snapper desymmetrization catalyst can catalyze the enantioselective activation of *meso*-diols using NsCl and *p*-methoxybenzenesulfonyl chloride as electrophiles. Thus, we predicted that the kinetic resolution of racemic diol **2.1** using NsCl and *p*-methoxybenzenesulfonyl chloride was possible as well. We went on to test this hypothesis and the results are shown in Table 2.4. The conversion was dependent on the reactivity of the electrophile. NsCl, which is more reactive than TsCl due to the electron withdrawing nitro group, led to 49% conversion; *p*-methoxybenzenesulfonyl chloride,

which is less reactive than TsCl due the electron donating methoxy group, led to 21% conversion. On the other hand, the difference in selectivity for all electrophiles tested was negligible ($s = 9-11$), proving that our catalyst can utilize different sulfonyl chlorides in resolving asymmetric diols.

Table 2.4 Sulfonyl Chloride Screening



2.2.4 Substrate scope

Using the optimal reaction conditions, we proceeded to expand the substrate scope of the kinetic resolution by sulfonylation reaction. Each substrate was reacted with 30 mol% catalyst, 1.25 equivalents of TsCl and DIPEA, in the presence of $t\text{-BuOMe}$ as solvent at $-30\text{ }^\circ\text{C}$ for an appropriate period of time. The results, which include secondary-secondary 1,2-diols and one example of a secondary-secondary 1,3-diol, are shown in Table 2.5. While the substrate scope is relatively wide, the majority of the selectivities are moderate. Our best substrate is diol **2.4** with an s value of 15 (Entry 1, Table 2.5).

Table 2.5 Substrate Scope

Entry	Substrate	Time	rsm Yield; ee	product Yield; ee	s
1	 2.4	60 h	41%; 70%	38% [*] ; 76%	15
2	 2.7	12 h	44%; 80%	47%; 60%	10
3	 2.8	48 h	38%; 68%	43%; 64%	9
4	 2.1	48 h	52%; 38%	34%; 68%	8
5	 2.9	48 h	28%; 88%	67%; 32%	5
6	 2.10	72 h	62%; 16%	28%; 68%	6
7	 2.11	12 h	22%; 84%	64%; 46%	7
8	 2.12	16 h	27%; 50%	51%; 36%	3
9	 2.13	12 h	12%; 50%	60%; 32%	3

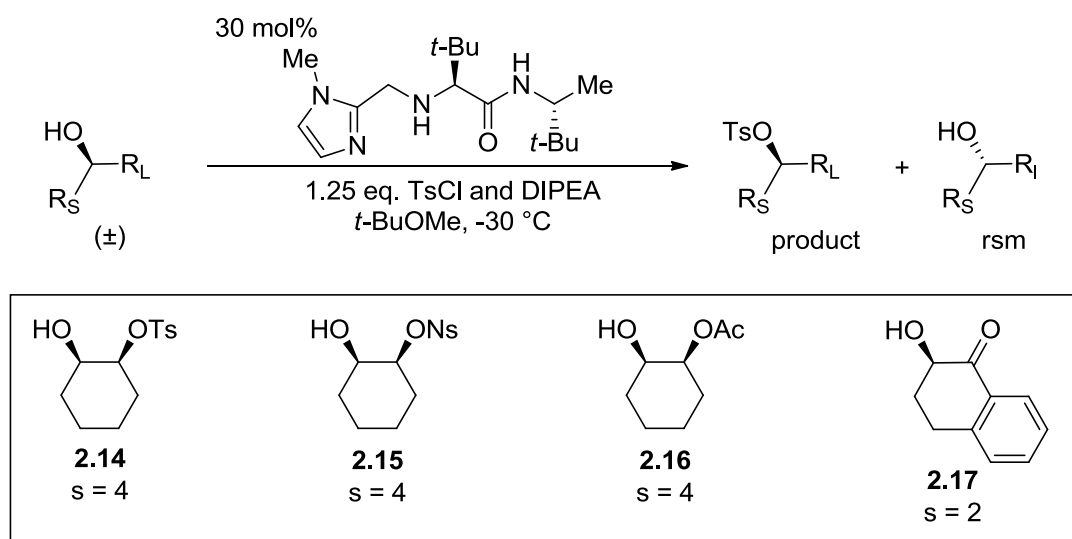
^{*}Minor sulfonyl ester isomer was isolated in 4% yield.

Interestingly, we encountered a problem with this substrate that we did not encounter with any other substrates: the minor formation of unexpected mono-tosylate. Fortunately, however, the production of bis-tosylate was negligible for all substrates. Entries 2-5 indicate that most cyclic and acyclic *syn*-1,2-diols are moderate substrates for the kinetic resolution by tosylation reaction ($s = 5-10$). Entry 6 is an example of an acyclic *syn*-1,3-diol that can be resolved by this method ($s = 6$), proving that the catalyst is not confined to 1,2-diols. Entries 7-9 reveal that primary-secondary and primary-tertiary 1,2-diols can also be resolved by enantioselective tosylation, albeit with poor to moderate selectivities ($s = 3-7$), which can be attributed to the greater freedom of rotation that a primary alcohol has over a more sterically hindered alcohol.

The Hoveyda-Snapper desymmetrization catalyst works best with diols, most likely because multiple hydrogen-bonding interactions are required in order for a substrate-catalyst complex to form; thus, we were surprised by the catalyst's ability to resolve mono-alcohols by tosylation. As previously stated, a secondary kinetic resolution is responsible for the production of bis-tosylate during our enantioselective tosylation reaction. When a racemic mixture of mono-tosylated diol **2.14** was subjected to the enantioselective tosylation conditions, the mono-tosylate was kinetically resolved (Scheme 2.4). Although the selectivity for this reaction was poor ($s = 4$), we were intrigued by the fact that the mono-tosylate could form a complex with the catalyst and we wondered if other mono-alcohols would perform the same way.

Not surprisingly, a racemic mixture of mono-nosylated diol **2.15** was resolved with the same selectivity as the mono-tosylate ($s = 4$). We hypothesize that the oxygens

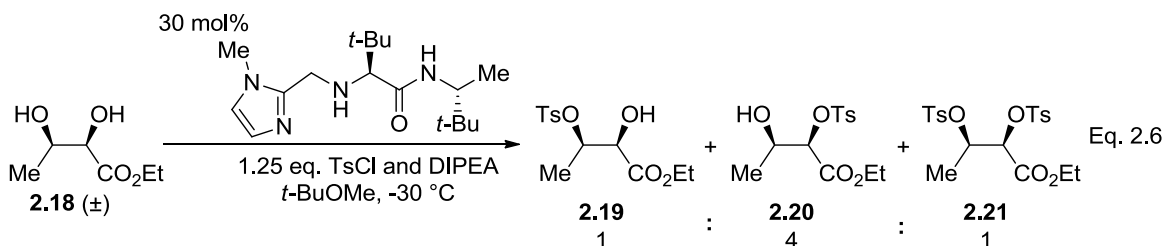
from the polarized S=O bonds on the substrate can hydrogen-bond with the catalyst and promote the formation of a substrate-catalyst complex. Likewise, the oxygen from the C=O bond on mono-acylated diol **2.16** can serve as a hydrogen-bond acceptor and interact with a hydrogen-bond donor on the catalyst. Substrate **2.16** was resolved with the same selectivity as both mono-sulfonates ($s = 4$). We then tested α -hydroxy-ketone **2.17**, which, unfortunately, exhibited the lowest selectivity ($s = 2$). This may be due to the substrate's conformation, which doesn't allow the carbonyl group and hydroxyl group to simultaneously hydrogen-bond to the catalyst.



Scheme 2.4 Mono-alcohol substrates

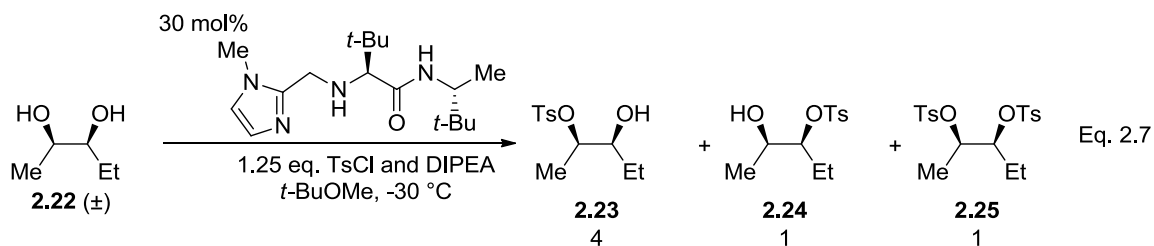
The catalyst's limitations in regard to kinetic resolution by tosylation include ester-containing substrates such as **2.18** (Eq. 2.6). When asymmetric diol **2.18** is subjected to the reaction conditions, the result is a ratio of 1:4:1 of expected mono-tosylate (**2.19**): unexpected mono-tosylate (**2.20**): bis-tosylate (**2.21**). The reason that the majority of the product is unexpected mono-tosylate may be because the ester group on

the substrate hydrogen-bonds with the catalyst in such a way that the tosyl group is delivered to the closest hydroxyl group.



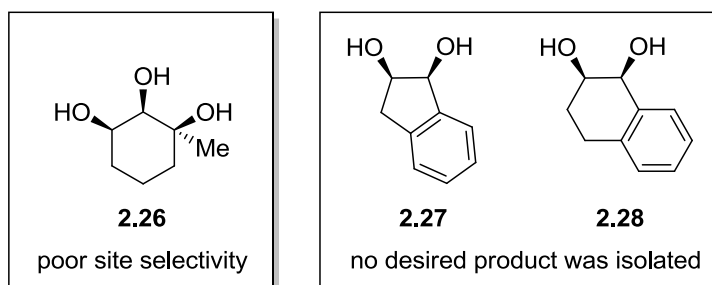
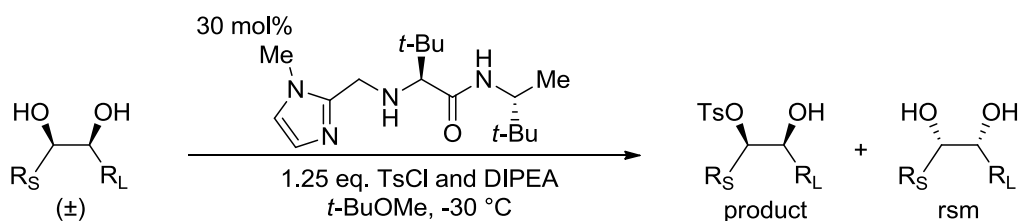
Another unsuccessful substrate is asymmetric diol **2.22** (Eq. 2.7); its ratio of products is 4:1:1 of expected mono-tosylate (**2.23**): unexpected mono-tosylate (**2.24**): bis-tosylate (**2.25**). The explanation for this ratio is the negligible size difference between a methyl group and an ethyl group. One of the ways to determine the size difference between two groups is to compare their “A values”, or the difference in Gibbs free energy (ΔG) between the higher energy conformation (axial substitution) and the lower energy conformation (equatorial substitution) of a mono-substituted cyclohexane ring. The A values for methyl and ethyl are 1.70 and 1.75²⁶, respectively. Such a small steric difference makes it difficult for the catalyst to discriminate between the two groups. The reason that this is not an issue for silylation may be because a *tert*-butyldimethylsilyl (TBS) group is larger a tosyl (Ts) group. The size of the group being transferred to the substrate may play a role in the energy barriers of the transition states leading to the expected and unexpected products.

²⁶ Hirsch, J. A. *Topics in Stereochemistry*. **1967**, 3, 199-222.



Asymmetric triol **2.26** is another substrate that challenges the catalyst's site selectivity (Scheme 2.5). The problem with asymmetric triols is that there are three possible combinations of diols that can dictate product formation. Moreover, the mono-protected product of a triol is a diol, which can undergo further protection. Both of these challenges lead to poor site-selectivity.

Other substrates that the catalyst cannot resolve by tosylation are asymmetric diols **2.27** and **2.28** (Scheme 2.5). Surprisingly, when these two substrates were reacted with the catalyst and TsCl, no desired product was isolated. It's possible that in each case, the mono-tosylate was produced, but it decomposed into the corresponding epoxide, a consequence of the free hydroxyl group nucleophilically attacking the tosylated carbon.



Scheme 2.5 Unsuccessful substrates

In conclusion, we have developed a method of kinetic resolution of diols and functionalized mono-alcohols by catalytic enantioselective sulfonylation. While the substrate scope is relatively wide, the majority of the selectivities are moderate. This method is useful because it produces enantioenriched alcohols and sulfonates that are difficult or impossible to synthesize otherwise. Furthermore, it is practical, economical, safe, and the substrates are easy to make through *syn*-dihydroxylation of their corresponding *cis*-alkenes, most of which are commercially available.

2.3 Experimental and Supporting Information

General Information

Infrared (**IR**) spectra were recorded on a Perkin Elmer 781 spectrophotometer, ν_{\max} in cm^{-1} . Bands are characterized as broad (br), strong (s), medium (m), and weak (w). ^1H NMR spectra were recorded on a Varian GN-400 (400 MHz) and a Varian Inova-500 (500 MHz). Chemical shifts are reported in ppm with the solvent reference as the internal standard (CHCl_3 : δ 7.26). Data are reported as follows: chemical shift, integration, multiplicity (s = singlet, d = doublet, t = triplet, q = quartet, m = multiplet, br = broad), and coupling constants (Hz). ^{13}C NMR spectra were recorded on a Varian GN-400 (100 MHz) and a Varian Inova-500 (125 MHz) with complete proton coupling. Chemical shifts are reported in ppm with the solvent reference as the internal standard (CHCl_3 : δ 77.23). Melting points (**MP**) were taken with a Laboratory Device Melt-Temp and were uncorrected. **Enantiomeric ratios** were determined by analytical liquid chromatography (HPLC) and chiral gas liquid chromatography (GLC). **Optical rotations** were measured on a Rudolph Research Analytical Autopol IV Automatic Polarimeter. High resolution mass spectrometry (**HRMS**) was performed at the mass spectrometry facility at Boston College.

All reactions were conducted under an open atmosphere in 10 x 75 mm test tubes. All commercially available reagents other than tosyl chloride (TsCl) were used directly for the reaction without any further purification. Liquid reagents were handled with a Gilson Pipetman. Solvents other than *tert*-butylmethyl ether (*t*-BuOMe) were dried on alumina columns using a solvent dispensing system. Tosyl chloride was purchased from Aldrich and was purified from CHCl_3 /hexanes (1:5). *tert*-Butylmethyl ether was purchased from Aldrich and was used without distillation. Diisopropylethylamine (DIPEA) and 3,3-dimethylbutane-1,2-diol were purchased from Aldrich. 1-Methylcyclohexane-1,2-diol, 2,3,3-trimethylbutane-1,2-diol, and 2,3-

dimethylbutane-1,2-diol were synthesized by *cis*-dihydroxylation of the corresponding commercially available *cis*-alkenes.²⁷ 1,1-Diethoxybutane-2,3-diol and 1-phenylpropane-1,2-diol were synthesized by Lindlar reduction of the corresponding commercially available alkynes followed by *cis*-dihydroxylation. 4,4-Dimethylpentane-2,3-diol and 1-cyclohexylpropane-1,2-diol were synthesized by *cis*-dihydroxylation of the corresponding *cis*-alkenes (synthesized by Wittig olefination of the corresponding commercially available aldehydes). 1-Phenylbutane-1,3-diol was synthesized by the sodium borohydride reduction of the corresponding β -hydroxyketone (synthesized by Aldol reaction of commercially available acetophenone and acetaldehyde). The catalyst was synthesized according to literature procedure.²⁸

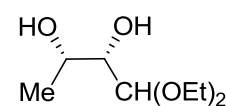
General procedure for the kinetic resolution of syn-diols by catalytic enantioselective sulfonylation

The catalyst (9.0 mg, 0.030 mmol) and the diol substrate (0.10 mmol) were weighed into a 10 x 75 mm test tube. DIPEA (22 μ L, 0.13 mmol) was added with a Gilson Pipetman. The contents were dissolved in *t*-BuOMe (180 μ L), the tube was capped with a rubber septum, and the mixture was cooled to -78 °C. TsCl (19 mg, 0.10 mmol) was dissolved in *t*-BuOMe (200 μ L) and added to the test tube with a Gilson Pipetman. The test tube was capped with a rubber septum, wrapped with Teflon tape and the mixture was allowed to stir at -30 °C in a cryocool apparatus for the reported period of time. The reaction was quenched by the addition of methanol (25 μ L). The mixture was allowed to warm to 22 °C and directly purified by silica gel chromatography. The product and unreacted starting material were analyzed by chiral GLC or HPLC.

²⁷ Donohoe, T. J., et al. *Org. Biomol. Chem.* **2003**, *1*, 2173-2186.

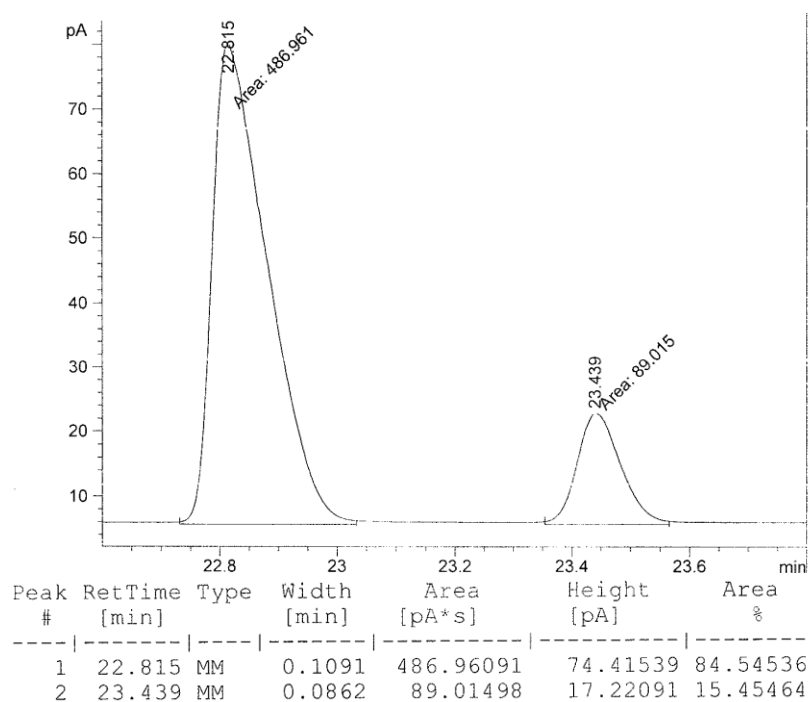
²⁸ Zhao, Y.; Rodrigo, J.; Hoveyda, A. H.; Snapper, M. L. *Nature.* **2006**, *443*, 67-70.

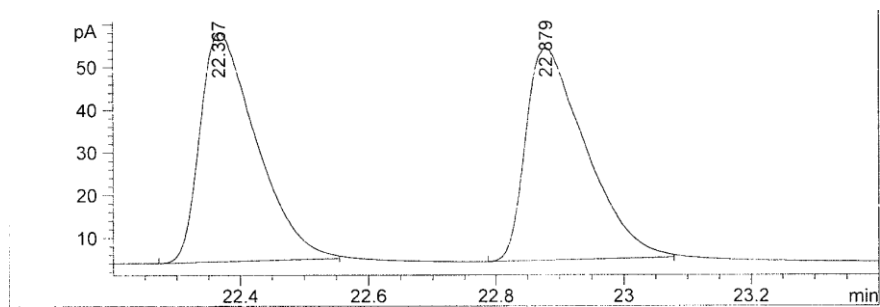
(2S,3S)-1,1-diethoxybutane-2,3-diol


IR (neat, thin film): 3421 (br), 2975 (w), 2930 (w), 1375 (w), 1121 (m), 1056 (s), 995 (m). **¹H NMR** (CDCl₃, 400 MHz); δ 4.48 (1 H, d, *J* = 5.6 Hz), 3.86 (1 H, qd, *J* = 6.2, 6.4 Hz), 3.76 (2 H, m), 3.59 (2 H, m), 3.45 (1 H, dd, *J* = 8.6, 5.6 Hz), 2.77 (1 H, br), 2.35 (1 H, d, *J* = 3.2 Hz), 1.22 (9 H, m). **¹³C NMR** (CDCl₃, 400 MHz); δ 103.5, 74.1, 68.0, 63.6, 63.5, 18.5, 15.4, 15.2. **HRMS** (*m/z* + NH₄): Calculated: 196.155; Found: 196.155.

Optical Rotation: $[\alpha]_D^{25}$ -10 (*c* = 1.0, CHCl₃).

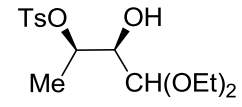
Optical purity was established by chiral GLC analysis (Supelco Beta Dex 120 (30 m x 0.15 mm x 0.25 μm), 80-140 °C at 2 °C/min, 25 psi.); chromatograms are illustrated below for a 70 % ee sample:



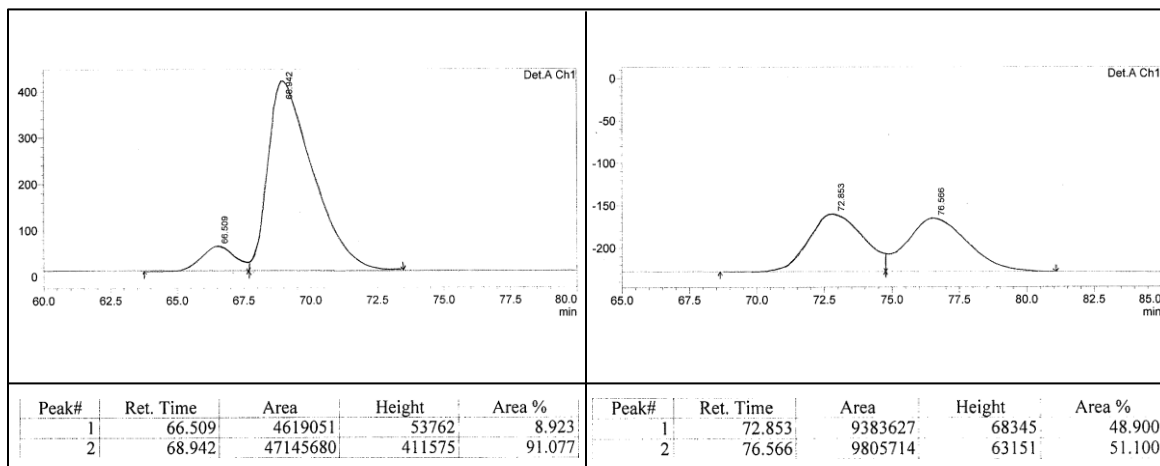


Peak #	RetTime [min]	Type	Width [min]	Area [pA*s]	Height [pA]	Area %
1	22.367	PB	0.0895	329.66263	53.79398	50.42191
2	22.879	PB	0.0951	324.14560	49.69032	49.57809

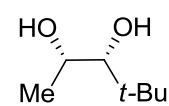
(2R,3R)-4,4-diethoxy-3-hydroxybutan-2-yl 4-methylbenzenesulfonate


IR (neat, thin film): 3540 (br), 2977 (w), 2927 (w), 1357 (m), 1189 (m), 1177 (s), 1060 (m), 919 (m), 904 (m), 556 (m). **¹H NMR** (CDCl₃, 400 MHz); δ 7.78 (2 H, d, *J* = 4.0 Hz), 7.32 (2 H, d, *J* = 4.0 Hz), 4.74 (1 H, qd, *J* = 6.4, 4.0 Hz), 4.34 (1 H, d, *J* = 5.2 Hz), 3.70 (2 H, m), 3.61 (1 H, m), 3.49 (2 H, m), 2.43 (3 H, s), 2.31 (1 H, d, *J* = 4.8 Hz), 1.26 (3 H, d, *J* = 6.8 Hz), 1.18 (6 H, q, *J* = 6.8 Hz). **¹³C NMR** (CDCl₃, 400 MHz); δ 144.6, 134.3, 129.7, 127.8, 101.2, 79.3, 73.2, 63.7, 62.8, 21.6, 15.6, 15.2. **HRMS** (*m/z* + NH₄): Calculated: 350.164; Found: 350.163. **Optical Rotation**: [α]_D²⁵ -1.0 (*c* = 1.0, CHCl₃).

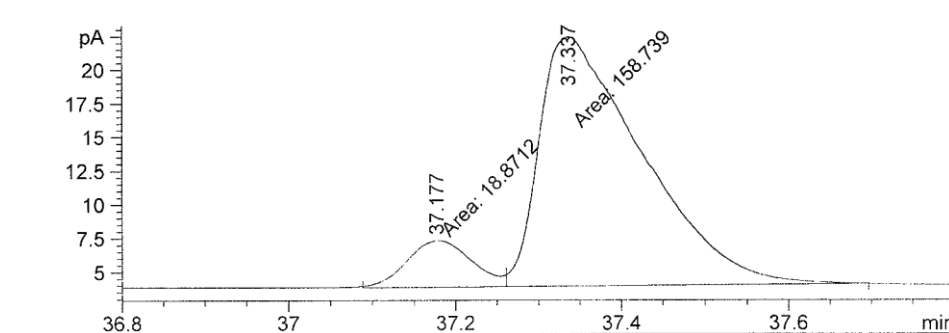
Optical purity was established by HPLC analysis (Chiralpak OD-H column (25 cm x 0.46 cm), 95/5 hexanes/*i*-PrOH, 0.5 mL/min, 220 nm); chromatograms are illustrated below for a 82 % ee sample:



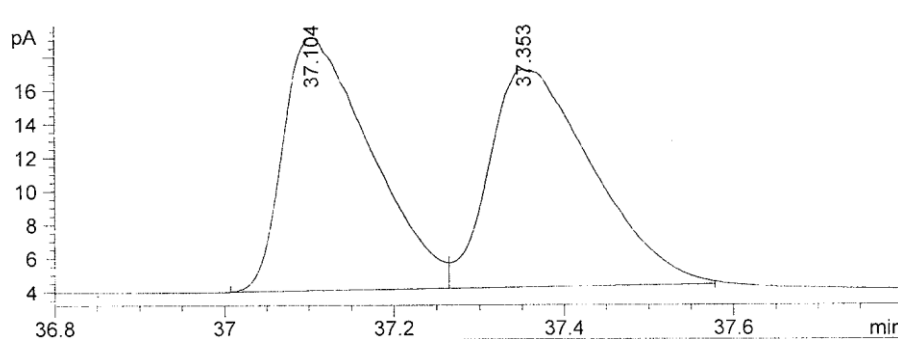
(2S,3R)-4,4-dimethylpentane-2,3-diol


¹H NMR (CDCl₃, 400 MHz); δ 3.93 (1 H, m), 3.37 (1 H, t, *J* = 3.6 Hz), 2.15 (1 H, br), 1.90 (1 H, br), 1.21 (3 H, d, *J* = 6.4 Hz), 0.95 (9 H, s). ¹³C NMR (CDCl₃, 400 MHz); δ 85.2, 71.1, 36.7, 29.3, 21.0. **Optical Rotation:** [α]_D²⁵ -16 (*c* = 0.50, CHCl₃).

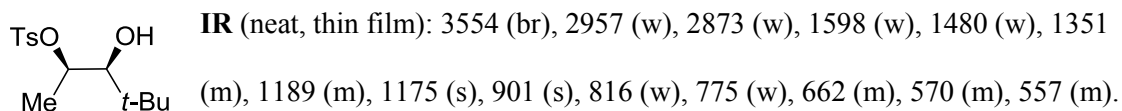
Optical purity was established by chiral GLC analysis (Supelco Beta Dex 120 (30 m x 0.15 mm x 0.25 μm), 80 °C for 20 min, 2 °C/min to 140 °C, 25 psi.); chromatograms are illustrated below for a 78 % ee sample:



Peak #	RetTime [min]	Type	Width [min]	Area [pA*s]	Height [pA]	Area %
1	37.177	MF	0.0907	18.87118	3.46918	10.62505
2	37.337	FM	0.1430	158.73907	18.49880	89.37495

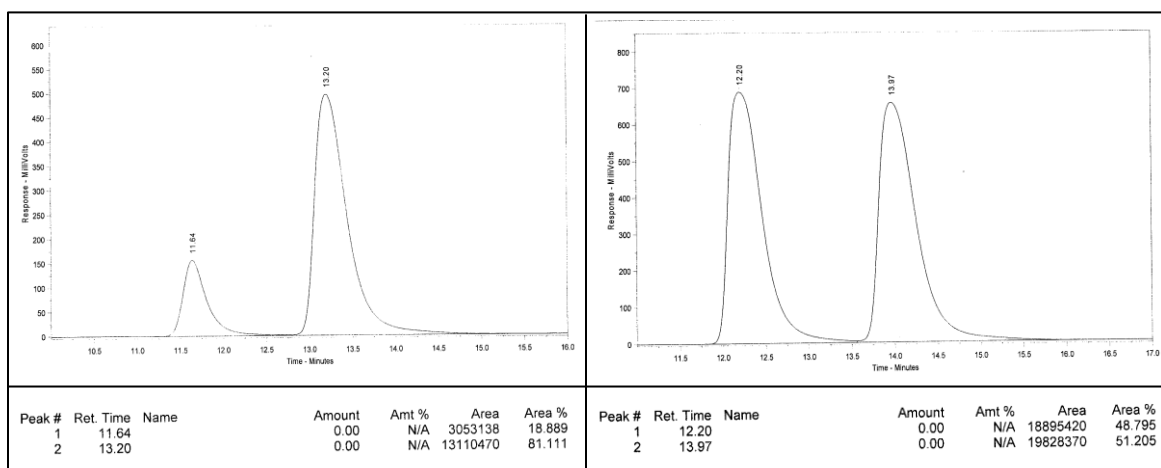


Peak #	RetTime [min]	Type	Width [min]	Area [pA*s]	Height [pA]	Area %
1	37.104	PV	0.0980	108.49735	15.07702	49.55098
2	37.353	VB	0.1226	110.46371	12.93288	50.44902

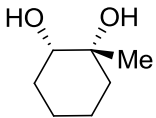
(2R,3S)-3-hydroxy-4,4-dimethylpentan-2-yl 4-methylbenzenesulfonate

¹H NMR (CDCl₃, 400 MHz); δ 7.76 (2 H, d, *J* = 8.4 Hz), 7.31 (2 H, d, *J* = 8.4 Hz), 4.76 (1 H, qd, *J* = 6.4, 2.0 Hz), 3.49 (1 H, d, *J* = 2.0 Hz), 2.42 (3 H, s), 2.00 (1 H, s), 1.24 (3 H, d, *J* = 6.4 Hz), 0.85 (9 H, s). **¹³C NMR** (CDCl₃, 400 MHz); δ 147.4, 137.0, 132.5, 130.4, 84.2, 83.1, 36.8, 29.1, 24.3, 18.4. **HRMS** (*m/z* + NH₄): Calculated: 304.158; Found: 304.159. **Optical Rotation**: [α]_D²⁵ +9.2 (*c* = 1.0, CHCl₃).

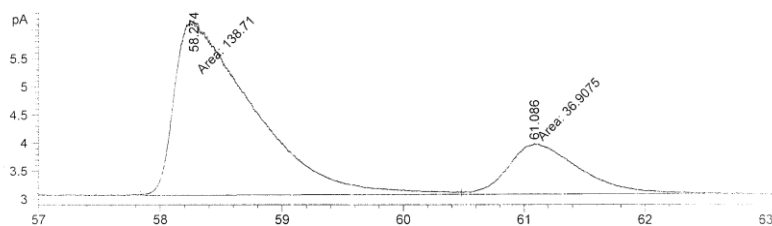
Optical purity was established by HPLC analysis (Chiralpak OJ-H column (25 cm x 0.46 cm), 85/15 hexanes/*i*-PrOH, 0.5 mL/min, 220 nm); chromatograms are illustrated below for a 62 % ee sample:



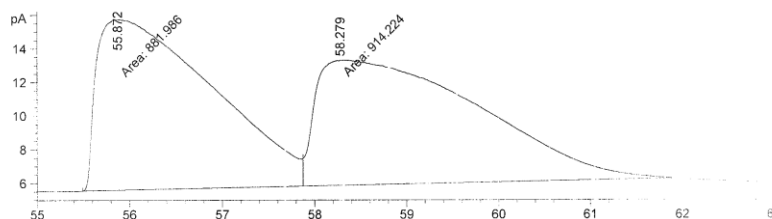
(1R,2S)-1-methylcyclohexane-1,2-diol


mp: 66-68 °C. **IR** (neat, thin film): 3389 (br), 2935 (s), 2862 (m), 1449 (w), 1373 (w), 1164 (w), 1125 (w), 1066 (m), 1045 (m), 1002 (w), 948 (m). **¹H NMR** (CDCl₃, 400 MHz); δ 3.39 (1 H, dd, *J* = 9.0, 4.0 Hz), 2.10 (1 H, br), 1.99 (1 H, br), 1.78-1.24 (8 H, m), 1.25 (3 H, s). **¹³C NMR** (CDCl₃, 400 MHz); δ 74.8, 71.5, 36.8, 30.4, 26.5, 23.1, 21.5. **HRMS** (m/z + NH₄): Calculated: 148.134; Found: 148.134. **Optical Rotation:** [α]_D²⁵ +1.2 (*c* = 1.0, CHCl₃).

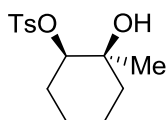
Optical purity was established by chiral GLC analysis (Supelco Beta Dex 120 (30 m x 0.15 mm x 0.25 μm), 90 °C for 90 min, 25 psi.); chromatograms are illustrated below for a 58 % ee sample:



Peak #	RetTime [min]	Type	Width [min]	Area [pA*s]	Height [pA]	Area %
1	58.274	MF	0.7462	138.71016	3.09818	78.98416
2	61.086	FM	0.6782	36.90753	9.06975e-1	21.01584

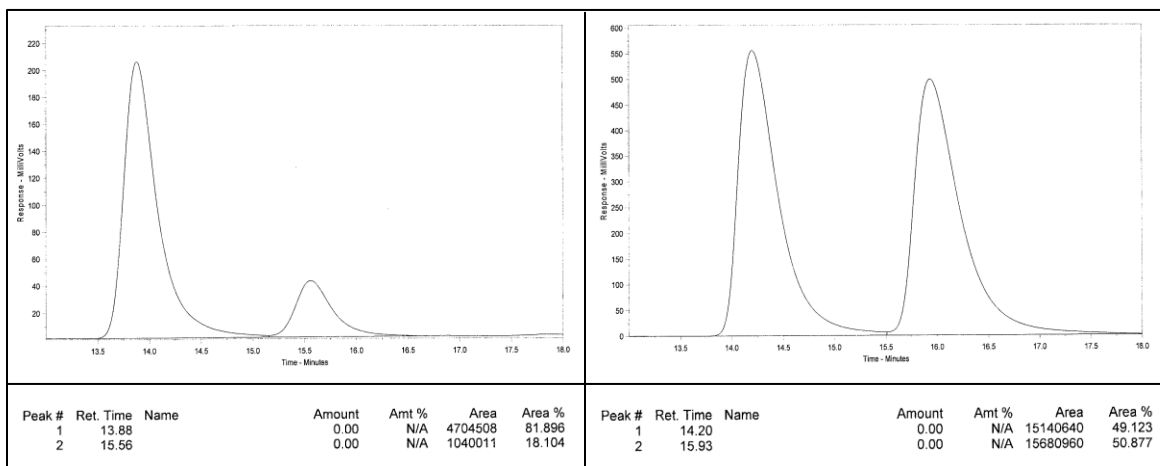


Peak #	RetTime [min]	Type	Width [min]	Area [pA*s]	Height [pA]	Area %
1	55.872	MF	1.4498	881.98572	10.13915	49.10260
2	58.279	FM	2.0471	914.22424	7.44329	50.89740

(1R,2S)-2-hydroxy-2-methylcyclohexyl 4-methylbenzenesulfonate

IR (neat, thin film): 3546 (br), 2938 (m), 2865 (w), 1449 (w), 1359 (m), 1175 (s), 1097 (w), 941 (m), 879 (m), 669 (m). **¹H NMR** (CDCl₃, 400 MHz); δ 7.78 (2 H, d, *J* = 8.4 Hz), 7.32 (2 H, d, *J* = 8.4 Hz), 4.34 (1 H, dd, *J* = 10.2, 4.0 Hz), 2.43 (3 H, s), 1.82-1.25 (9 H, m), 1.11 (3 H, s). **¹³C NMR** (CDCl₃, 400 MHz); δ 144.7, 134.4, 129.8, 127.7, 87.0, 70.6, 37.5, 28.0, 26.9, 23.5, 21.6, 20.7. **HRMS** (m/z + NH₄): Calculated: 302.143; Found: 302.142. **Optical Rotation**: [α]_D²⁵ +1.2 (*c* = 1.0, CHCl₃).

Optical purity was established by HPLC analysis (Chiralpak OJ-H column (25 cm x 0.46 cm), 85/15 hexanes/*i*-PrOH, 0.5 mL/min, 220 nm); chromatograms are illustrated below for a 64 % ee sample:

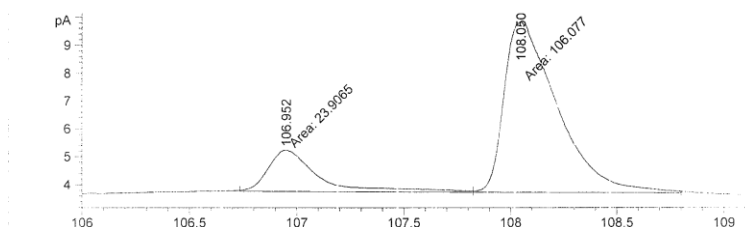


(1R,2S)-1-phenylpropane-1,2-diol

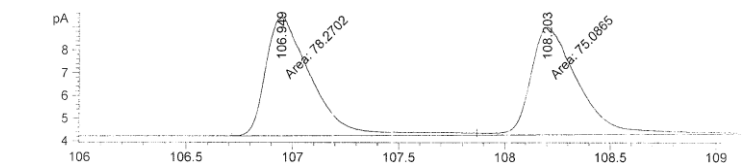
C[C@@H](O)[C@H](O)c1ccccc1 ¹H NMR (CDCl₃, 400 MHz); δ 7.36-7.26 (5 H, m), 4.67 (1 H, d, *J* = 4.4 Hz), 4.00 (1 H, qd, *J* = 6.2, 4.8 Hz), 2.53 (1 H, br), 2.02 (1 H, br), 1.08 (3 H, d, *J* = 6.4 Hz).

¹³C NMR (CDCl₃, 400 MHz); δ 140.3, 128.4, 127.8, 126.6, 77.5, 71.3, 17.3. **Optical Rotation:** [α]_D²⁵ -14 (*c* = 1.0, CHCl₃).

Optical purity was established by chiral GLC analysis (Supelco Beta Dex 120 (30 m x 0.15 mm x 0.25 μm), 100 °C for 98 min, 20 °C/min to 140 °C, hold for 30 min, 25 psi); chromatograms are illustrated below for a 64 % ee sample:

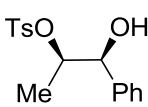


Peak #	RetTime [min]	Type	Width [min]	Area [pA*s]	Height [pA]	Area %
1	106.952	MF	0.2696	23.90651	1.47798	18.39191
2	108.050	FM	0.2888	106.07729	6.12208	81.60809

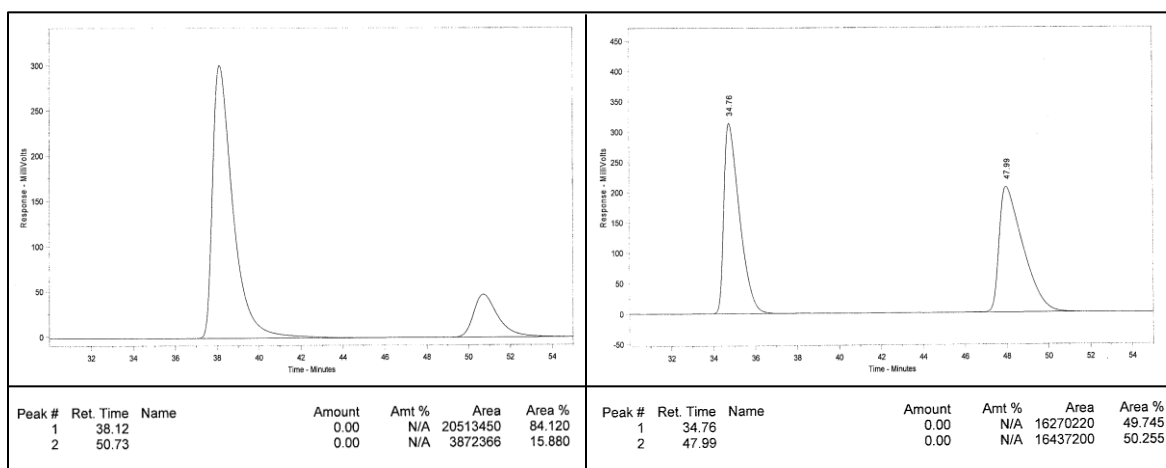


Peak #	RetTime [min]	Sig	Type	Area [pA*s]	Height [pA]	Area %
1	106.949	2	MF	78.27019	5.20102	51.71242
2	108.203	2	FM	75.08647	4.70248	49.60896

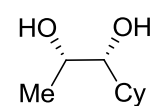
(1S,2R)-1-hydroxy-1-phenylpropan-2-yl 4-methylbenzenesulfonate


IR (neat, thin film): 3533 (br), 3064 (w), 2988 (w), 1354 (m), 1189 (m), 1174 (s), 912 (s), 891 (s), 702 (m), 624 (m), 555 (s). **¹H NMR** (CDCl₃, 400 MHz); δ 7.67 (2 H, d, *J* = 8.4 Hz), 7.24-7.17 (7 H, m), 4.84 (1 H, d, *J* = 3.2 Hz), 4.67 (1 H, qd, *J* = 6.4, 3.6 Hz), 2.37 (3 H, s), 2.08 (1 H, s), 1.08 (3 H, d, *J* = 6.4 Hz). **¹³C NMR** (CDCl₃, 400 MHz); δ 144.7, 138.7, 133.9, 129.8, 128.4, 128.0, 127.7, 126.3, 82.8, 75.3, 21.6, 14.0. **HRMS** (m/z): Calculated: 307.100; Found: 307.100. **Optical Rotation**: [α]_D²⁵ +8.0 (*c* = 1.0, CHCl₃).

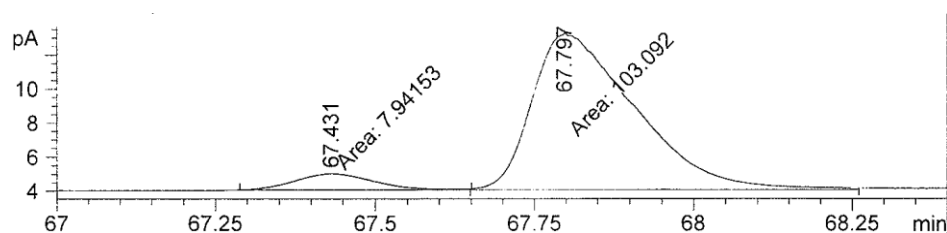
Optical purity was established by HPLC analysis (Chiralpak OJ-H column (25 cm x 0.46 cm), 85/15 hexanes/*i*-PrOH, 0.5 mL/min, 220 nm); chromatograms are illustrated below for a 68 % ee sample:



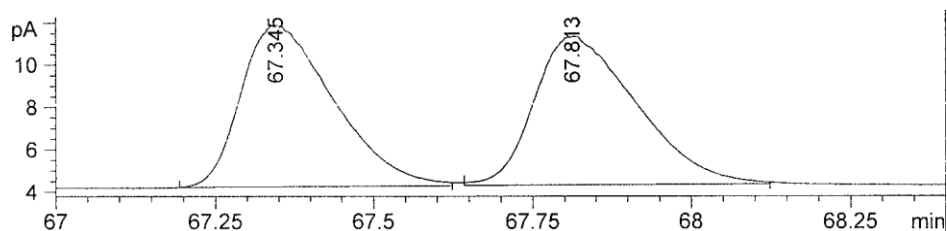
(1R,2S)-1-cyclohexylpropane-1,2-diol


¹H NMR (CDCl₃, 400 MHz); δ 3.90 (1 H, qd, *J* = 6.4, 3.6 Hz), 3.35 (1 H, dd, *J* = 8.2, 3.6 Hz), 2.01 (3 H, m), 1.77-1.65 (3 H, m), 1.55 (1 H, d, *J* = 11.2 Hz), 1.43-1.18 (4 H, m), 1.15 (3 H, d, *J* = 6.4 Hz), 1.00 (2 H, qd, *J* = 12.2, 2.4 Hz). ¹³C NMR (CDCl₃, 400 MHz); δ 78.9, 68.0, 40.0, 29.3, 28.7, 26.3, 25.9, 25.7, 16.0. **Optical Rotation:** [α]_D²⁵ +1.4 (*c* = 1.0, CHCl₃).

Optical purity was established by chiral GLC analysis (Supelco Beta Dex 120 (30 m x 0.15 mm x 0.25 μm), 110 °C for 60 min, 20 °C/min to 140 °C, 25 psi.); chromatograms are illustrated below for a 86 % ee sample:

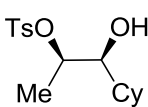


Peak #	RetTime [min]	Sig	Type	Area [pA*s]	Height [pA]	Area %
1	67.431	2	MM	7.94153	9.55845e-1	7.15239
2	67.797	2	MM	103.09164	9.18635	92.84761

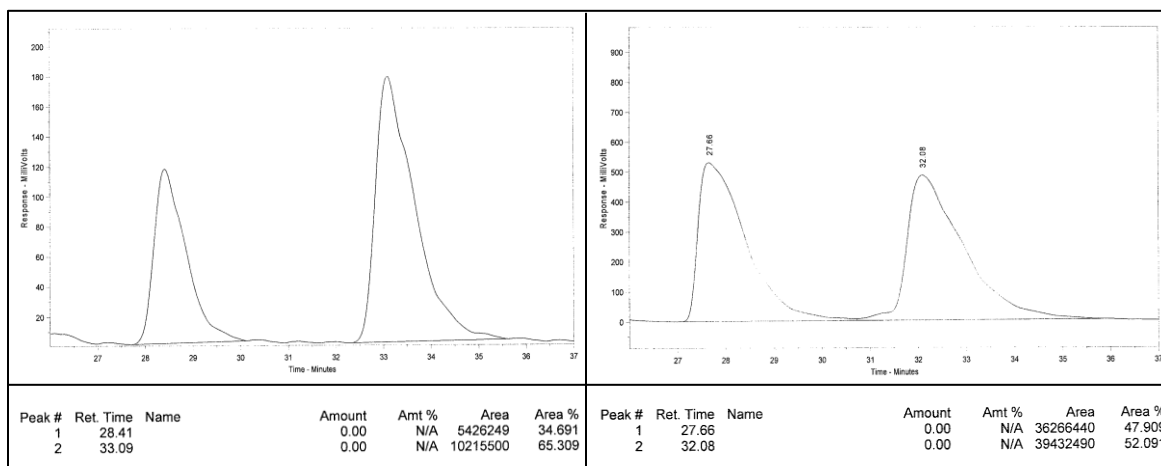


Peak #	RetTime [min]	Sig	Type	Area [pA*s]	Height [pA]	Area %
1	67.345	2	BB	78.17459	7.66125	49.77829
2	67.813	2	BB	78.87097	7.00274	50.22171

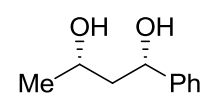
(1S,2R)-1-cyclohexyl-1-hydroxypropan-2-yl 4-methylbenzenesulfonate


IR (neat, thin film): 3537 (w), 2926 (m), 2853 (w), 1357 (m), 1189 (m), 1176 (s), 913 (s), 895 (m), 679 (w), 664 (w), 556 (m). **¹H NMR** (CDCl₃, 400 MHz); δ 7.76 (2 H, d, *J* = 8.4 Hz), 7.31 (2 H, d, *J* = 8.4 Hz), 4.67 (1 H, qd, *J* = 6.4, 3.6 Hz), 3.44 (1 H, m), 2.42 (3 H, s), 2.01 (1 H, s), 1.87 (1 H, *J* = 12.8 Hz), 1.66-1.59 (3 H, m), 1.41 (1 H, *J* = 14.0 Hz), 1.27-1.08 (7 H, m), 0.97-0.86 (2 H, m). **¹³C NMR** (CDCl₃, 400 MHz); δ 147.4, 136.8, 132.5, 130.3, 83.6, 42.0, 31.4, 31.3, 28.8, 28.4, 28.2, 24.3, 16.6. **HRMS** (m/z): Calculated: 313.147; Found: 313.147. **Optical Rotation**: [α]_D²⁵ +2.4 (*c* = 1.0, CHCl₃).

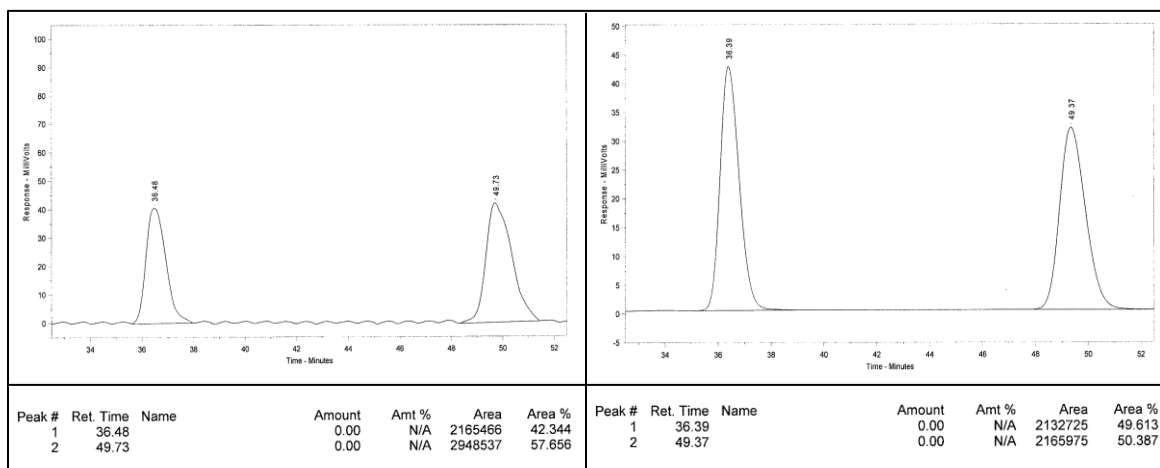
Optical purity was established by HPLC analysis (Chiralpak OJ-H column (25 cm x 0.46 cm), 95/5 hexanes/*i*-PrOH, 0.5 mL/min, 220 nm); chromatograms are illustrated below for a 30 % ee sample:



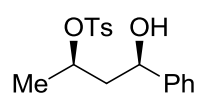
(1S,3S)-1-phenylbutane-1,3-diol


 $^1\text{H NMR}$ (CDCl_3 , 400 MHz); δ 7.36-7.32 (4 H, m), 7.29-7.25 (1 H, m), 4.92 (1 H, dd, $J = 10.2, 2.8$ Hz), 4.13 (1 H, m), 3.78 (1 H, br), 3.16 (1 H, br), 1.83 (1 H, dt, $J = 14.4, 10.0$ Hz), 1.73 (1 H, ddd, $J = 14.6, 2.8, 2.4$ Hz), 1.21 (3 H, d, $J = 6.0$ Hz). $^{13}\text{C NMR}$ (CDCl_3 , 400 MHz); δ 144.4, 128.5, 127.6, 125.6, 75.3, 68.8, 47.0, 24.1. **Optical Rotation:** $[\alpha]_{\text{D}}^{25} -8.6$ ($c = 1.0, \text{CHCl}_3$).

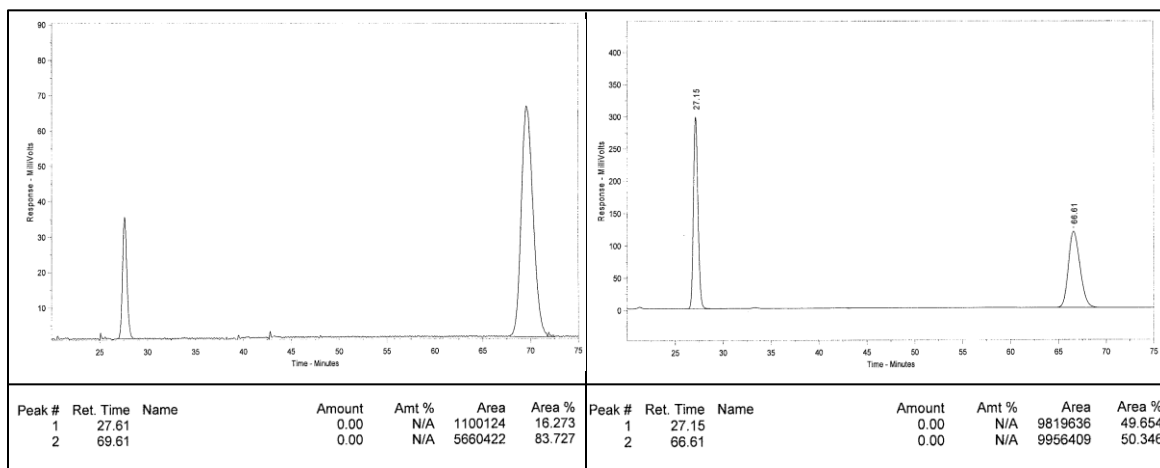
Optical purity was established by HPLC analysis (Chiralpak OD-H column (25 cm x 0.46 cm), 95/5 hexanes/*i*-PrOH, 0.5 mL/min, 220 nm); chromatograms are illustrated below for a 16 % ee sample:

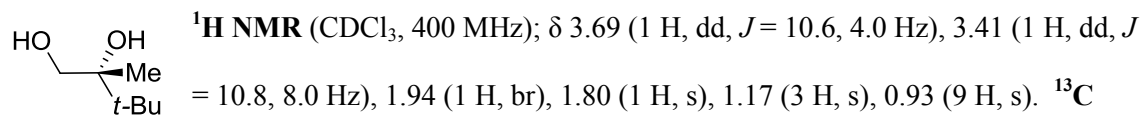


(2R,4R)-4-hydroxy-4-phenylbutan-2-yl 4-methylbenzenesulfonate


IR (neat, thin film): 3532 (br), 2924 (w), 2853 (w), 1355 (m), 1188 (m), 1173 (s), 913 (s), 887 (s), 701 (m), 665 (m), 555 (s). **¹H NMR** (CDCl₃, 400 MHz); δ 7.78 (2 H, d, *J* = 8.4 Hz), 7.33-7.23 (7 H, m), 4.74 (2 H, m), 2.44 (3 H, s), 2.19 (1 H, m), 1.87 (2 H, m), 1.31 (3 H, d, *J* = 6.4 Hz). **¹³C NMR** (CDCl₃, 400 MHz); δ 144.5, 143.5, 134.4, 129.8, 128.6, 128.0, 127.7, 125.9, 78.2, 71.3, 45.5, 21.6, 21.0. **HRMS** (*m/z* + NH₄): Calculated: 338.143; Found: 338.144. **Optical Rotation**: [α]_D²⁵ +25 (*c* = 1.0, CHCl₃).

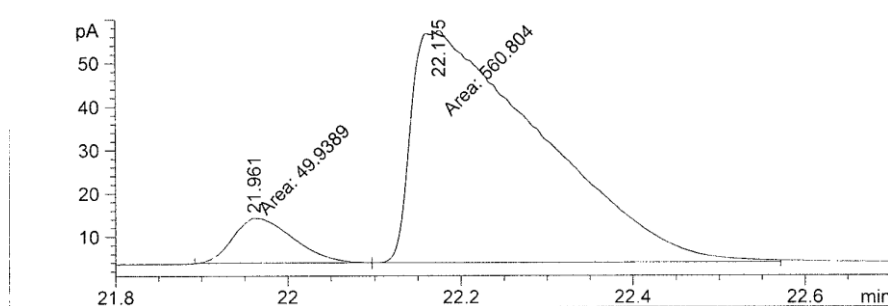
Optical purity was established by HPLC analysis (Chiralpak AD-H column (25 cm x 0.46 cm), 85/15 hexanes/*i*-PrOH, 0.5 mL/min, 220 nm); chromatograms are illustrated below for a 68 % ee sample:



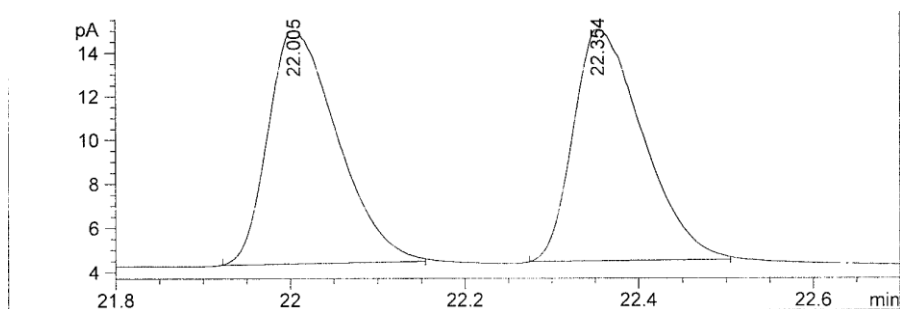
(R)-2,3,3-trimethylbutane-1,2-diol

NMR (CDCl_3 , 400 MHz); δ 76.4, 66.0, 36.4, 25.3, 19.6. **Optical Rotation:** $[\alpha]_D^{25} +8.0$ ($c = 0.33$, CHCl_3).

Optical purity was established by chiral GLC analysis (Supelco Beta Dex 120 (30 m x 0.15 mm x 0.25 μm), 80-140 $^\circ\text{C}$ at 2 $^\circ\text{C}/\text{min}$, 25 psi.); chromatograms are illustrated below for a 84 % ee sample:

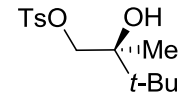


Peak #	RetTime [min]	Type	Width [min]	Area [pA*s]	Height [pA]	Area %
1	21.961	MF	0.0805	49.93894	10.33961	8.17676
2	22.175	FM	0.1748	560.80353	53.47699	91.82324

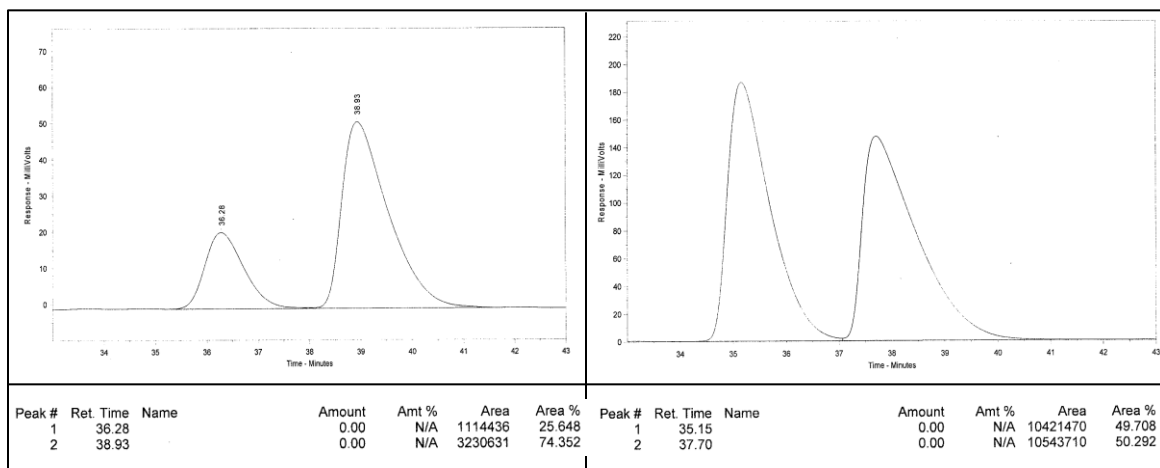


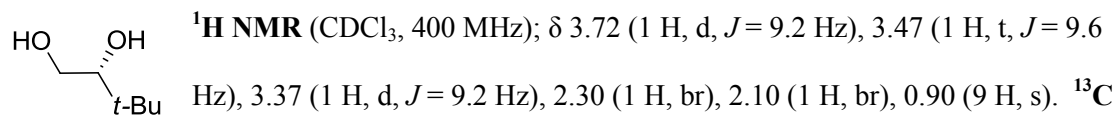
Peak #	RetTime [min]	Type	Width [min]	Area [pA*s]	Height [pA]	Area %
1	22.005	BB	0.0829	58.86150	10.58558	50.18229
2	22.354	PB	0.0778	58.43385	10.51898	49.81771

(S)-2-hydroxy-2,3,3-trimethylbutyl 4-methylbenzenesulfonate


IR (neat, thin film): 3545 (br), 2959 (w), 2877 (w), 1357 (m), 1189 (m), 1175 (s), 1097 (w), 975 (s), 841 (m), 814 (m), 665 (m), 556 (m). **¹H NMR** (CDCl₃, 400 MHz); δ 7.78 (2 H, d, *J* = 8.4 Hz), 7.34 (2 H, d, *J* = 8.4 Hz), 4.05 (1 H, d, *J* = 9.6 Hz), 3.98 (1 H, d, *J* = 9.6 Hz), 2.44 (3 H, s), 1.67 (1 H, s), 1.45 (1 H, s), 0.90 (9 H, s). **¹³C NMR** (CDCl₃, 400 MHz); δ 147.6, 135.5, 132.6, 130.6, 77.6, 77.2, 39.3, 27.9, 24.3, 22.7. **HRMS** (m/z + NH₄): Calculated: 304.158; Found: 304.158. **Optical Rotation**: [α]_D²⁵ -130 (*c* = 0.50, CHCl₃).

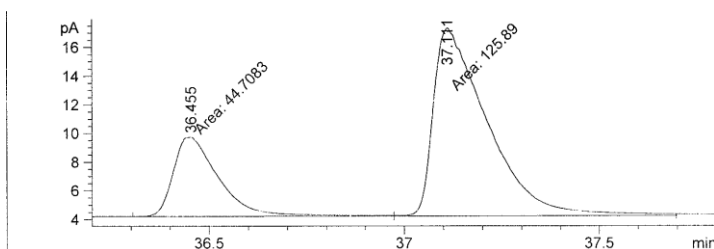
Optical purity was established by HPLC analysis (Chiralpak OD-H column (25 cm x 0.46 cm), 98/2 hexanes/*i*-PrOH, 0.5 mL/min, 220 nm); chromatograms are illustrated below for a 48 % ee sample:



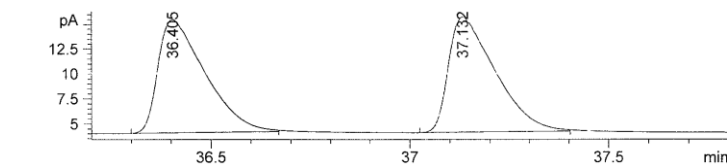
(R)-3,3-dimethylbutane-1,2-diol

NMR (CDCl_3 , 400 MHz); δ 79.7, 63.2, 33.5, 25.8. **Optical Rotation:** $[\alpha]_{\text{D}}^{25} -10$ ($c = 0.50$, CHCl_3).

Optical purity was established by chiral GLC analysis (Supelco Beta Dex 120 (30 m x 0.15 mm x 0.25 μm), 90 $^\circ\text{C}$ for 40 min, 25 psi.); chromatograms are illustrated below for a 48 % ee sample:

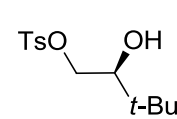


Peak #	RetTime [min]	Type	Width [min]	Area [pA*s]	Height [pA]	Area %
1	36.455	MF	0.1348	44.70827	5.52655	26.20679
2	37.111	MF	0.1601	125.88979	13.10171	73.79321

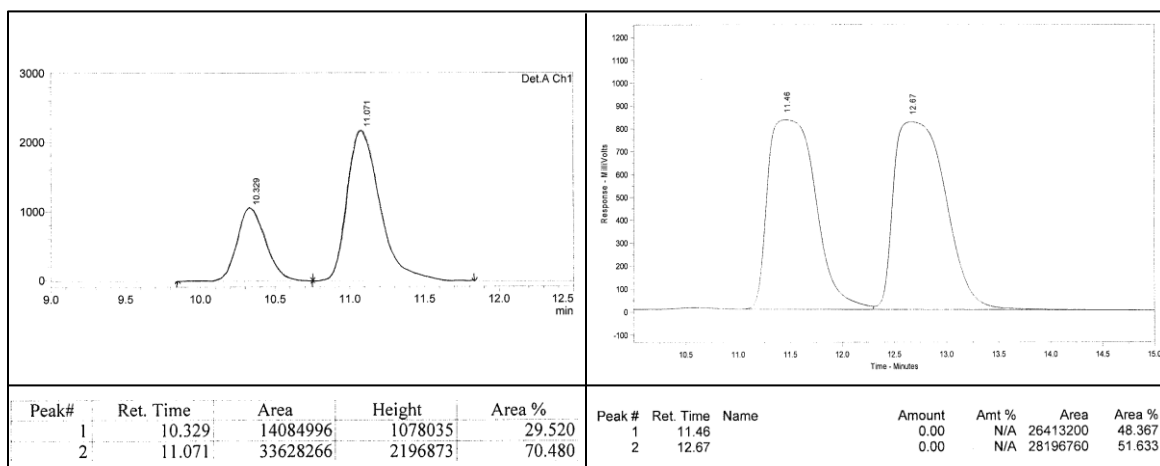


Peak #	RetTime [min]	Sig	Type	Area [pA*s]	Height [pA]	Area %
1	36.405	2	PB	92.97523	11.38344	49.84417
2	37.132	2	PB	93.55659	11.57559	50.15583

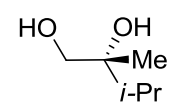
(S)-2-hydroxy-3,3-dimethylbutyl 4-methylbenzenesulfonate


¹H NMR (CDCl₃, 400 MHz); δ 7.77 (2 H, d, *J* = 8.4 Hz), 7.32 (2 H, d, *J* = 8.4 Hz), 4.15 (1 H, dd, *J* = 10.2, 2.0 Hz), 3.85 (1 H, dd, 10.0, 8.8 Hz), 3.49 (1 H, d, *J* = 8.8 Hz), 2.42 (3 H, s), 2.26 (1 H, s), 0.86 (9 H, s). ¹³C NMR (CDCl₃, 400 MHz); δ 147.7, 135.5, 132.6, 130.5, 79.4, 74.9, 36.4, 28.4, 24.3. **Optical Rotation:** [α]_D²⁵ +9.6 (*c* = 1.0, CHCl₃).

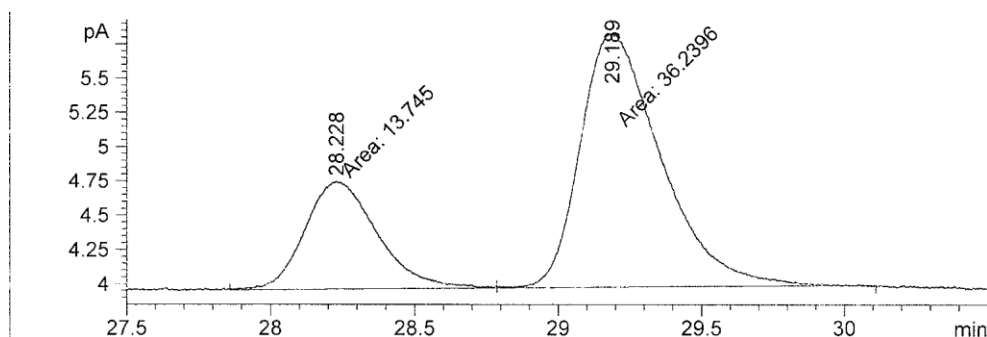
Optical purity was established by HPLC analysis (Chiralpak OD-H column (25 cm x 0.46 cm), 85/15 hexanes/*i*-PrOH, 0.5 mL/min, 220 nm); chromatograms are illustrated below for a 40 % ee sample:



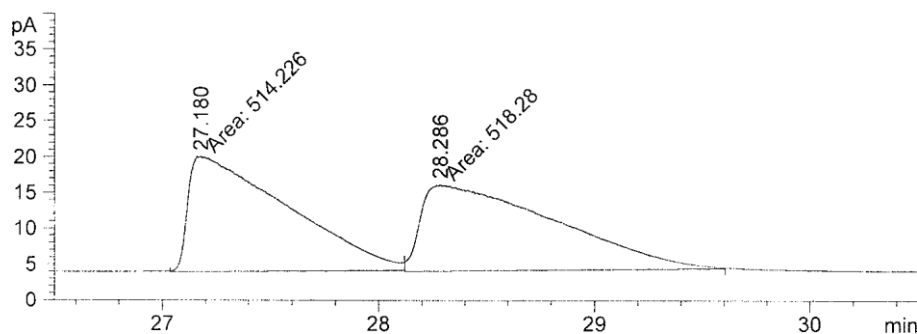
(R)-2,3-dimethylbutane-1,2-diol


 $^1\text{H NMR}$ (CDCl_3 , 400 MHz); δ 3.52 (1 H, d, $J = 10.8$ Hz), 3.40 (1 H, d, $J = 10.8$ Hz), 2.43 (1 H, br), 2.14 (1 H, br), 1.80 (1 H, septet, $J = 6.8$ Hz), 1.03 (3 H, s), 0.93 (3 H, d, $J = 7.2$ Hz), 0.85 (3 H, d, $J = 6.8$ Hz). $^{13}\text{C NMR}$ (CDCl_3 , 400 MHz); δ 75.2, 68.4, 34.2, 18.8, 17.6, 16.6. **Optical Rotation:** $[\alpha]_D^{25} +3.6$ ($c = 0.33$, CHCl_3).

Optical purity was established by chiral GLC analysis (Supelco Beta Dex 120 (30 m x 0.15 mm x 0.25 μm), 90 $^\circ\text{C}$ for 40 min, 25 psi.); chromatograms are illustrated below for a 46 % ee sample:

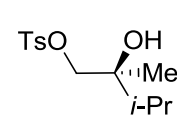


Peak #	RetTime [min]	Type	Width [min]	Area [pA*s]	Height [pA]	Area %
1	28.228	MF	0.2911	13.74498	7.86987e-1	27.49847
2	29.189	FM	0.3248	36.23956	1.85976	72.50153

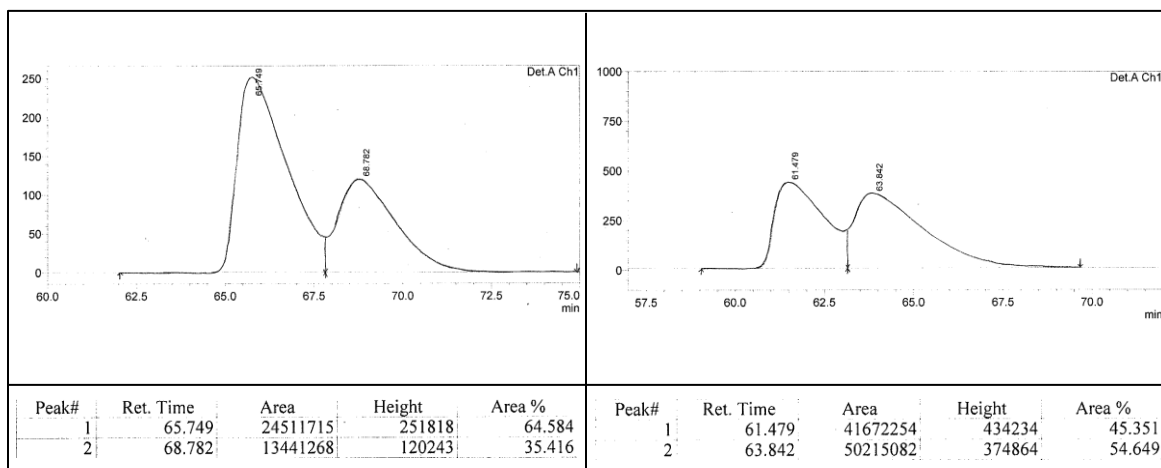


Peak #	RetTime [min]	Type	Width [min]	Area [pA*s]	Height [pA]	Area %
1	27.180	MM	0.5333	514.22601	16.06929	49.80370
2	28.286	MM	0.7161	518.27960	12.06316	50.19630

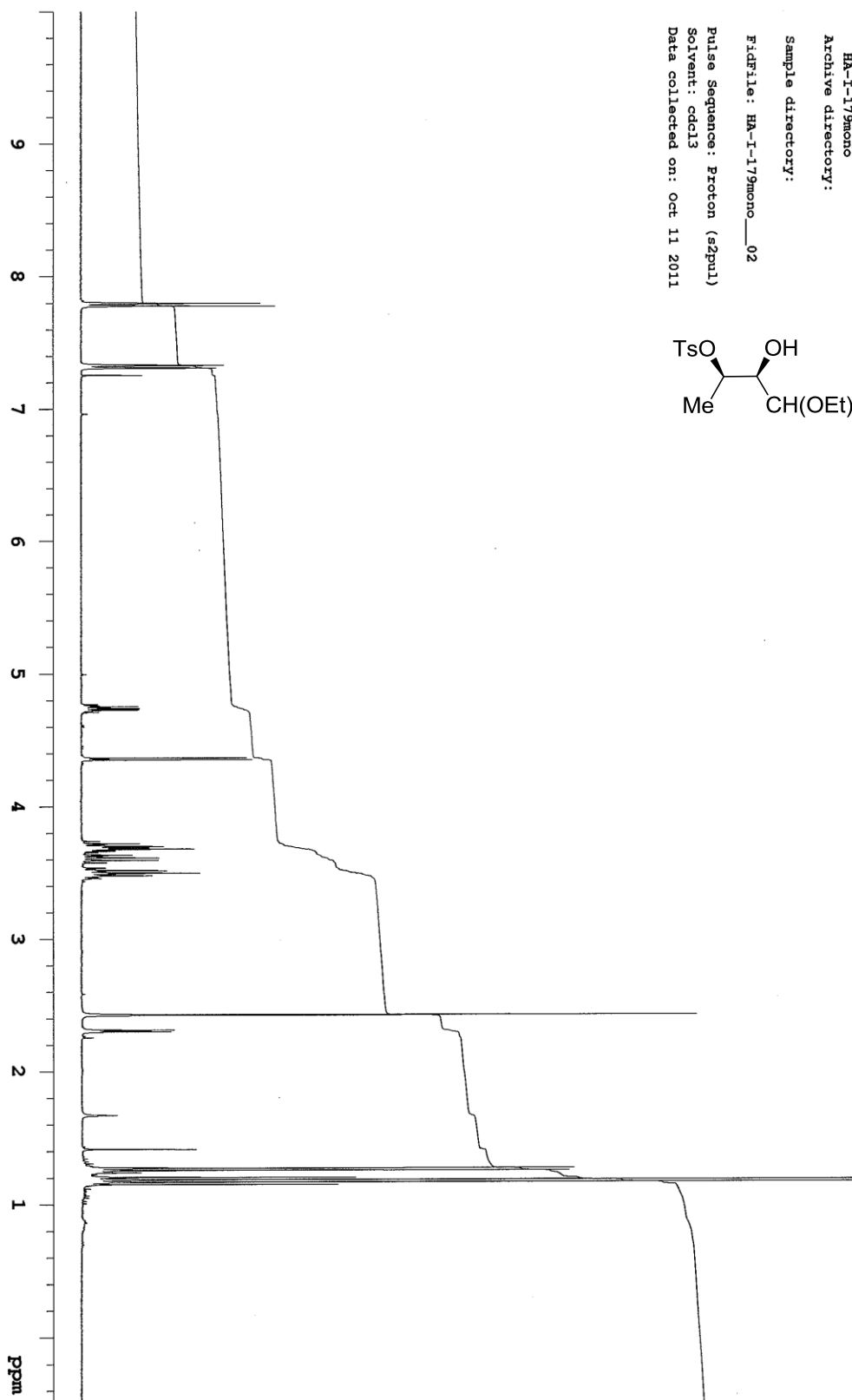
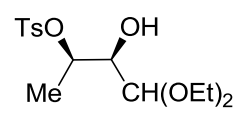
(S)-2-hydroxy-2,3-dimethylbutyl 4-methylbenzenesulfonate


 $^1\text{H NMR}$ (CDCl_3 , 400 MHz); δ 7.78 (2 H, d, $J = 8.4$ Hz), 7.34 (2 H, d, $J = 8.4$ Hz), 3.93 (1 H, d, $J = 9.6$ Hz), 3.86 (1 H, d, $J = 9.6$ Hz), 2.44 (3 H, s), 1.80 (2 H, m), 1.05 (3 H, s), 0.89 (3 H, d, $J = 7.2$), 0.81 (3 H, d, $J = 6.8$ Hz). $^{13}\text{C NMR}$ (CDCl_3 , 400 MHz); δ 147.7, 135.3, 132.6, 130.6, 78.1, 76.3, 36.8, 24.3, 22.0, 20.0, 19.1. **Optical Rotation:** $[\alpha]_D^{25}$ -2.8 ($c = 0.50$, CHCl_3).

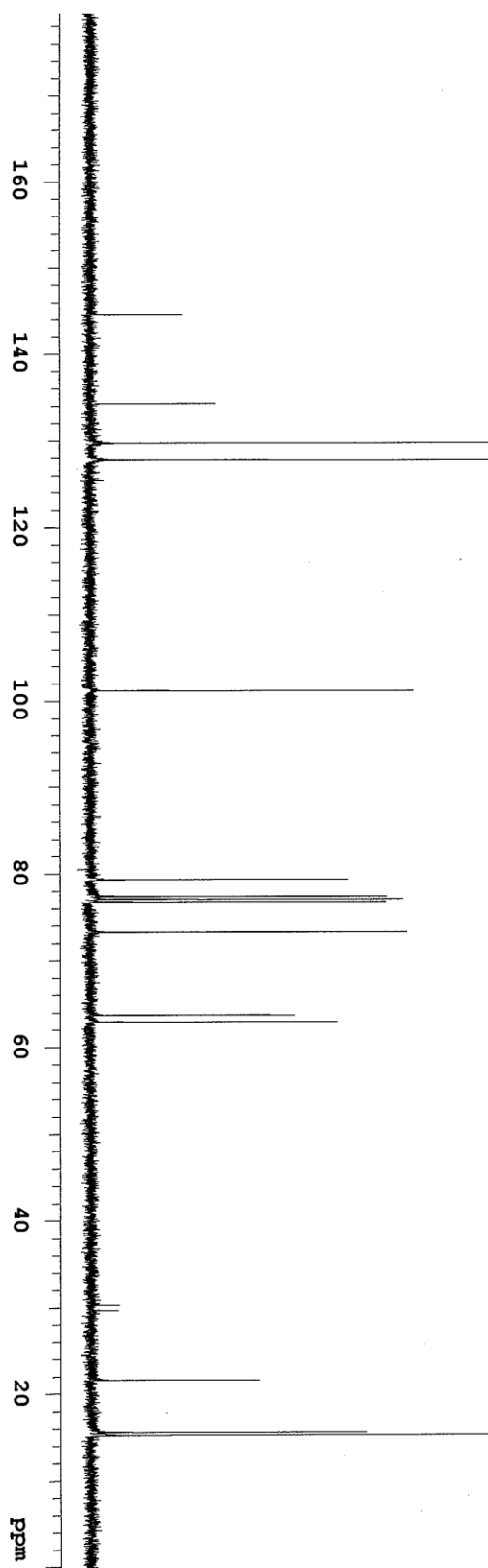
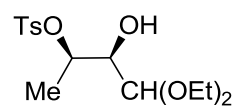
Optical purity was established by HPLC analysis (Chiralpak OD-H column (25 cm x 0.46 cm), 98/1 hexanes/*i*-PrOH, 0.5 mL/min, 220 nm); chromatograms are illustrated below for a 30 % ee sample:



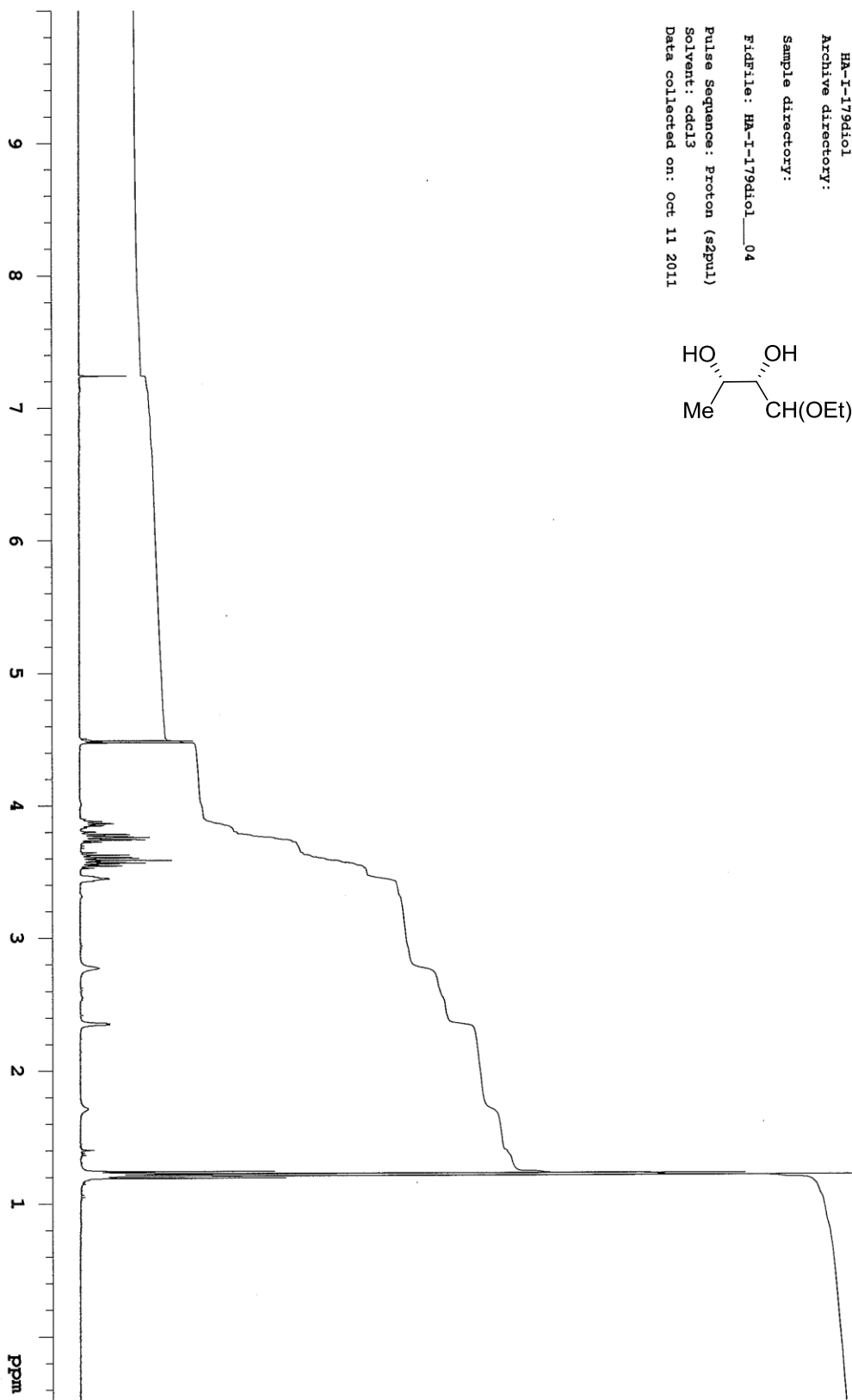
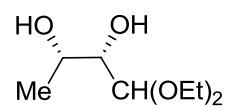
Sample Name:
HA-I-179mono
Archive directory:
Sample directory:
F1dFile: HA-I-179mono__02
Pulse Sequence: Proton (szpul)
Solvent: cdcl3
Data collected on: Oct 11 2011



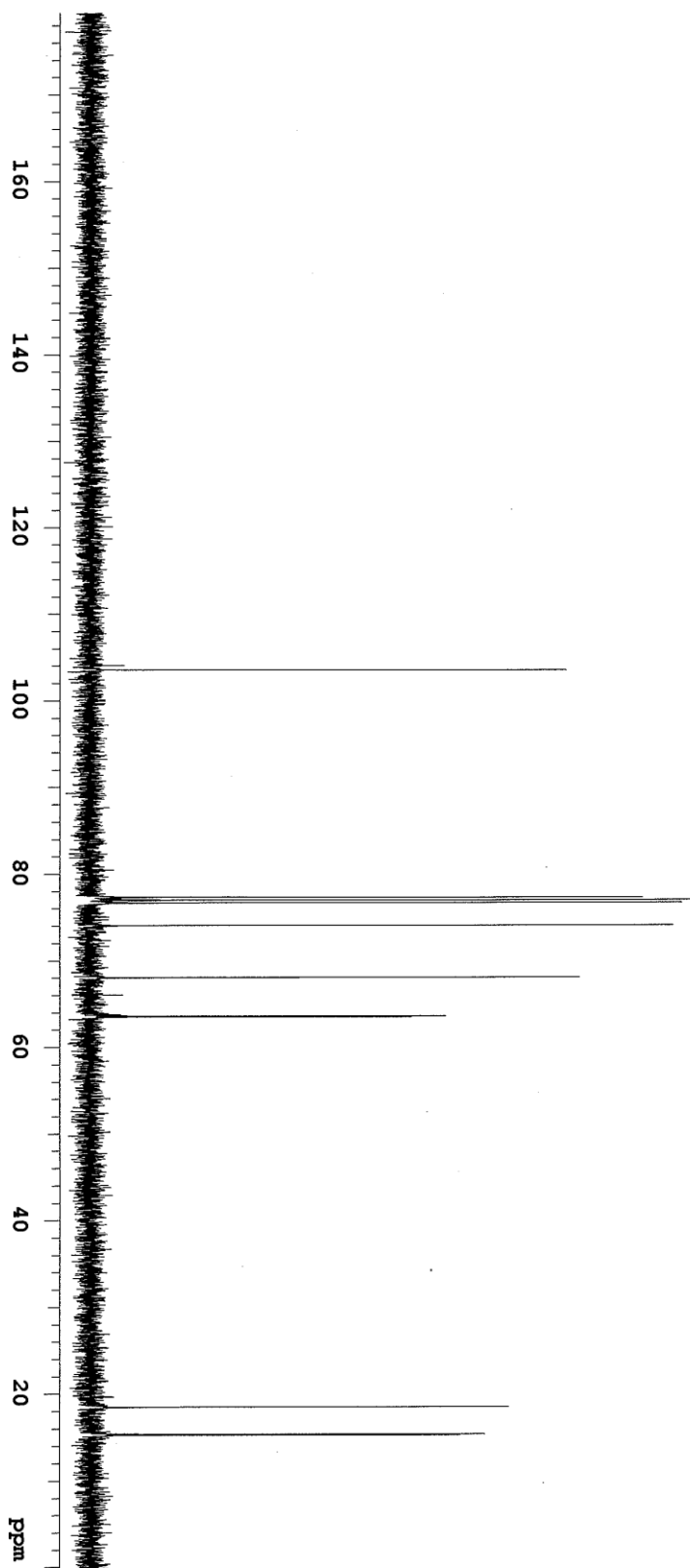
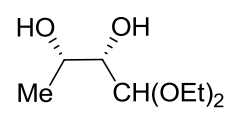
Sample Name:
HA-I-179mono
Archive directory:
Sample directory:
FidFile: HA-I-179mono_03
Pulse Sequence: Carbon (sZpu1)
Solvent: cdcl3
Data collected on: Oct 11 2011



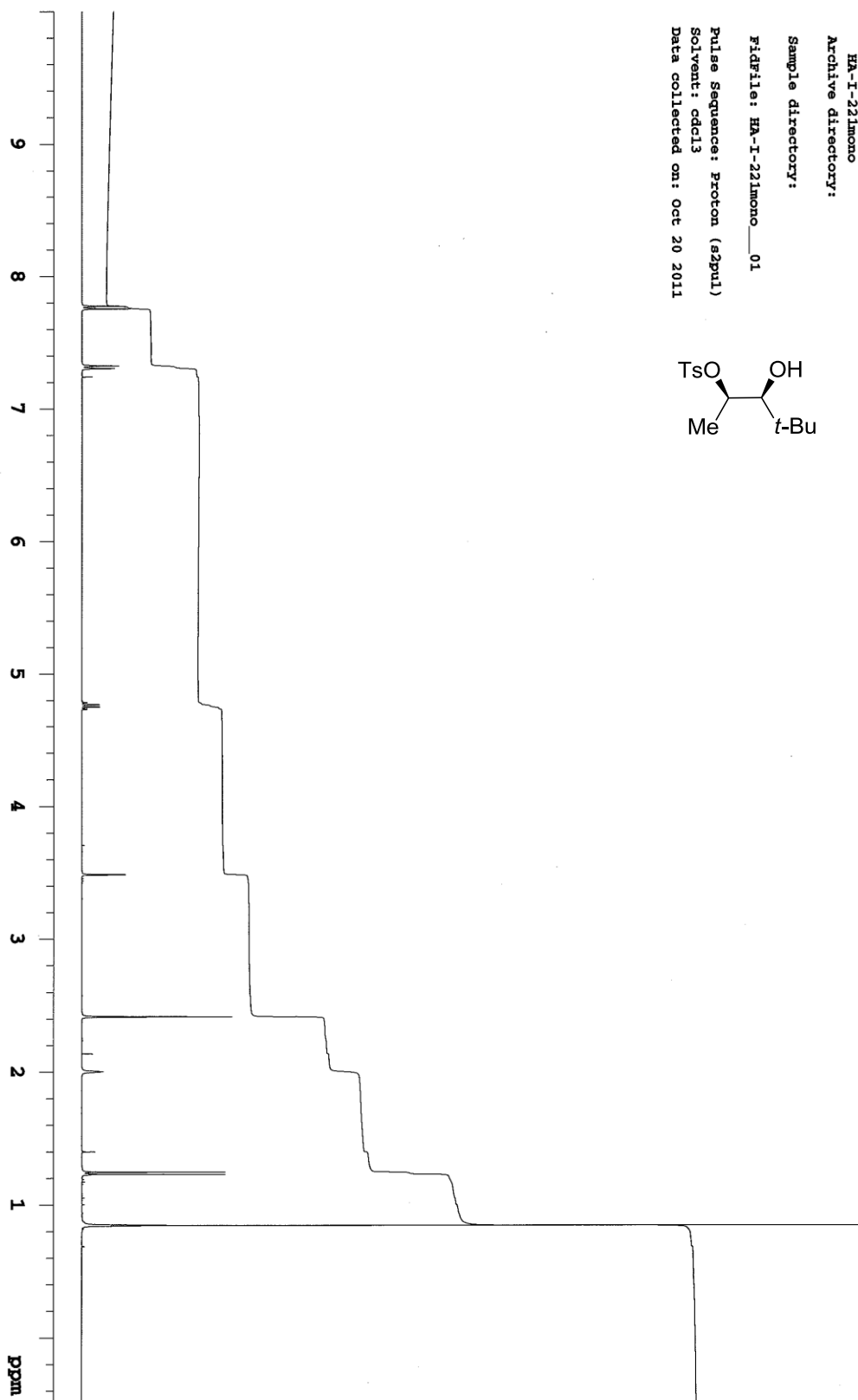
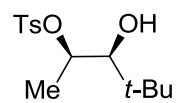
Sample Name:
HA-I-179d101
Archive directory:
Sample directory:
FidFile: HA-I-179d101_04
Pulse Sequence: Proton (s2pul)
Solvent: cdcl3
Data collected on: Oct 11 2011



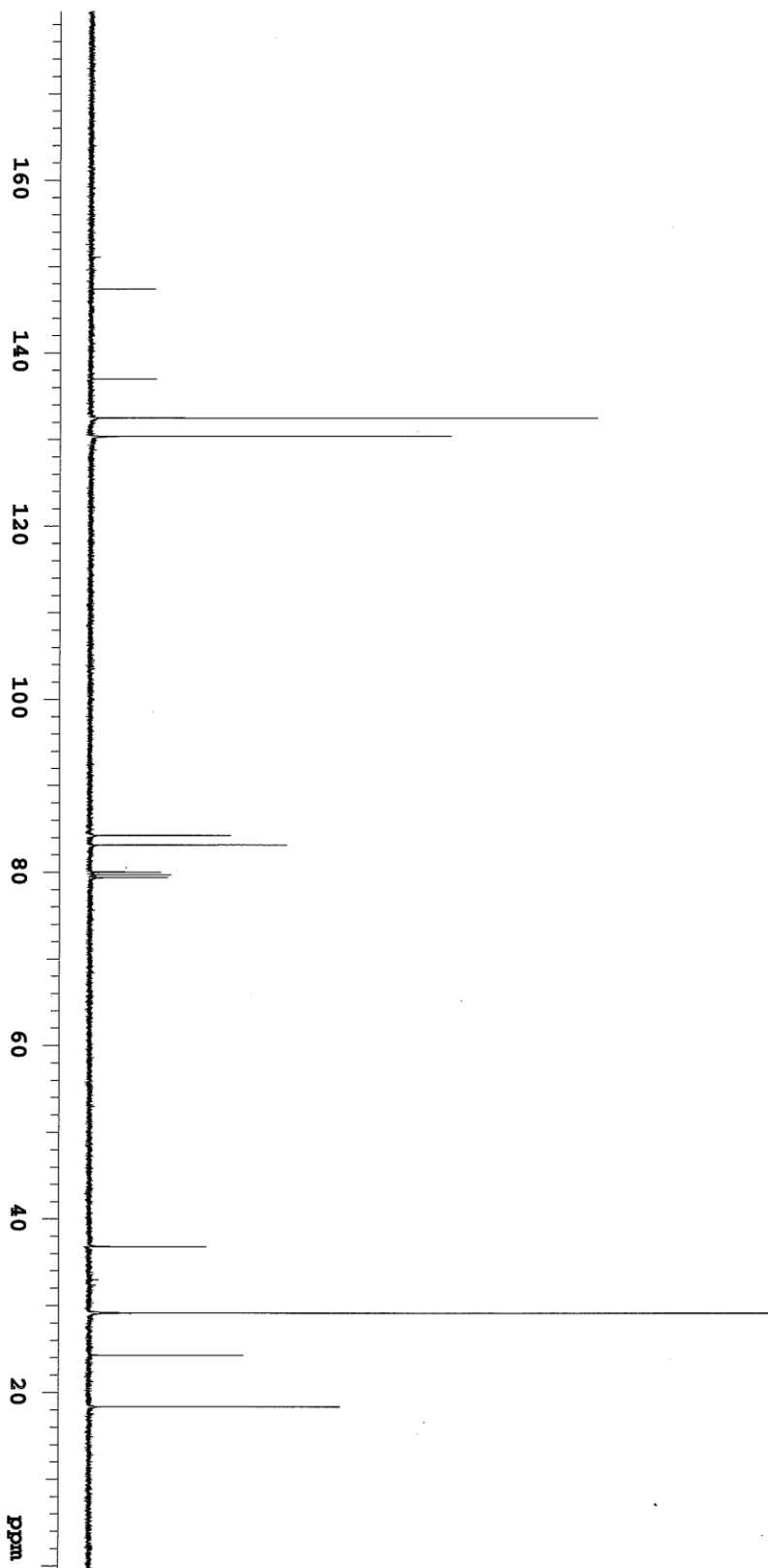
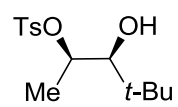
Sample Name: HR-I-179diol
Archive directory:
Sample directory:
FIDFile: HR-I-179diol_05
Pulse Sequence: Carbon (s2pu1)
Solvent: cdcl3
Data collected on: Oct 11 2011



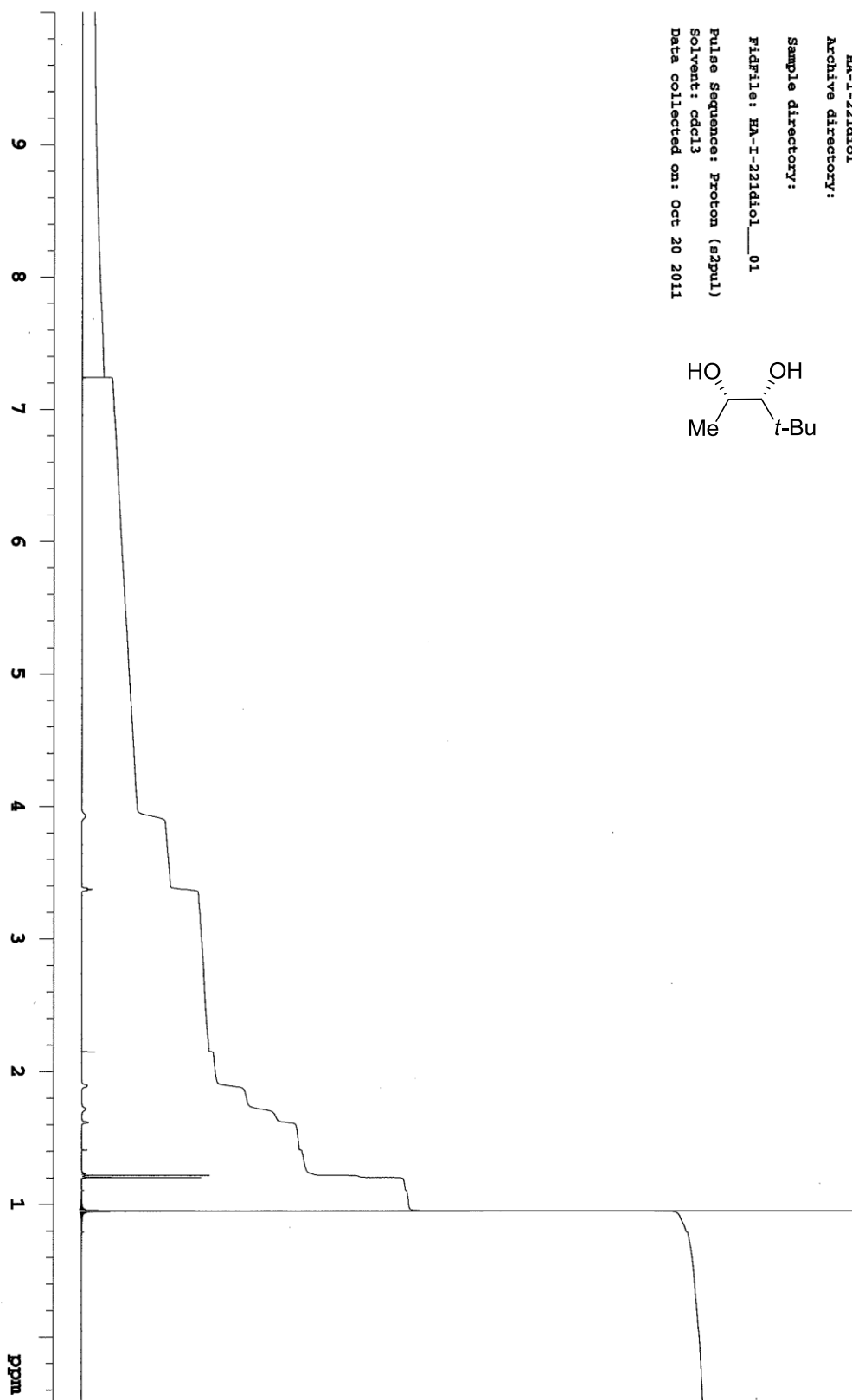
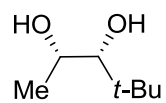
Sample Name:
HA-I-221mono
Archive directory:
Sample directory:
Fidfile: HA-I-221mono_01
Pulse Sequence: Proton (s2pu1)
Solvent: cdcl3
Data collected on: Oct 20 2011



Sample Name:
HA-I-22Imono
Archive directory:
Sample directory:
FidFile: HA-I-22Imono_02
Pulse Sequence: Carbon (s2pu1)
Solvent: cdcl3
Data collected on: Oct 20 2011



Sample Name:
HA-I-221diol
Archive directory:
Sample directory:
Fidfile: HA-I-221diol_01
Pulse Sequence: Proton (s2pu1)
Solvent: cdcl3
Data collected on: Oct 20 2011

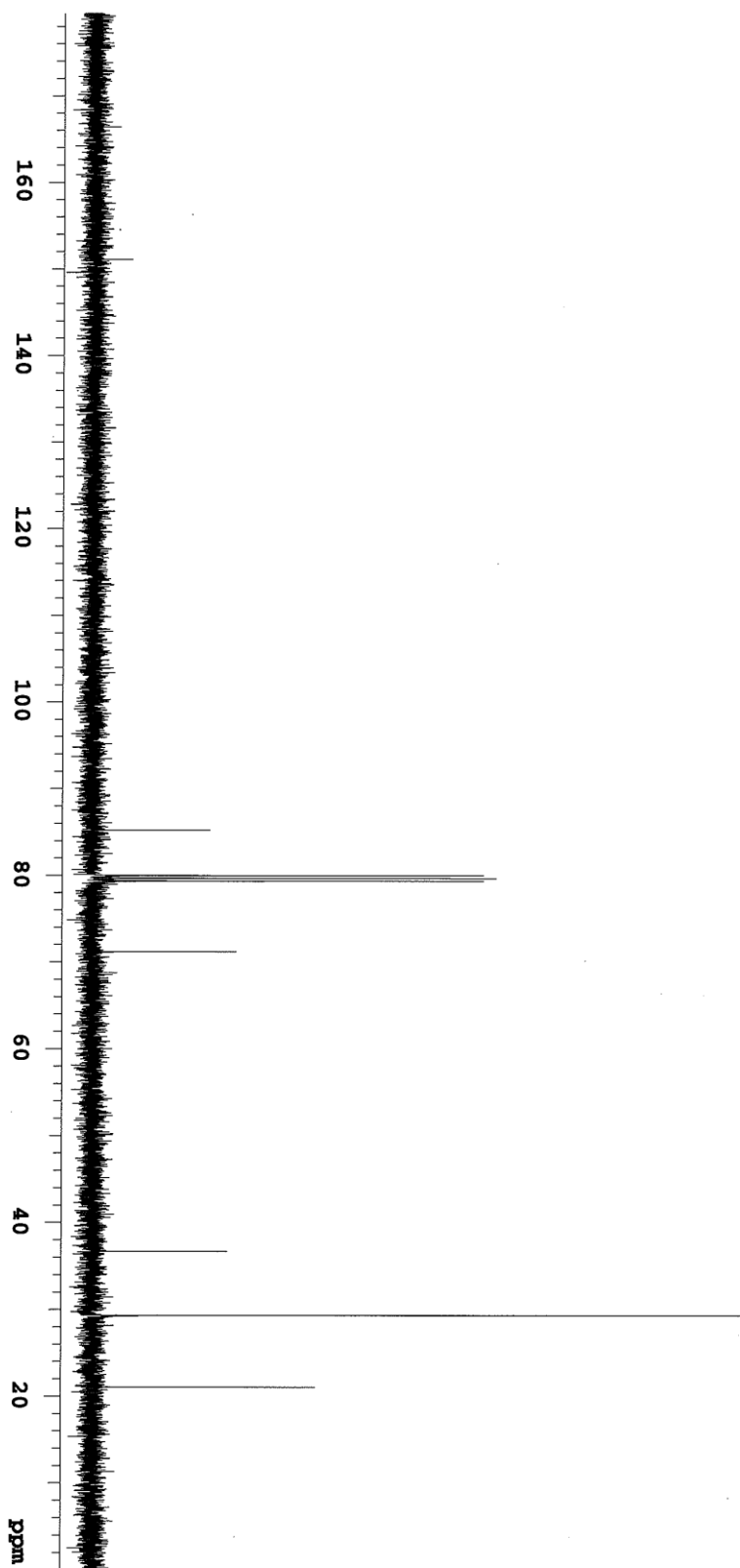
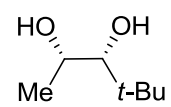


Sample Name:
HA-I-221diol
Archive directory:

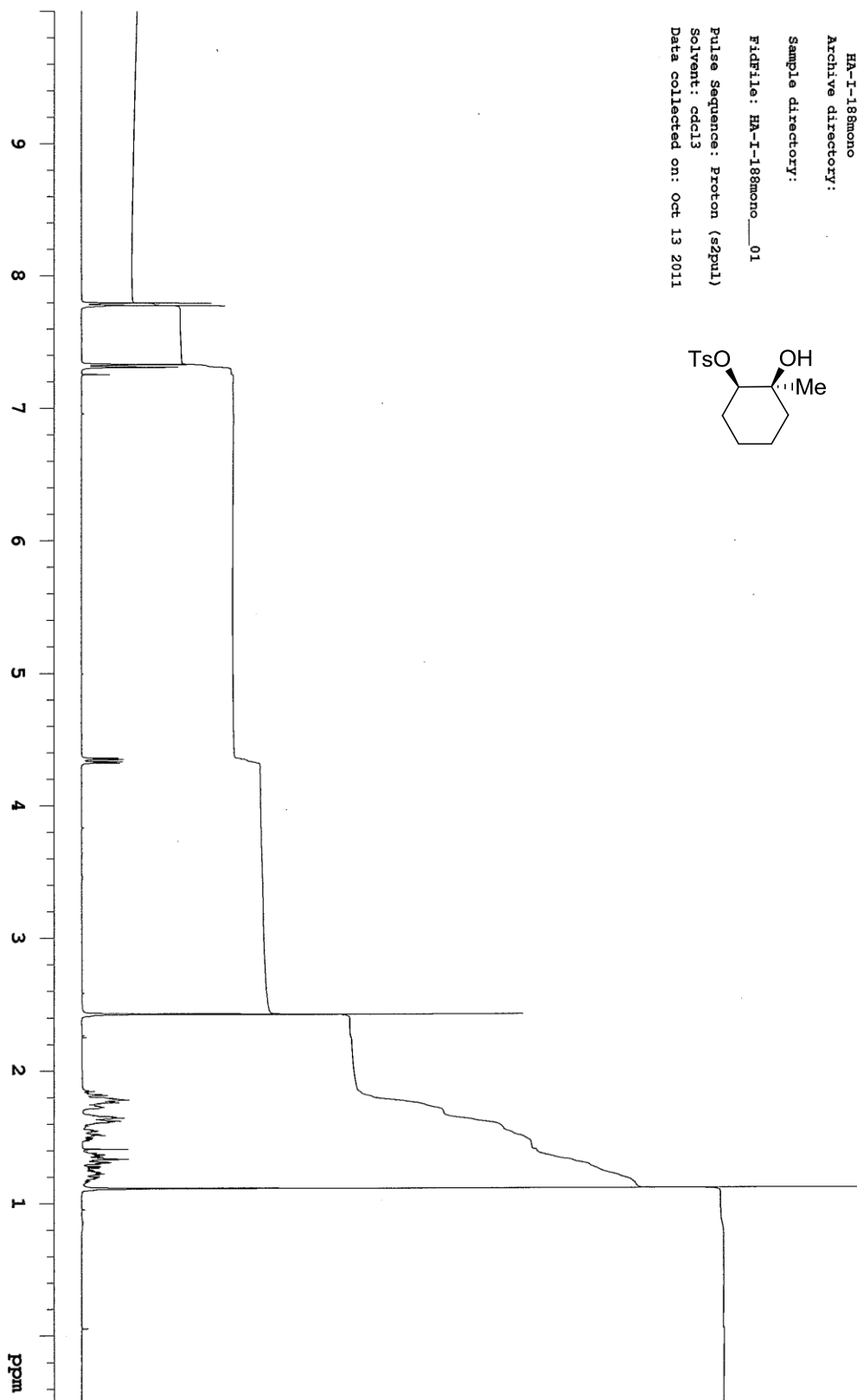
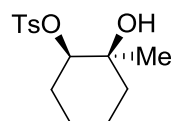
Sample directory:

Fidfile: HA-I-221diol_02

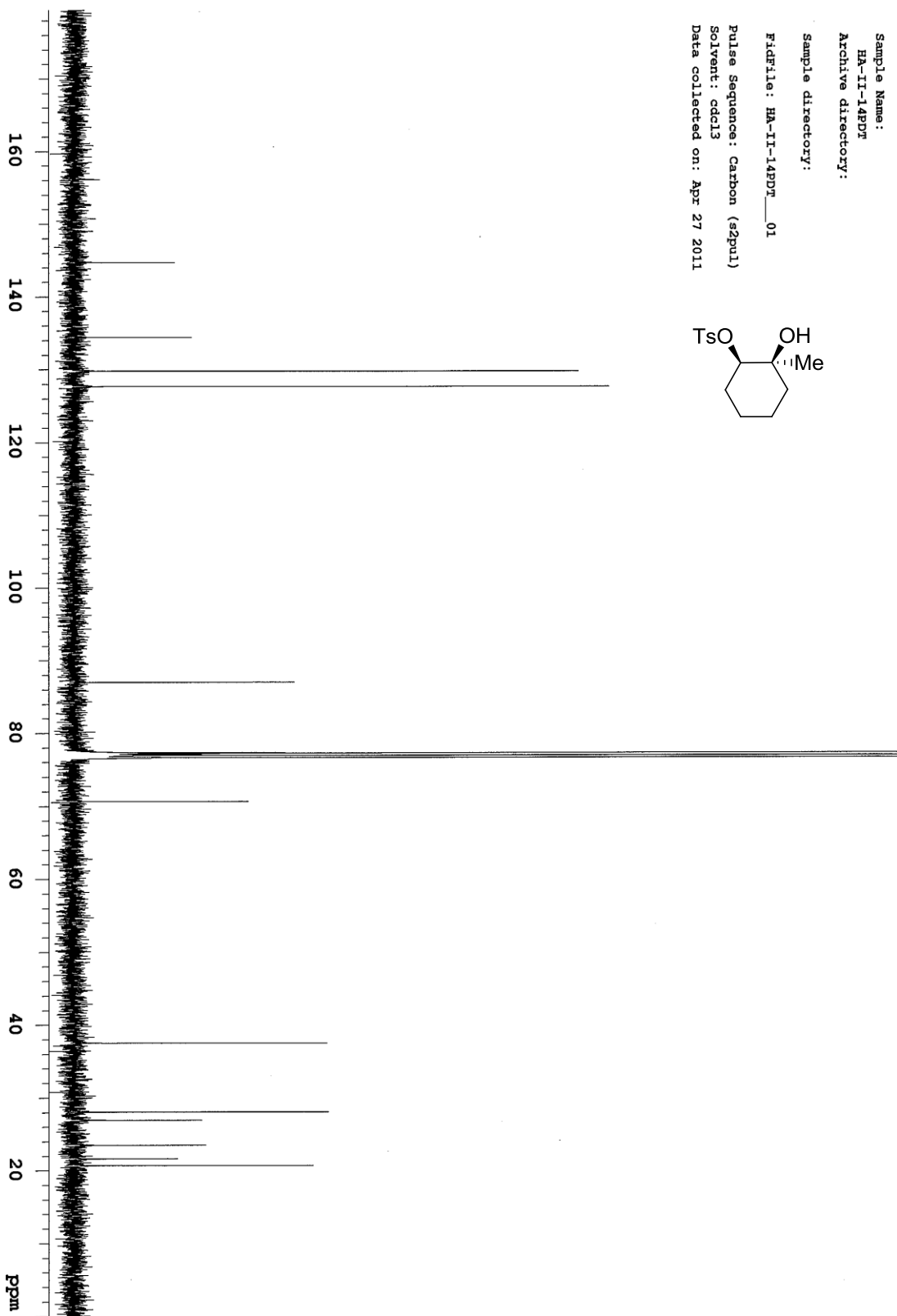
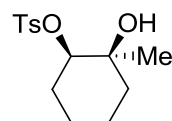
Pulse Sequence: Carbon (s2pul)
Solvent: cdcl3
Data collected on: Oct 20 2011



Sample Name: HA-I-18monone
Archive directory:
Sample directory:
FIDFile: HA-I-18monone_01
Pulse Sequence: Proton (s2pul)
Solvent: cdcl3
Data collected on: Oct 13 2011



Sample Name:
HA-II-14PPT
Archive directory:
Sample directory:
FidFile: HA-II-14PPT_01
Pulse Sequence: Carbon (s2pul)
Solvent: cdcl3
Data collected on: Apr 27 2011



Sample Name:
HA-I-188diol

Archive directory:

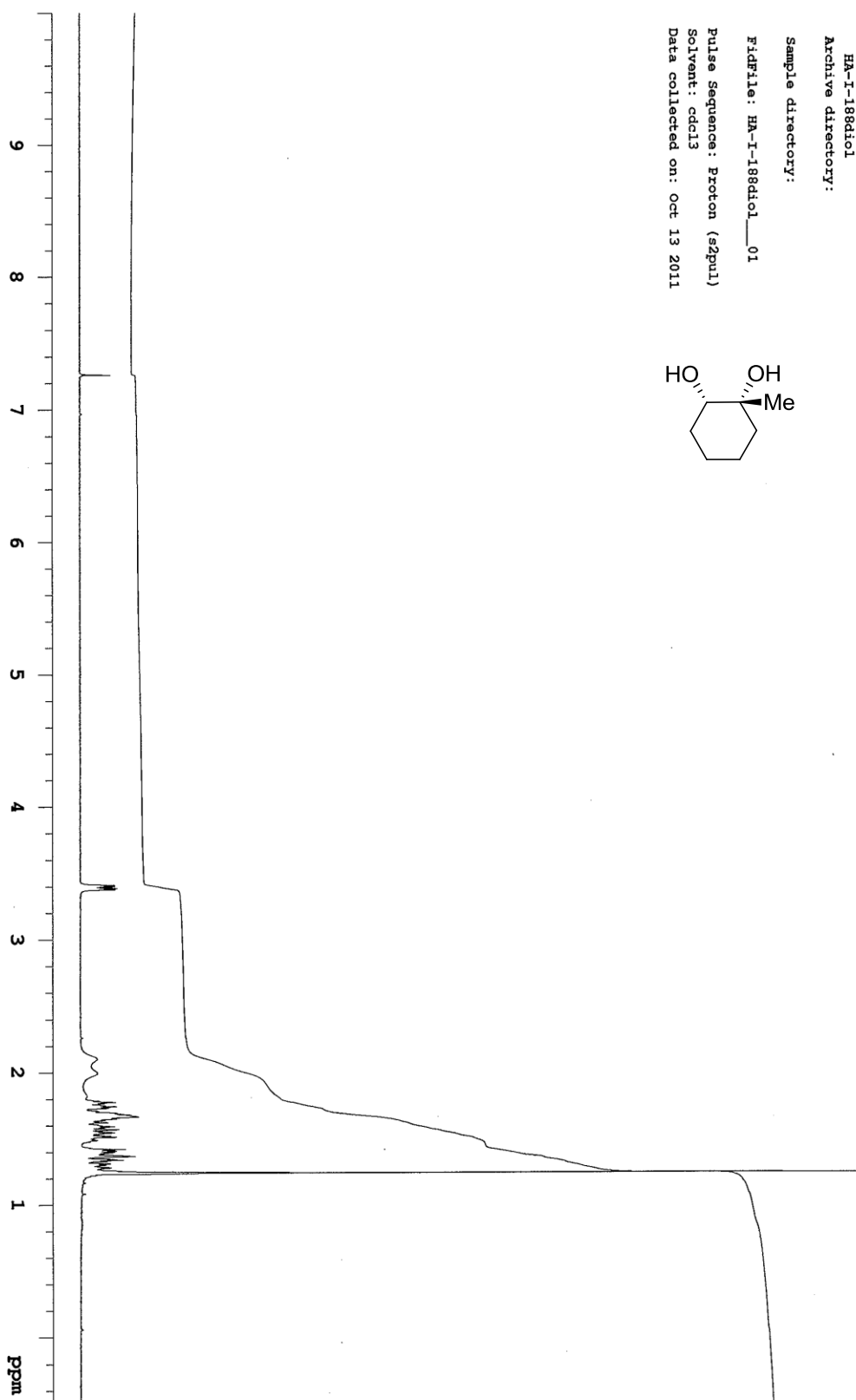
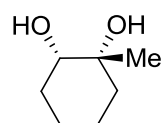
Sample directory:

FidFile: HA-I-188diol_01

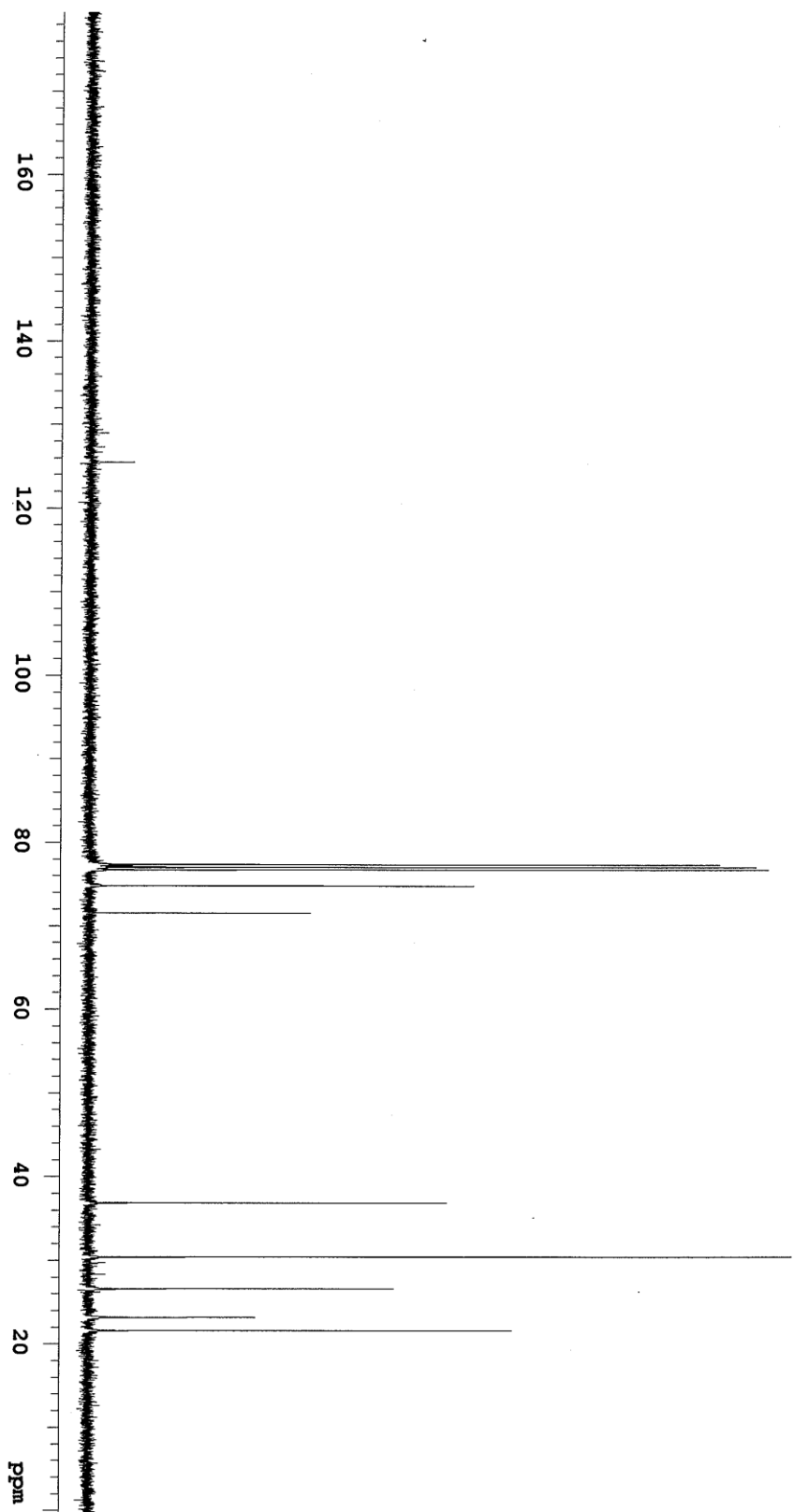
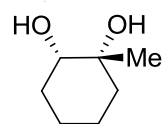
Pulse Sequence: Proton (zgpg1)

Solvent: cdcl3

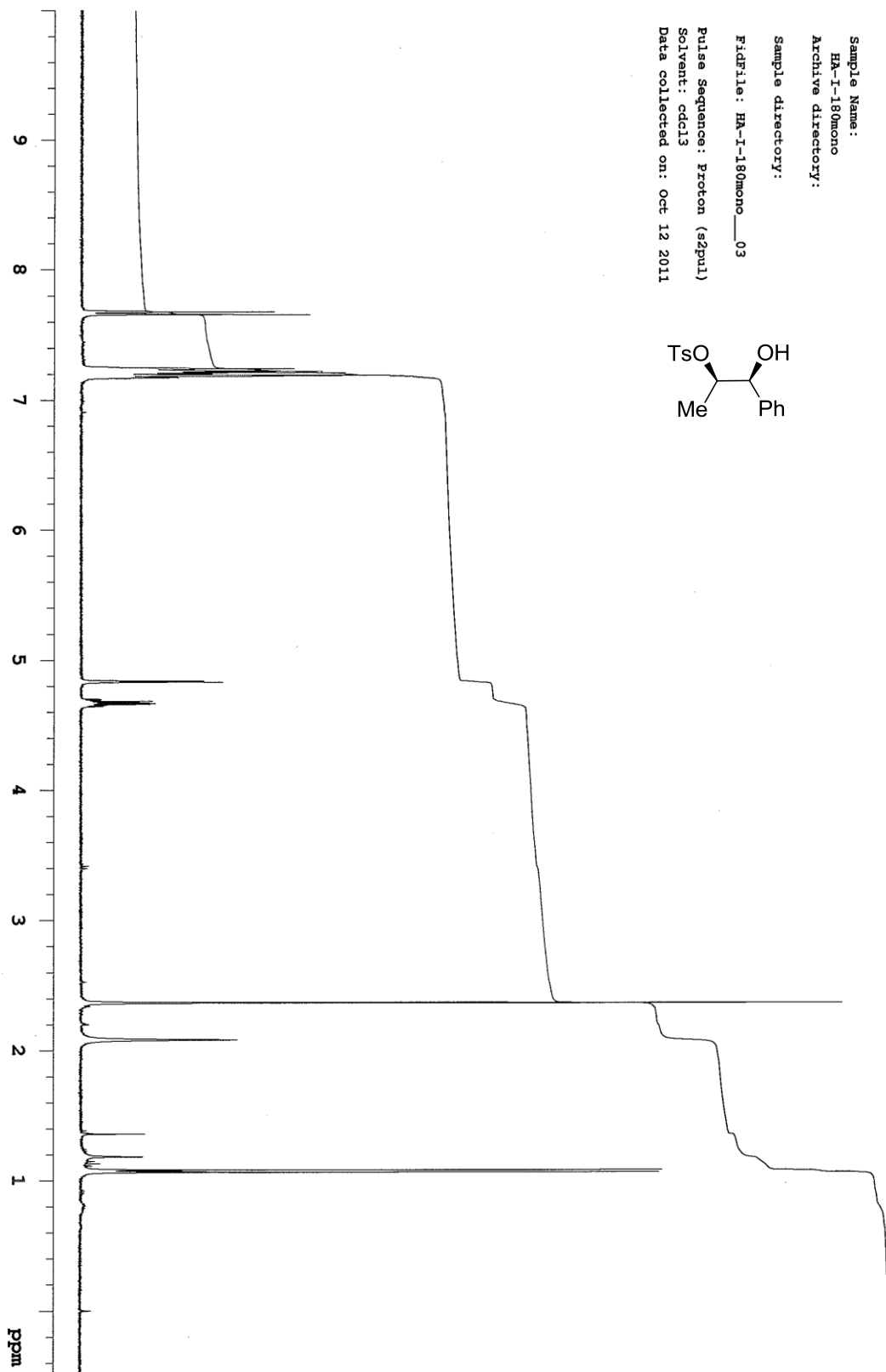
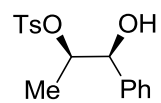
Data collected on: Oct 13 2011



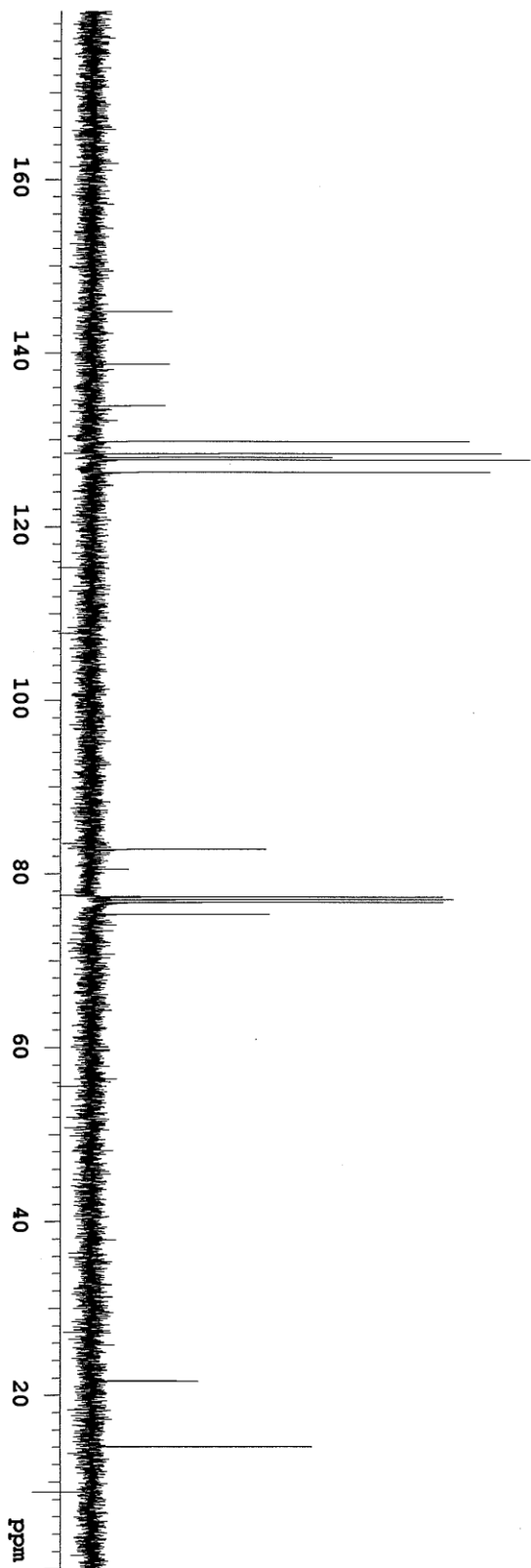
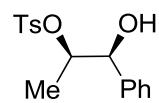
Sample Name:
HA-II-14RSM
Archive directory:
Sample directory:
FidFile: HA-II-14RSM_04
Pulse Sequence: Carbon (szpu1)
Solvent: cdcl3
Data collected on: Apr 26 2011



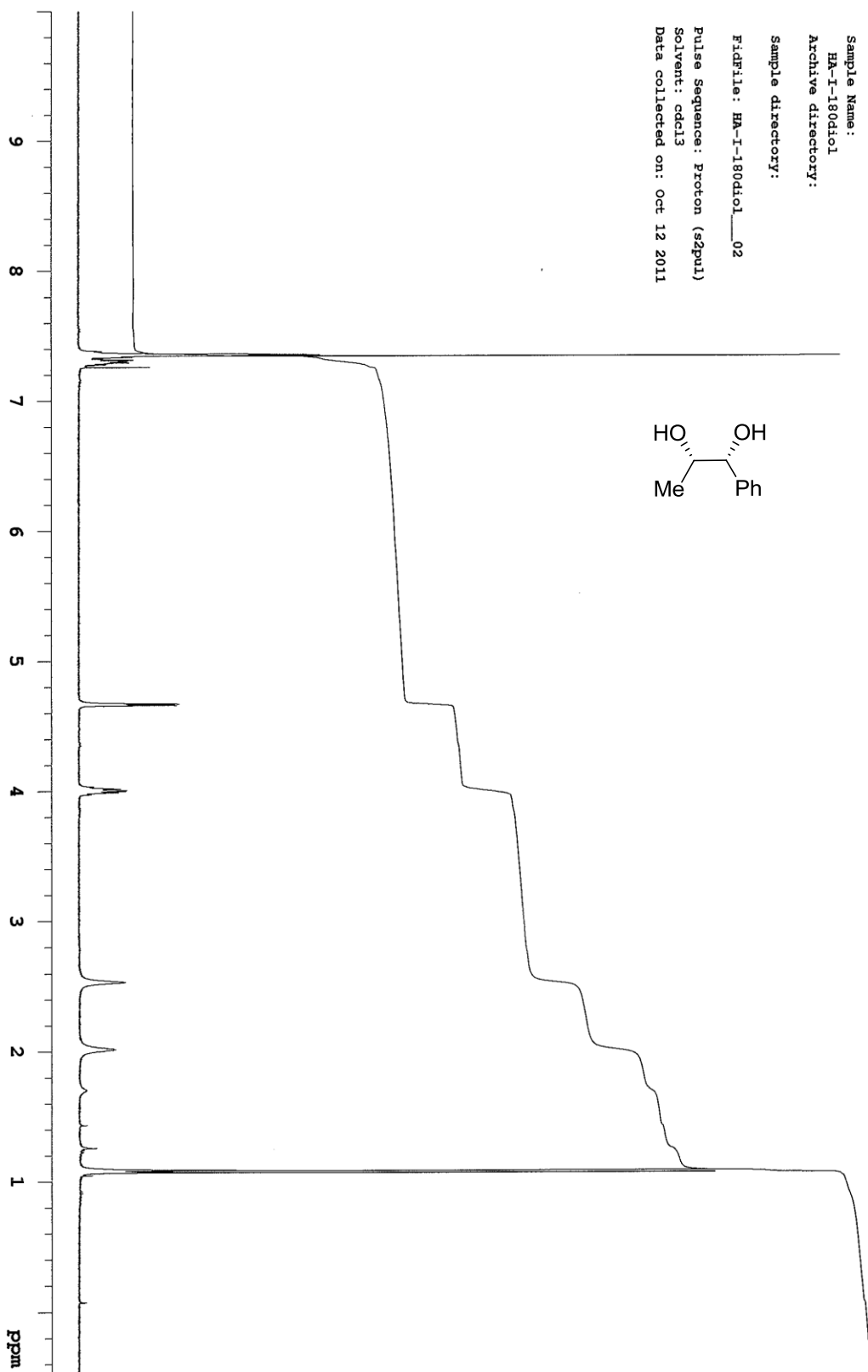
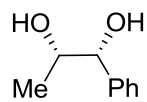
Sample Name: HA-I-180mono
Archive directory:
Sample directory:
FidFile: HA-I-180mono_03
Pulse Sequence: Proton (szpu1)
Solvent: cdcl3
Data collected on: oct 12 2011



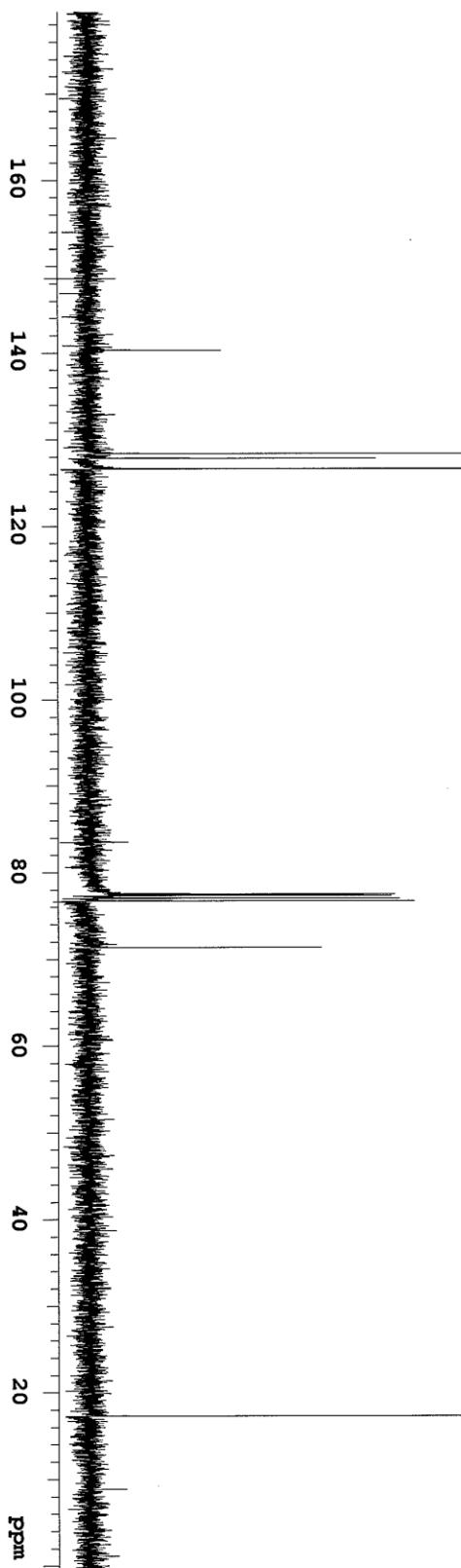
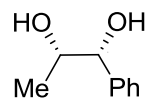
Sample Name:
HA-I-180mono
Archive directory:
Sample directory:
F1DF1le: HA-I-180mono__04
Pulse Sequence: Carbon (s2pu1)
Solvent: cdcl3
Data collected on: Oct 12 2011



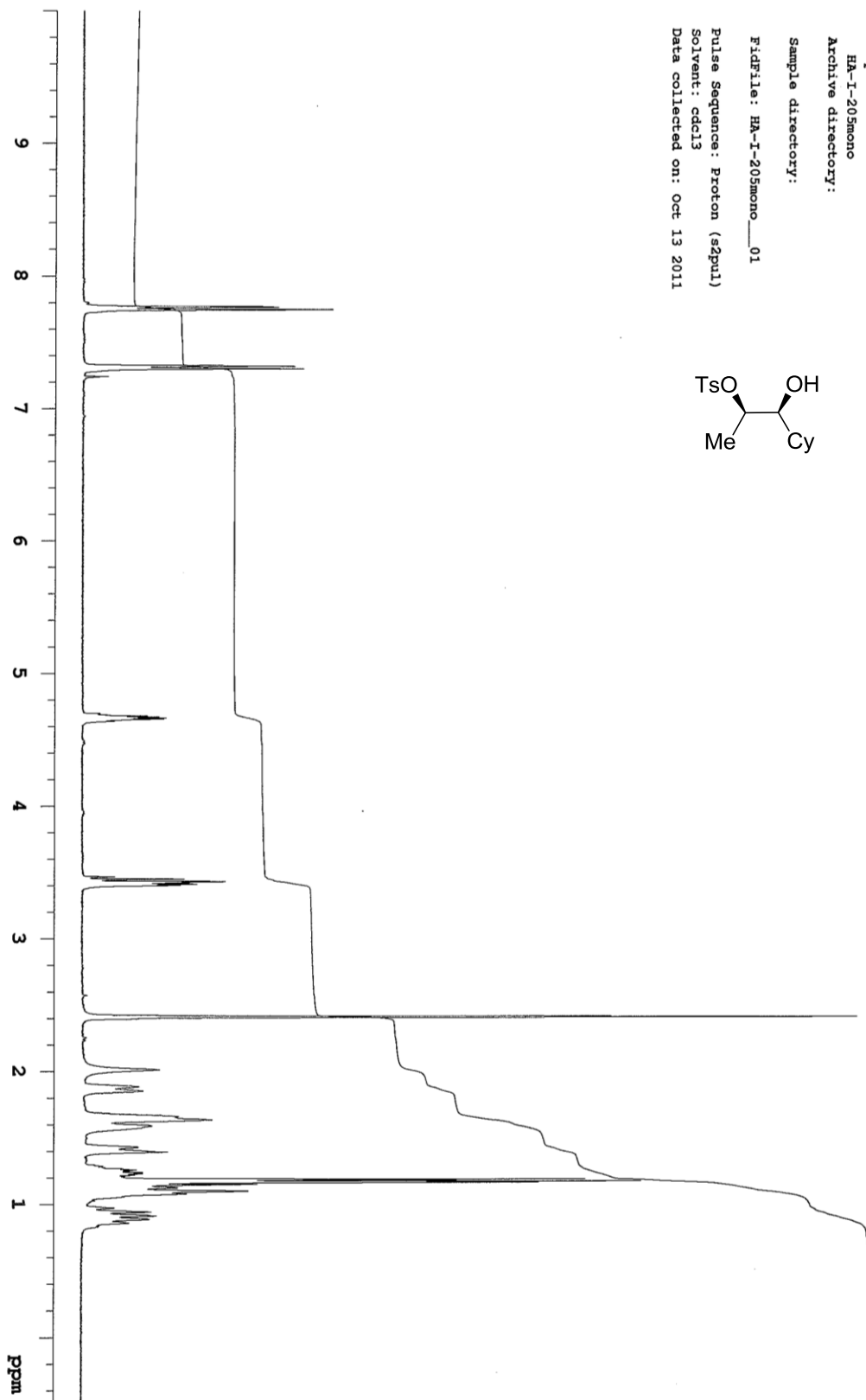
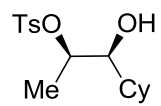
Sample Name:
HA-I-180d101
Archive directory:
Sample directory:
F1: HA-I-180d101_02
Pulse Sequence: Proton (zgpg30)
Solvent: cdcl3
Data collected on: Oct 12 2011



Sample Name:
HR-I-180diol
Archive directory:
Sample directory:
FIDFile: HR-I-180diol_03
Pulse Sequence: Carbon (s2pu1)
Solvent: cdcl3
Data collected on: oct 12 2011



Sample Name:
HA-I-205mono
Archive directory:
Sample directory:
FidFile: HA-I-205mono__01
Pulse Sequence: Proton (zgpg3)
Solvent: cdcl3
Data collected on: Oct 13 2011

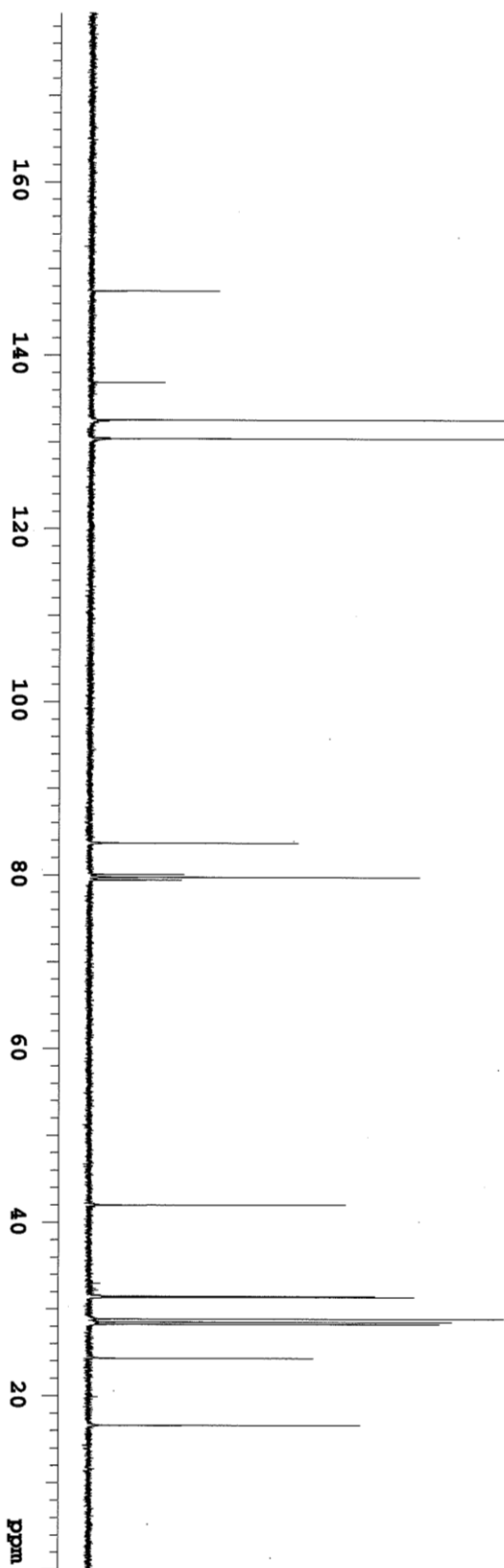
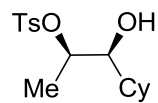


Sample Name:
HA-I-253mono
Archive directory:

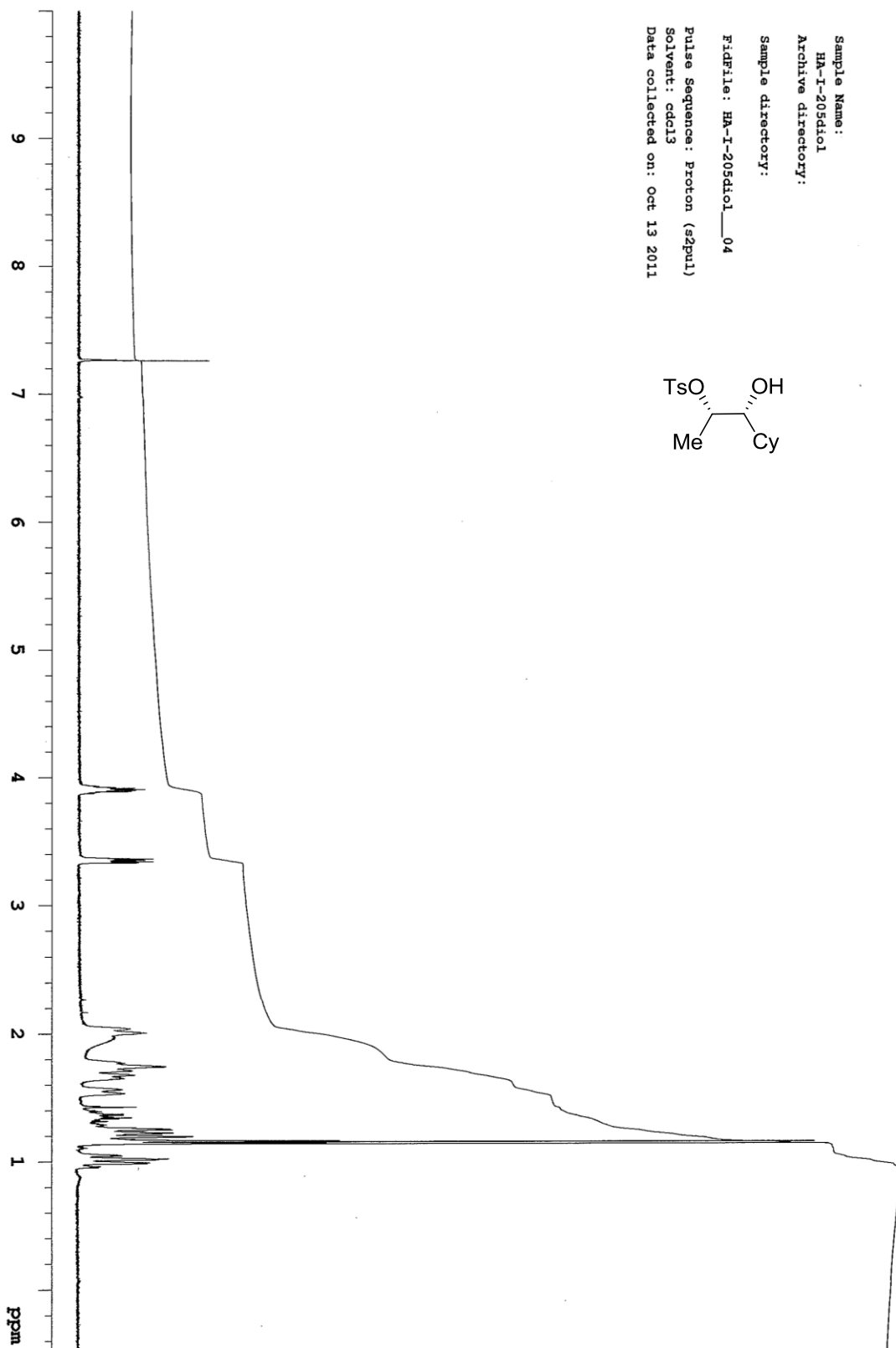
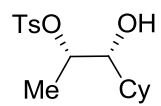
Sample directory:

FidFile: HA-I-253mono__02

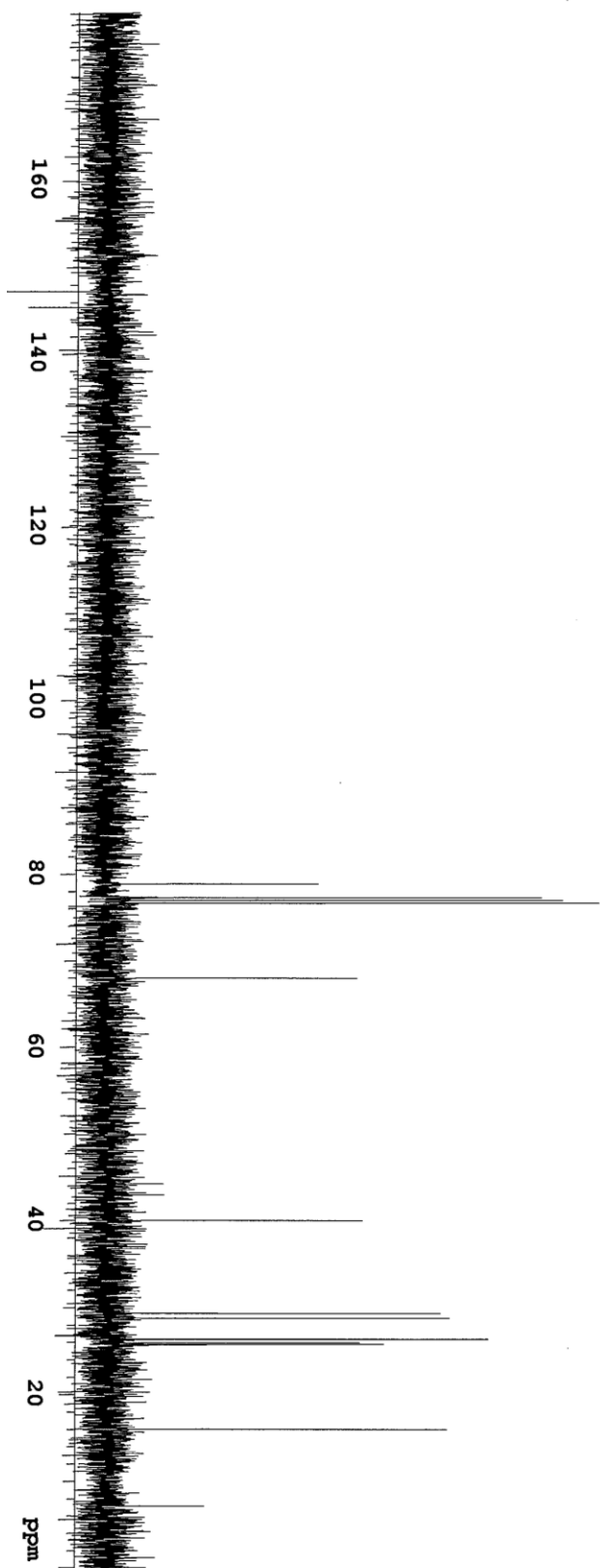
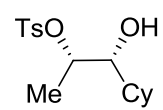
Pulse Sequence: Carbon (zgpg1)
Solvent: cdcl3
Data collected on: Oct 22 2011



Sample Name:
HA-I-205diol
Archive directory:
Sample directory:
FidFile: HA-I-205diol_04
Pulse Sequence: Proton (s2pul)
Solvent: cdcl3
Data collected on: Oct 13 2011



Sample Name:
HA-I-205diol
Archive directory:
Sample directory:
FidFile: HA-I-205diol_05
Pulse Sequence: Carbon (sZpu1)
Solvent: cdcl3
Data collected on: Oct 13 2011



CHAPTER 3:

SIGNIFICANT IMPROVEMENT ON CATALYTIC ENANTIOSELECTIVE SILYLATION OF *SYN*-DIOLS AND TRIOLS THROUGH THE USE OF A TETRAZOLE ADDITIVE

3.1 Catalytic enantioselective silylation of *syn*-diols and triols using amino-acid-derived catalyst

The Hoveyda-Snapper desymmetrization catalyst can successfully catalyze the enantioselective silylation and sulfonylation of symmetric diols and triols, as well as the kinetic resolution of asymmetric diols by both silylation and sulfonylation. As mentioned before, the catalyst contains an N-methylimidazole moiety that acts as a Lewis base to activate each electrophile, and a secondary amine that acts as a Bronsted base to deprotonate the product. Also discussed, the peptide catalyst works best with diols, most likely because multiple hydrogen-bonding interactions are required in order for an active complex to form. Although we have speculated upon the mechanism of this catalyst, we have yet to provide a transition state model. The reason for this is because new findings have led us to revise our previously reported transition state model⁵.

3.1.1 *Previously proposed transition state*

The original transition state models for enantioselective silylation and sulfonylation are shown in Figures 3.1 and 3.2, respectively. In both cases, *meso*-1,2-cyclopentanediol is portrayed as hydrogen-bonding to the amino acid unit of the catalyst. The hydroxyl groups on the substrate act as hydrogen-bond donors, while the secondary amine and carbonyl group on the catalyst act as hydrogen-bond acceptors. In the case of

silylation, the imidazole unit of the catalyst forms a loose bond with silicon; next, the closest hydroxyl group on the substrate attacks the silyl chloride and displaces Cl^- (Figure 3.1). In the case of sulfonylation, the imidazole unit forms a covalent bond with sulfur by attacking the sulfonyl chloride and displacing Cl^- ; next, the closest hydroxyl group attacks the sulfur and displaces the imidazole (Figure 3.2). Finally, in both cases, the secondary amine on the catalyst deprotonates the diol. These two models account for the multiple hydrogen-bonding interactions, the Lewis base activation, and the Bronsted base deprotonation; however, the models don't explain why relatively high catalyst loadings and long reaction times are needed.

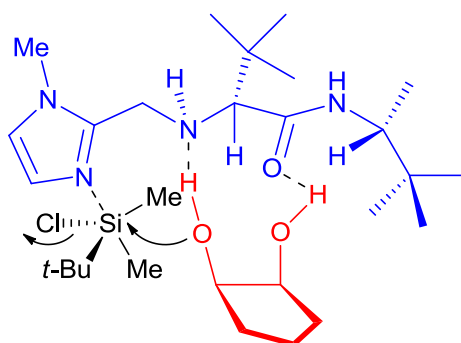


Figure 3.1 Previously proposed transition state model for enantioselective silylation

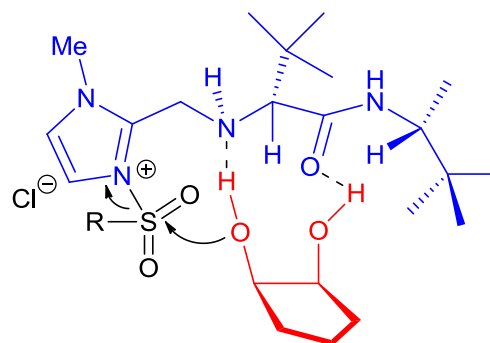


Figure 3.2 Previously proposed transition state model for enantioselective sulfonylation

In order to learn more about the catalyst's mechanism, we decided to perform DFT calculations on the proposed transition state model for enantioselective silylation. Dr. Frederick Haeffner, who performed the DFT calculations, had difficulty finding a low energy pathway for the substrate-catalyst complex that we had suggested. As a result, he simplified the problem down to understanding the mechanism of the imidazole-catalyzed silylation of methanol. Since imidazole qualifies as both a Lewis base and Bronsted base,

it is capable of electrophile activation and alcohol deprotonation. What we wanted to learn from this simple system was whether the reaction proceeds through a concerted or step-wise mechanism and whether one or two molecules of imidazole are responsible for the required activation and deprotonation steps. The conclusions of Dr. Haeffner's computational studies on the imidazole-catalyzed silylation of methanol are shown in the following reaction coordinate diagram (Figure 3.3).

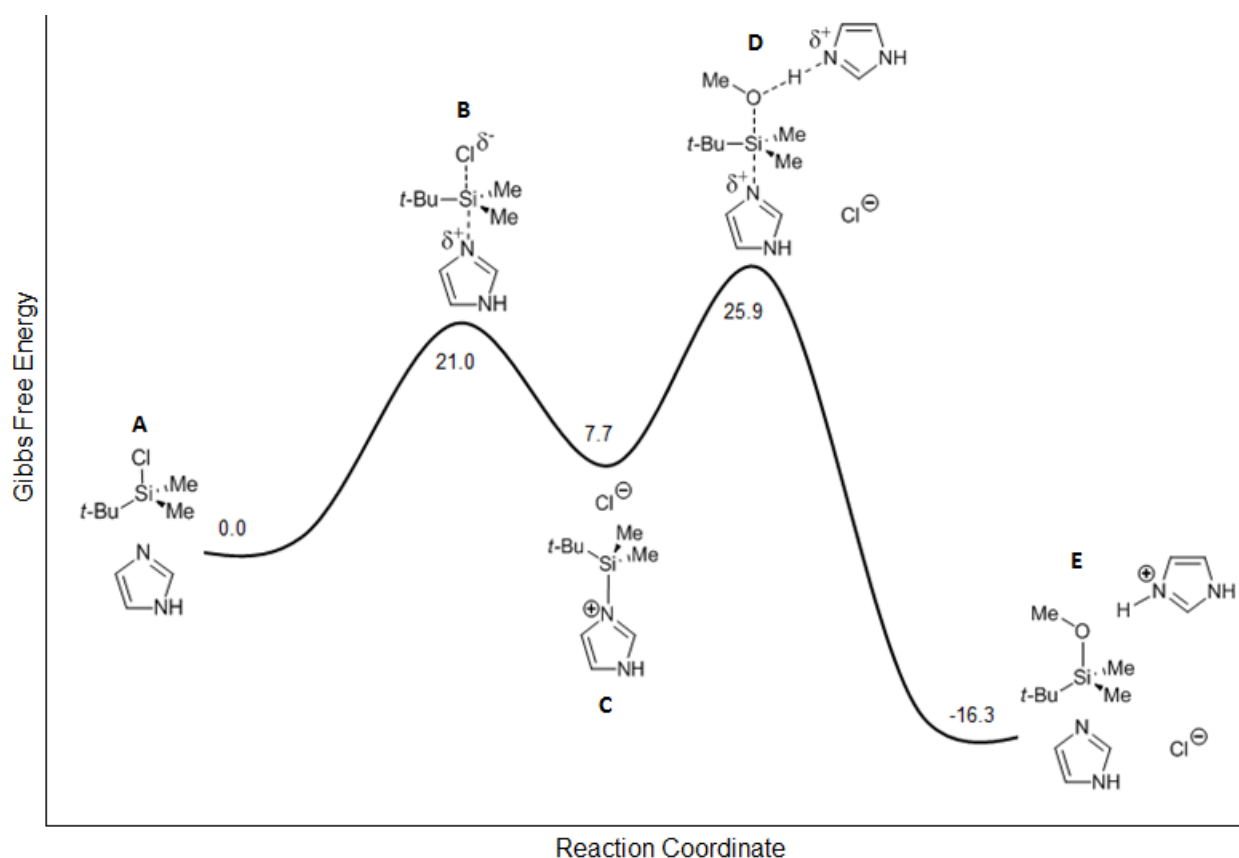


Figure 3.3 Mechanism of imidazole-catalyzed silylation of methanol determined by DFT calculations

The diagram suggests that the overall reaction is a two-step process. In the first step (A \rightarrow B \rightarrow C), one molecule of imidazole nucleophilically attacks the silyl chloride and displaces Cl^- , forming a silylimidazolium salt. In the second step (C \rightarrow D \rightarrow E), the

silylimidazolium salt transfers its silyl group to methanol, whilst another molecule of imidazole simultaneously deprotonates the hydroxyl group. The second step is the rate-determining step because it has the highest activation energy. This means that the rate-determining step involves two molecules of imidazole.

3.1.2 Additive study and discovery of rate enhancement

With new mechanistic insight into the imidazole-catalyzed silylation of methanol, we considered the possibility that the rate-determining step of enantioselective silylation also involves two molecules of catalyst. To test this hypothesis, we attempted kinetic studies; unfortunately, the studies were hindered by the fact that the reaction is heterogeneous. Then, as an alternate way to test our hypothesis, an additive study was performed.

The additive study that we designed was made up of three silylation reactions catalyzed by: (1) 20 mol% chiral catalyst, (2) 20 mol% N-methylimidazole, and (3) 20 mol% chiral catalyst and 20 mol% N-methylimidazole. In all three cases, *meso*-1,2-cyclooctanediol was reacted with 2 equivalents of TBSCl, 1.25 equivalents of DIPEA, in the presence of THF as solvent at -40 °C for 6 hours. The exciting results of this study, performed by Nathan Manville, are shown in Table 3.1.

Before looking at the results, however, it is important to understand the logic behind our additive study. Assuming that the rate-determining step of silylation involves two molecules of catalyst, it is possible for N-methylimidazole and our catalyst to act cooperatively in one reaction. N-methylimidazole is a better Lewis base than the catalyst, simply because it is smaller and less sterically hindered; therefore, it should

compete with the catalyst for the activation role. However, N-methylimidazole may or may not compete with the catalyst for the deprotonation role. If N-methylimidazole outcompetes the catalyst during the deprotonation step, the product should be racemic. On the other hand, if N-methylimidazole does not outcompete the catalyst during the deprotonation step and the enantioselectivity of the reaction is determined by the Bronsted base, the product should be enantioenriched.

Table 3.1 Initial additive study

Entry	Catalyst (mol%)	N-methylimidazole (mol%)	Conversion (%)	ee (%)
1	20	-	9	87
2	-	20	69	-
3	20	20	92	56
4	20	15	88	63
5	20	10	79	66
6	20	7.5	71	71
7	20	5	49	73

The reaction with just chiral catalyst in 6 hours resulted in low conversion (9%) but highly enriched product (87% ee, Entry 1). The reaction with just N-methylimidazole resulted in moderate conversion (69%) but racemic product (Entry 2). Most importantly though, using both chiral catalyst and N-methylimidazole led to high conversion (92%) and moderately enriched product (56% ee, Entry 3). Compared to Entry 1, the

conversion drastically increased and the ee suffered but it was not completely diminished; thus, we concluded that some of the N-methylimidazole was acting cooperatively with the catalyst, and some of it was acting independently. To prevent the loss in ee, but maintain the rate enhancement, we chose to lower the N-methylimidazole loading (whilst keeping the catalyst loading the same). At 7.5 mol% N-methylimidazole, the reaction went to 71% completion and the ee was 71%, an improvement, yet still lacking in enantioselectivity.

Realizing that N-methylimidazole was still functioning as base, we decided to explore new additives that would not compete with the catalyst for deprotonation. We predicted that the ideal additive would be a strong Lewis base, yet weak Bronsted base. In the search for an improved additive, Nathan Manville screened several Lewis bases and some representative results are shown in Table 3.2. In all cases, *meso*-1,2-cyclooctanediol was reacted with 20 mol% catalyst, 7.5 mol% Lewis base, 2 equivalents of TBSCl, 1.25 equivalents of DIPEA, in the presence of THF as solvent at -40 °C for 3 hours.

With imidazole as an additive, the conversion at 3 hours was low (13%, Entry 1), forcing us to dismiss imidazole as a useful additive. As expected, N-methylimidazole considerably enhanced the rate of the reaction (58% conversion) but the ee suffered (81%, Entry 2). When compared to N-methylimidazole, reactions with 4,5-dicyanoimidazole and tetrazole resulted in slightly lower conversions (~50%) but higher ee's (92%, Entries 3 and 4), which were encouraging. With 5-ethylthiotetrazole as an additive, however, the reaction went to completion and the ee was 94% (Entry 5)! This

was exciting news, especially considering that with 30 mol% catalyst, but no additive, the reaction takes 120 hours and the ee is 95%. Upon further optimization, we learned that the reaction with 5-ethylthiotetrazole is complete in 1 hour, which translates into a >100-fold rate enhancement.

Table 3.2 Additive Screening Study

Entry	Azole	Conversion (%)	ee (%)
1	3.3	13	86
2	3.4	58	81
3	3.5	47	92
4	3.6	55	92
5	3.7	100	94

Not surprisingly, 5-ethylthiotetrazole, which has a pKa of 4.3²⁹, is the weakest Bronsted base that was screened; in fact, it is a Bronsted acid. This is in accordance with our theory that the optimal additive would be a weak Bronsted base. Moreover, due to

²⁹ Wong, C.; Wittmann, V. *J. Org. Chem.* **1997**, *62*, 2144-2147.

the highly electron rich amine, 5-ethylthiotetrazole is a great nucleophilic activator, which explains the remarkable rate enhancement.

3.1.3 *Newly proposed transition state*

With some validation that the rate-determining step of enantioselective silylation involves two molecules of catalyst, we revised our original transition state model. In the new model, the diol is portrayed as both intramolecularly H-bonding with itself and as intermolecularly H-bonding with the chiral catalyst. We presume that in the first step of the reaction, DIPEA deprotonates the tetrazole. Then, the tetrazole activates the silyl chloride and the activated complex approaches and binds to the substrate-catalyst complex, which is followed by silyl group transfer. We are still unsure about the final step, the deprotonation step. Depending on the H-bonding of the substrate-catalyst complex, one possibility is that the secondary amine deprotonates directly the silylated hydroxyl group (Figure 3.4, **A**). Another possibility is that the secondary amine deprotonates the un-silylated hydroxyl group, which, in turn, deprotonates the neighboring hydroxyl group in a relay deprotonation (Figure 3.4, **B**).

This new model accounts for the multiple hydrogen-bonding interactions, the Lewis base activation, and the Bronsted base deprotonation. In addition, the new model explains why, in the absence of tetrazole, relatively high catalyst loadings and long reaction times are needed. Without an additive, the transition state involves two molecules of chiral catalyst; thus, there is a large entropic and steric barrier that must be overcome in order for the reaction to take place.

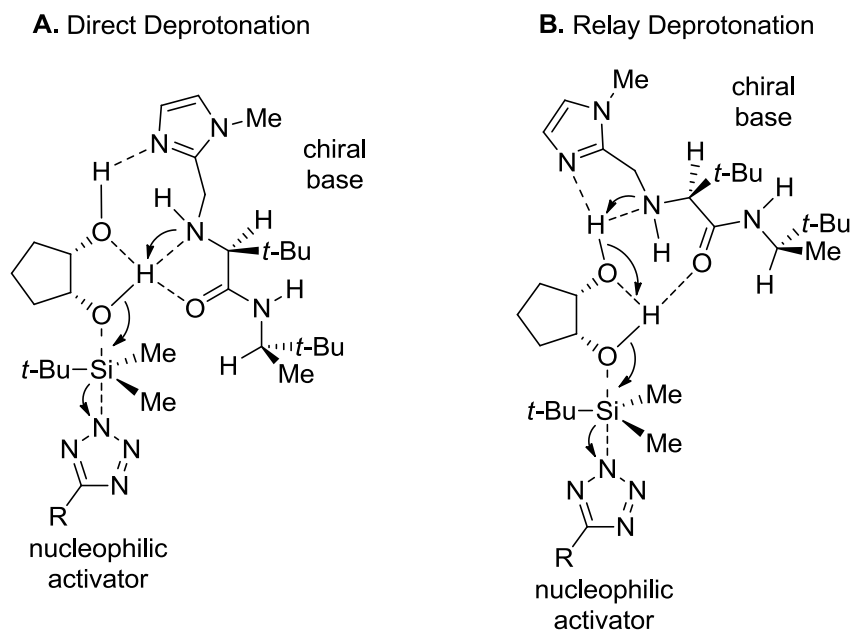


Figure 3.4 Newly proposed transition state models for enantioselective silylation

3.2 Rate enhancement for previously successful substrates

3.2.1 *meso*-diols and triols

Having discovered an additive for our catalyst that is capable of 120-fold rate enhancement, we tested the rest of our previously successful silylation substrates in the presence of 5-ethylthiotetrazole. We were happy to find that most of our *meso*-diols could undergo enantioselective silylation significantly faster in the presence of 5-ethylthiotetrazole, while the ee's remained unchanged (Table 3.3).

When testing a cyclic *meso*-triol, we encountered a solubility issue (Table 3.4, Entry 2). For the reaction without additive, in 120 hours, the yield is 65%; for the reaction with 5-ethylthiotetrazole, in 6 hours, the yield was only 51%. We concluded that due to the poor solubility of the triol in THF at -30 °C, it takes a long time for the substrate to go into solution; therefore, in this case, the longer reaction time is necessary.

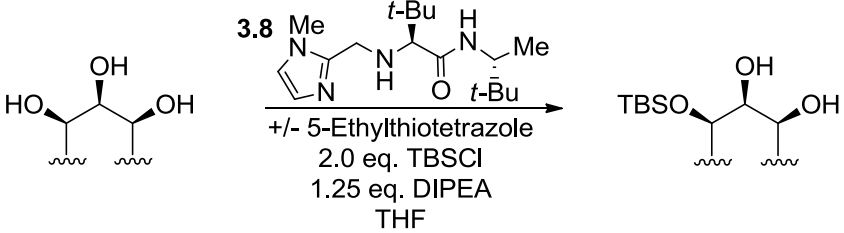
On the other hand, an acyclic *meso*-triol underwent enantioselective silylation approximately 100 times faster with 5-ethylthiotetrazole, and the yield was comparable to the reaction without additive (Table 3.4, Entry 1).

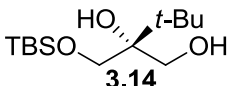
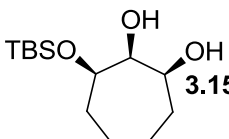
Table 3.3 Rate enhancement for *meso*-diols

3.8

+/- 5-Ethylthiotetrazole
2.0 eq. TBSCl
1.25 eq. DIPEA
THF

Entry	Product	3.8 (mol%)	5-Ethylthiotetrazole (mol%)	Time (h)	Temp. (°C)	Yield (%)	ee (%)
1		30	-	60	-40	96	88
		20	7.5	1	-40	97	91
2		20	-	120	-28	82	92
		20	7.5	1	-40	93	94
3		30	-	72	-40	75	94
		20	7.5	1	-40	82	95
4		30	-	72	-40	93	93
		20	7.5	1	-40	93	93
5		30	-	120	-40	96	95
		20	7.5	1	-40	96	95
6		30	-	72	-40	80	93
		20	7.5	1	-40	93	95
7		30	-	48	-78	82	96
		20	7.5	1	-78	78	92

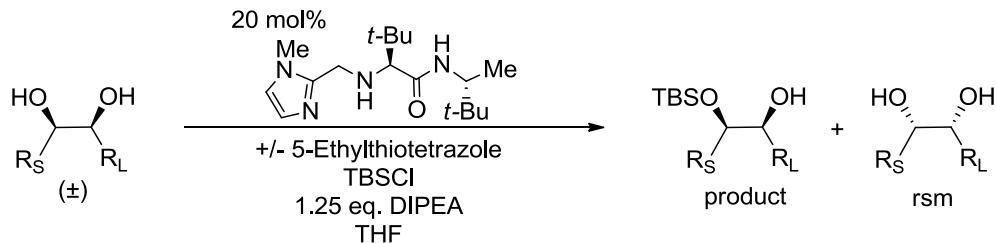
Table 3.4 Rate enhancement for *meso*-triols


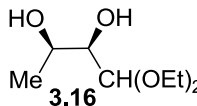
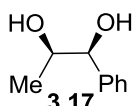
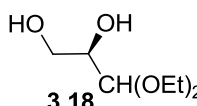
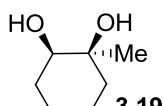
Entry	Product	3.8 (mol%)	5-Ethylthiotetrazole (mol%)	Time (h)	Temp. (°C)	Yield (%)	ee (%)
1	 3.14	30	-	96	-30	78	93
		20	7.5	1	-40	74	92
2	 3.15	30	-	120	-30	65	>98
		20	7.5	6	-30	51	>98

3.2.2 Kinetic resolution substrates

Given the importance of rate on kinetic resolution, we were curious to find out what effect 5-ethylthiotetrazole would have on our kinetic resolution reactions (Table 3.5). For *syn*-1,2-diol **3.16** and primary-secondary 1,2-diol **3.18**, the reactions with 5-ethylthiotetrazole went to ~50% completion 24 times faster than the reactions without additive (Entries 1 and 3). In both cases, the presence of the additive did not affect the selectivity of the kinetic resolution. On the other hand, we were pleasantly surprised with substrate **3.17**; not only did 5-ethylthiotetrazole enhance the rate of the original reaction 72-fold, but the selectivity value increased dramatically from 8 to 43 (Entry 2)! Yet another exciting result was the successful kinetic resolution of asymmetric diol **3.19**, which was previously not possible. In the presence of 5-ethylthiotetrazole, diol **3.19** was resolved in 12 hours with great selectivity ($s = 39$, Entry 4).

Table 3.5 Rate enhancement for kinetic resolution substrates

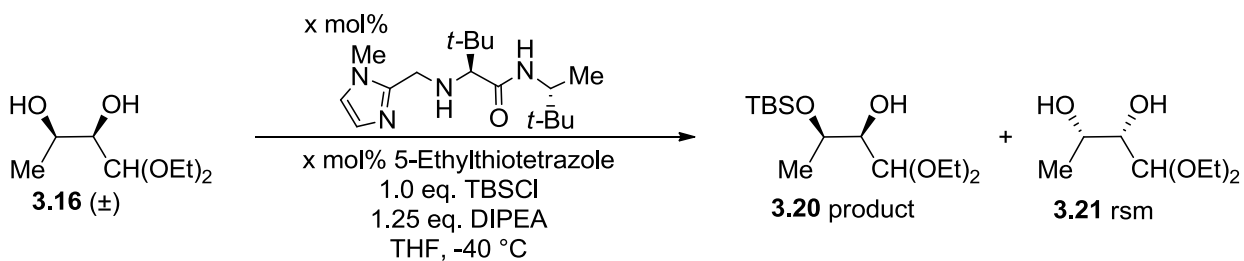


Entry	Substrate	Temp.; Time; 5-Ethylthiotetrazole; TBSCl	rsm Yield; ee	product Yield; ee	s
1	 3.16	-30 °C; 24 h; 0 mol %; 1.0 eq.	44%; >98%	52%; 80%	>50
		-40 °C; 1 h; 7.5 mol %; 0.6 eq.	52%; 79%	35%; 90%	46
2	 3.17	-15 °C; 72 h; 0 mol %; 1.0 eq.	30%; 96%	68%; 39%	8
		-40 °C; 1 h; 7.5 mol %; 0.6 eq.	47%; 92%	52%; 86%	43
3	 3.18	-78 °C; 24 h; 0 mol %; 1.0 eq.	25%; 84%	55%; 68%	14
		-78 °C; 1 h; 7.5 mol %; 1.0 eq.	41%; 82%	49%; 70%	14
4	 3.19	-30 °C; 24 h; 0 mol %; 1.0 eq.	-; -	<5% conversion	-
		-40 °C; 12 h; 20 mol %; 0.6 eq.	62%; 57%	36%; 90%	39

Having solved the issue of long reaction time, we decided to address the related issue of high catalyst loading. To this end, a catalyst loading study was performed with *syn*-1,2-diol **3.16** (Table 3.6). In the study, we maintained a 1:1 ratio of catalyst to additive as we lowered the catalyst loading. By doing this, we found that with 5 mol% catalyst and 5-ethylthiotetrazole, the reaction goes to 43% completion in 1 hour (Entry 2). As we lowered the catalyst loading further, the best result that we achieved was 45% completion in 6 hours with 2.5 mol% catalyst and 5-ethylthiotetrazole (Entry 4). The

difference between 20 mol% and 2.5 mol% is significant and it renders our kinetic resolution reaction much more efficient.

Table 3.6 Catalyst loading study for kinetic resolution substrates



Entry	x; Time	rsm ee	product ee	Conversion	s
1	5.0; 2 h	92%	86%	52%	43
2	5.0; 1 h	70%	92%	43%	50
3	5.0; 6 h	93%	69%	57%	18
4	2.5; 6 h	74%	92%	45%	53
5	1.0; 6 h	18%	95%	16%	47
6	0.5; 6 h	6%	93%	6%	29

3.3 Previously unsuccessful substrates

After improving upon our previously successful enantioselective silylation reactions, we chose to re-explore substrates that were initially problematic. Two of these substrates are shown in Table 3.7. We concluded that *meso*-1,2-diols **3.22** and **3.23** could not undergo catalytic silylation, even at relatively high temperatures, because they were too sterically hindered. Fortunately, our prediction that 5-ethylthiotetrazole could speed up these two reactions was correct. Of the two, *meso*-1,2-diol **3.23** is the best example. Without the additive, in 24 hours, the mono-silylated product of substrate **3.23** is obtained

in <10% yield; with the additive, in 12 hours, the product was obtained in a highly impressive 93% yield and 90% ee (Entry 2).

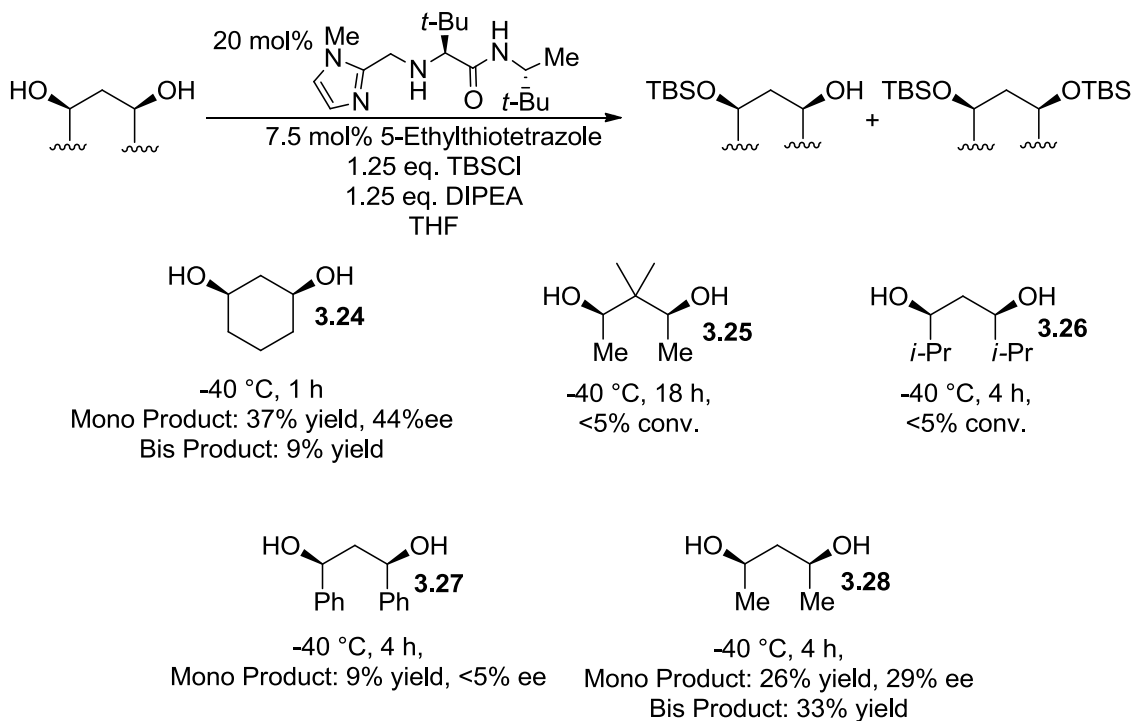
Table 3.7 Rate enhancement for sterically hindered *meso*-diols

3.8

 +/- 5-Ethylthiotetrazole
 2.0 eq. TBSCl
 1.25 eq. DIPEA
 THF

Entry	Product	3.8 (mol%)	5-Ethylthiotetrazole (mol%)	Time (h)	Temp. (°C)	Yield (%)	ee (%)
1	 Ph 3.22 Ph	20	-	24	4	<5%	-
		20	20	14	-40	51	67
2	 Et 3.23 Et	20	-	24	-30	<10%	-
		20	20	12	-40	93	90

Table 3.8 Unsuccessful *meso*-diols



Acyclic *meso*-1,3-diols were previously poor substrates for our catalytic enantioselective silylation reaction. Unfortunately, testing these substrates in the presence of 5-ethylthiotetrazole was not met with success. As shown in Table 3.8, the reactions suffer from no conversion, low conversion, and/or the formation of an excessive amount of bis-silylated product. It's possible that the lowest energy conformation of an acyclic *meso*-1,3-diol is not conducive to multiple hydrogen-bonding interactions with the catalyst, and so a tightly-bound substrate-catalyst complex cannot form. This would explain the low conversions and selectivities.

Table 3.9 Unsuccessful kinetic resolution substrates

Entry	Substrate	Temp.; Time	rsm Yield; ee	product Yield; ee	s
1	 3.29	-40 °C; 8 h	90%; <5%	10%; 9%	<2
2	 3.30	-40 °C; 12 h	78%; 5%	7%; 44%	3

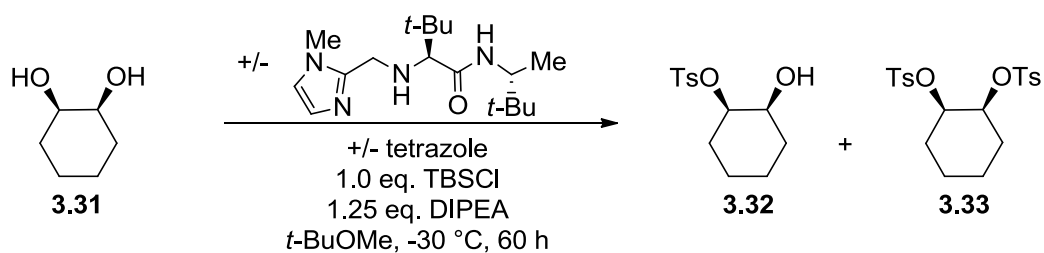
anti-1,2-Diols were previously unsuccessful substrates for our kinetic resolution by silylation reaction. However, 5-ethylthiotetrazole was not able to speed up the kinetic resolutions of *anti*-1,2-diols **3.29** and **3.30** (Table 3.9). Moreover, the selectivities were very poor ($s = <2$ and $s = 3$). To explain this, we deduced that the lowest energy

conformation of an *anti*-1,2-diol does not favor the formation of the active substrate-catalyst complex.

3.4 Rate enhancement for catalytic enantioselective sulfonylation?

Given the similarities of our original transition state models for catalytic enantioselective silylation and sulfonylation, we thought that the new transition state model for silylation could apply to sulfonylation as well. More importantly, we hoped that a strong Lewis base but weak Bronsted base could enhance the rate of our sulfonylation reaction. To test this hypothesis, we performed a study similar to the initial additive study for silylation. The study was made up of three tosylation reactions catalyzed by: (1) 20 mol% chiral catalyst, (2) 20 mol% tetrazole, and (3) 20 mol% chiral catalyst and 20 mol% tetrazole. In all three cases, *meso*-1,2-cyclohexanediol was reacted with 1 equivalent of TsCl, 1.25 equivalents of DIPEA, in the presence of *t*-BuOMe as solvent at -30 °C for 60 hours. Unfortunately, when comparing Entries 1 and 3 in Table 3.10, there was only minor rate enhancement and the ee of the mono-tosylated product

Table 3.10 Tosylation additive study



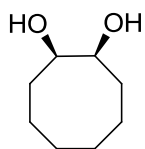
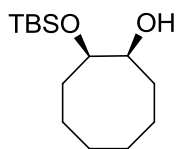
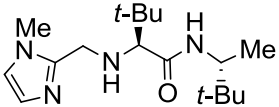
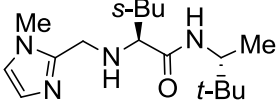
Entry	Catalyst (mol%)	Tetrazole (mol%)	Conversion (%)	ee (%)	mono:bis
1	20	-	65	84	3.1:1
2	-	20	<5%	-	-
3	20	20	95	70	4.3:1

decreased, while the mono:bis ratio increased. This led us to believe that the transition state for sulfonylation is different from the one for silylation.

3.5 Catalyst modification

While most modifications to the Hoveyda-Snapper desymmetrization catalyst cannot be tolerated due to loss in reactivity and/or selectivity, we found one valuable modification that did not decrease the catalyst's effectiveness when used in conjunction with 5-ethylthiotetrazole. The catalyst is derived from the unnatural amino acid *t*-leucine, which is relatively expensive. When the *t*-Leucine component was exchanged with the less expensive, natural amino acid Isoleucine, a negligible drop on the catalyst's ability to enantioselectively silylate *meso*-diols was observed (Table 3.11). In other words, a less expensive version of the catalyst is nearly as effective as the original.

Table 3.11 Catalyst modification

 3.1	$\xrightarrow[\text{THF, -40 } ^\circ\text{C, 1 h}]{\begin{array}{l} 20 \text{ mol\% catalyst} \\ 7.5 \text{ mol\% 5-ethylthiotetrazole} \\ 2.0 \text{ eq. TBSCl} \\ 1.25 \text{ eq. DIPEA} \end{array}}$	 3.2	
Entry	Catalyst	Yield (%)	ee (%)
1		96	95
2		90	92

3.6 Conclusion and future outlook

So far, we have demonstrated that the Hoveyda-Snapper desymmetrization catalyst can successfully catalyze the enantioselective silylation and sulfonylation of symmetric diols and triols, as well as the kinetic resolution of asymmetric diols by both silylation and sulfonylation. In the process of understanding the catalyst's mechanism of action, we have gained new insight into the imidazole-catalyzed silylation of simple alcohols, and we have discovered a nucleophilic activator that can assist our catalyst during silylation. Given the benefits of enantioselective functionalization, our next goal is to develop the first method of catalytic enantioselective alkylation of diols.

3.7 Experimental and Supporting Information

General Information[#]

tert-Butyldimethylsilyl chloride (TBSCl), 5-ethylthiotetrazole, and diisopropylethylamine (DIPEA) were purchased from Aldrich. *cis*-1,2-Cyclopentanediol, *cis*-1,2-cyclohexanediol, and *cis*-1,2-cyclooctanediol were purchased from Aldrich. *cis*-4-Cyclopentan-1,3-diol was synthesized via hydrogenation of commercially available *cis*-4-cyclopenten-1,3-diol. *cis*-Cycloheptane-1,2-diol, *cis*-cyclohex-4-ene-1,2-diol, *cis*-cyclooct-5-ene-1,2-diol, *cis*-hexane-3,4-diol, *cis*-1,2-diphenylethane-1,2-diol, (\pm)-3,3-diethoxypropane-1,2-diol, and *cis*-1-methylcyclohexane-1,2-diol were synthesized by *cis*-dihydroxylation of the corresponding commercially available alkenes. 2-(*tert*-Butyl)propane-1,2,3-triol was synthesized according to literature procedure.³⁰ *cis*-1,1-Diethoxybutane-2,3-diol and *cis*-1-phenylpropane-1,2-diol were synthesized by Lindlar reduction of the corresponding commercially available alkynes followed by *cis*-dihydroxylation. The catalyst was synthesized according to literature procedure.³¹

General procedure for the catalytic enantioselective silylation of meso-diols

The catalyst (18 mg, 0.060 mmol), 5-ethylthiotetrazole (2.9 mg, 0.023 mmol) and the diol substrate (0.30 mmol) were weighed into a 10 x 75 mm test tube. DIPEA (65 μ L, 0.38 mmol) was added with a Gilson Pipetman. The contents were dissolved in THF (240 μ L), the tube was capped with a rubber septum, and the mixture was cooled to -40 °C. In a separate test tube, TBSCl (91 mg, 0.60 mmol) was dissolved in THF (210 μ L), cooled to -40 °C, and added to the test tube with a Gilson Pipetman. The test tube was capped with a rubber septum, wrapped with Teflon tape, and the mixture was allowed to stir at -40 °C in a cryocool apparatus for the reported

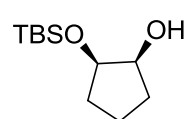
[#] See Chapter 2, page 36.

³⁰ Kang, S. H.; Jung, B. *Proc. Nat. Acad. Sci.* **2007**, *104*, 1471–1475.

³¹ Zhao, Y.; Rodrigo, J.; Hoveyda, A. H.; Snapper, M. L. *Nature.* **2006**, *443*, 67-70.

period of time. The reaction was quenched by the addition of DIPEA (52 μ L, 0.30 mmol) and methanol (25 μ L). The mixture was allowed to warm to 22 $^{\circ}$ C and directly purified by silica gel chromatography. The product was analyzed by chiral GLC or HPLC. The recovered catalyst was purified further by acid-base extraction and recrystallization.³¹

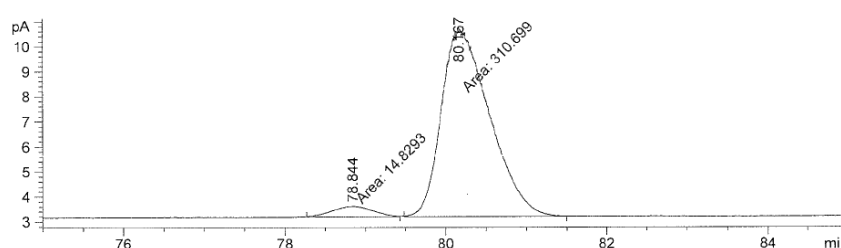
(1S,2R)-2-((tert-butyldimethylsilyl)oxy)cyclopentanol



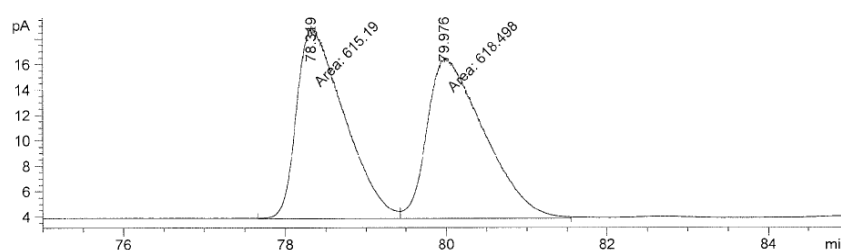
Optical Rotation: $[\alpha]_D^{25} -19$ ($c = 1.0$, CHCl_3). Optical purity was established

by chiral GLC analysis (Supelco Beta Dex 120 (30 m x 0.15 mm x 0.25 μ m), 80

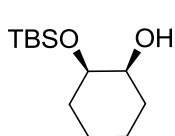
$^{\circ}$ C for 90 min, 15 psi.); chromatograms are illustrated below for a 91 % ee sample:



Peak #	RetTime [min]	Type	Width [min]	Area [pA*s]	Height [pA]	Area %
1	78.844	MM	0.5728	14.82929	4.31472e-1	4.55545
2	80.167	MM	0.6814	310.69891	7.59927	95.44455

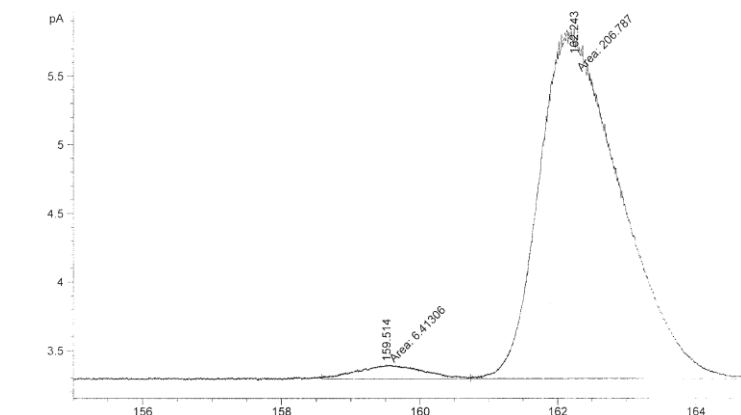


Peak #	RetTime [min]	Type	Width [min]	Area [pA*s]	Height [pA]	Area %
1	78.319	MF	0.6773	615.19025	15.13885	49.86593
2	79.976	FM	0.8163	618.49835	12.62848	50.13407

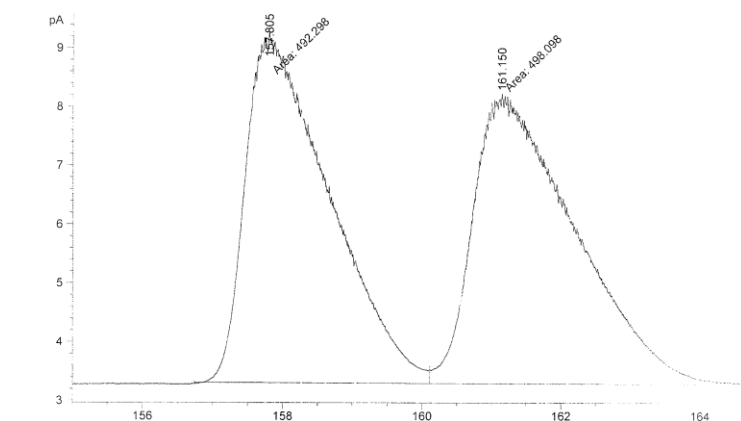
(1S,2R)-2-((tert-butyldimethylsilyl)oxy)cyclohexanol

Optical Rotation: $[\alpha]_D^{25} -11$ ($c = 1.0$, CHCl_3). Optical purity was established by chiral GLC analysis (Supelco Beta Dex 120 (30 m x 0.15 mm x 0.25 μm), 80

$^\circ\text{C}$ for 170 min, 15 psi.); chromatograms are illustrated below for a 94 % ee sample:

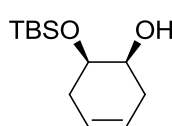


Peak #	RetTime [min]	Type	Width [min]	Area [pA*s]	Height [pA]	Area %
1	159.514	MF	1.0448	6.41306	1.02304e-1	3.00800
2	162.243	FM	1.3531	206.78725	2.54699	96.99200

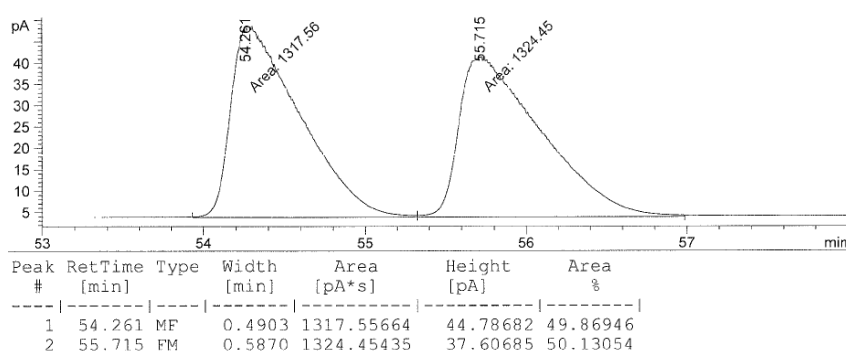
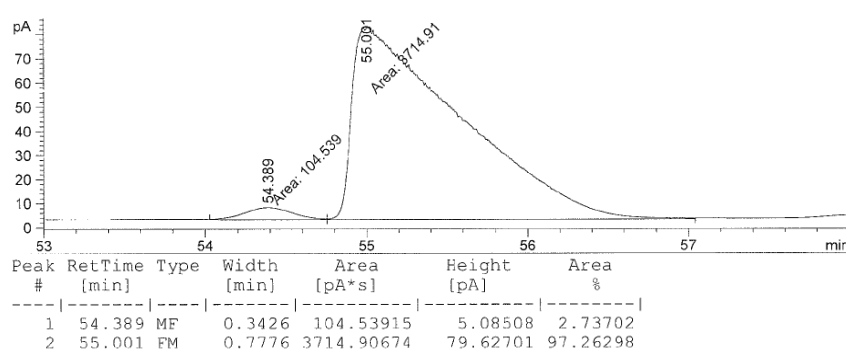


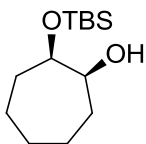
Peak #	RetTime [min]	Type	Width [min]	Area [pA*s]	Height [pA]	Area %
1	157.805	MF	1.3712	492.29807	5.98363	49.70720
2	161.150	FM	1.6823	498.09778	4.93473	50.29280

(1S,6R)-6-((tert-butyldimethylsilyl)oxy)cyclohex-3-enol

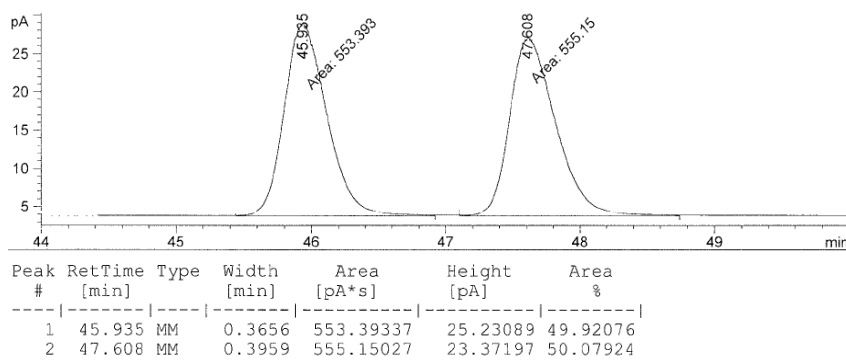
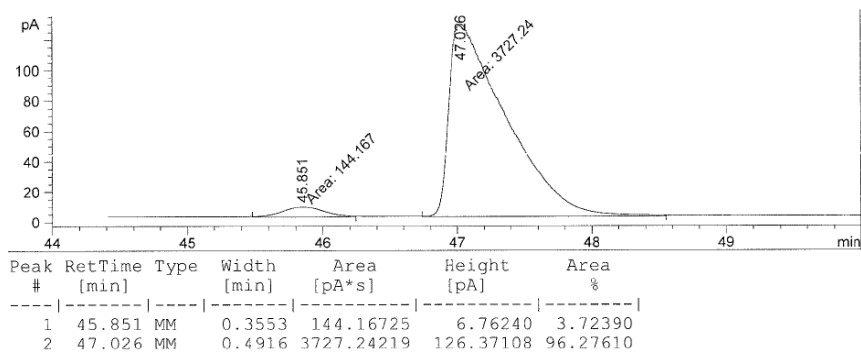

Optical Rotation: $[\alpha]^{25}_D -23$ ($c = 1.0$, CHCl_3). Optical purity was established

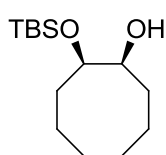
by chiral GLC analysis (Supelco Beta Dex 120 (30 m x 0.15 mm x 0.25 μm), 105 °C for 75 min, 15 psi.); chromatograms are illustrated below for a 95 % ee sample:



(1S,2R)-2-((tert-butyldimethylsilyl)oxy)cycloheptanol

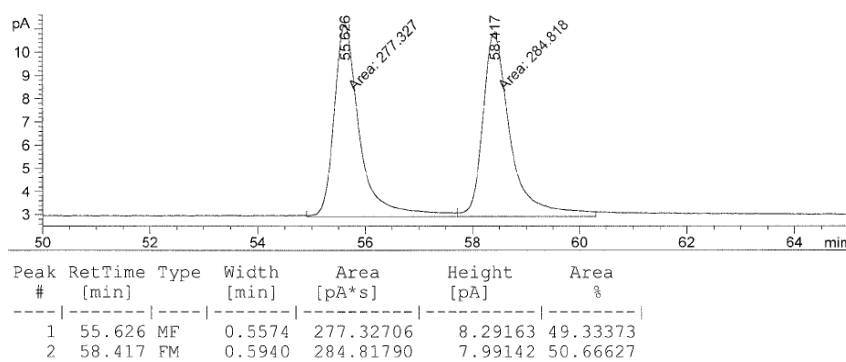
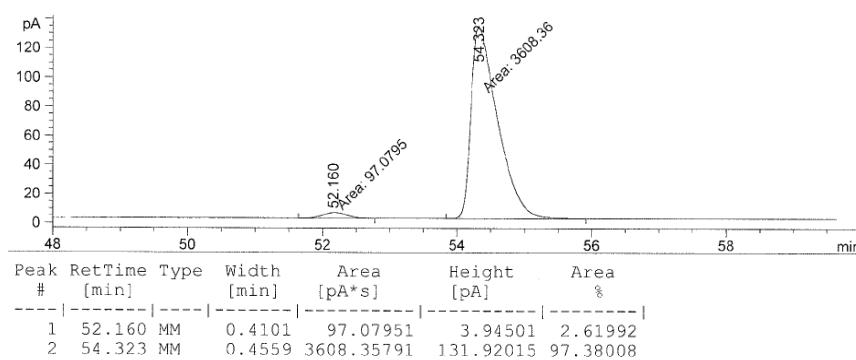
Optical Rotation: $[\alpha]_D^{25} -5.3$ ($c = 1.0$, CHCl_3). Optical purity was established by chiral GLC analysis (Supelco Beta Dex 120 (30 m x 0.15 mm x 0.25 μm), 120 °C for 60 min, 15 psi.); chromatograms are illustrated below for a 93 % ee sample:

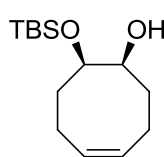


(1S,2R)-2-((tert-butyldimethylsilyl)oxy)cyclooctanol

Optical Rotation: $[\alpha]_D^{25} -5.3$ ($c = 1.0$, CHCl_3). Optical purity was established by chiral GLC analysis (Supelco Beta Dex 120 (30 m x 0.15 mm x 0.25 μm), 130 $^\circ\text{C}$ for 65 min, 15 psi.); chromatograms are illustrated below for a 95 % ee

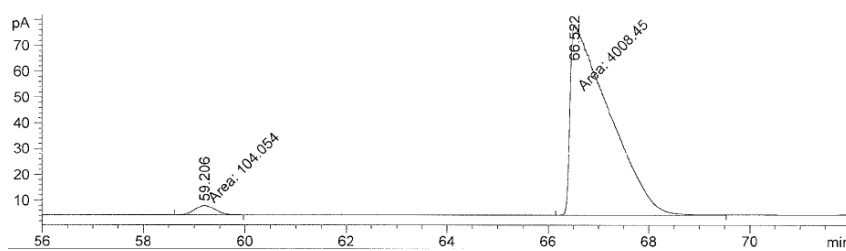
sample:



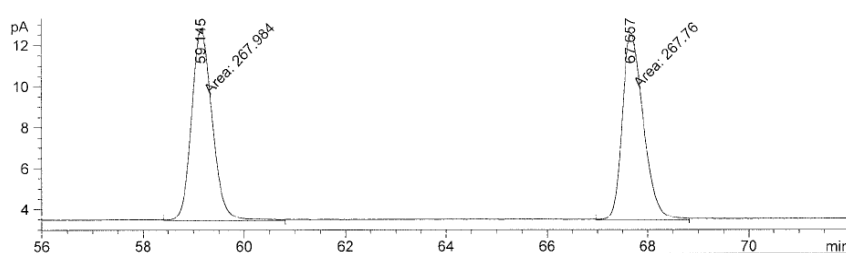
(1S,8R,Z)-8-((tert-butyldimethylsilyl)oxy)cyclooct-4-enol

Optical Rotation: $[\alpha]_D^{25} -2.3$ ($c = 1.0$, CHCl_3). Optical purity was established by chiral GLC analysis (Supelco Beta Dex 120 (30 m x 0.15 mm x 0.25 μm), 130 $^\circ\text{C}$ for 65 min, 15 psi.); chromatograms are illustrated below for a 95 % ee

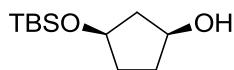
sample:



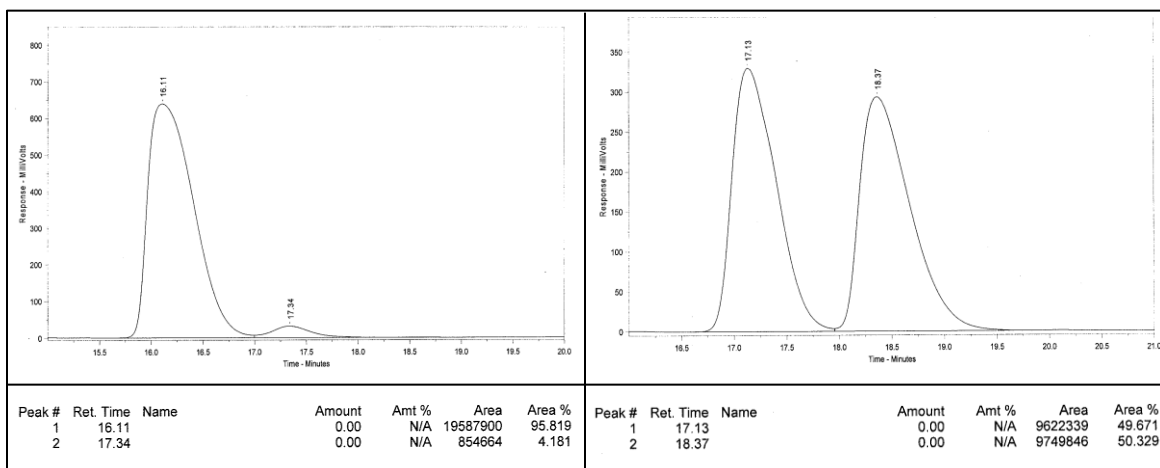
Peak #	RetTime [min]	Type	Width [min]	Area [pA*s]	Height [pA]	Area %
1	59.206	MM	0.4606	104.05386	3.76522	2.53019
2	66.522	MM	0.9038	4008.44604	73.92183	97.46981



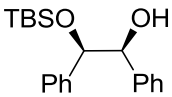
Peak #	RetTime [min]	Type	Width [min]	Area [pA*s]	Height [pA]	Area %
1	59.145	MM	0.4742	267.98425	9.41950	50.02094
2	67.667	MM	0.4884	267.75992	9.13810	49.97906

(1S,3R)-3-((tert-butyldimethylsilyl)oxy)cyclopentanol

Optical Rotation: $[\alpha]_D^{25} -4.6$ ($c = 1.0$, CHCl_3). Optical purity was established by HPLC analysis after conversion to the corresponding tosylate (Chiralpak AS-H column (25 cm x 0.46 cm), 98/2 hexanes/*i*-PrOH, 0.5 mL/min, 220 nm); chromatograms are illustrated below for a 92 % ee sample:

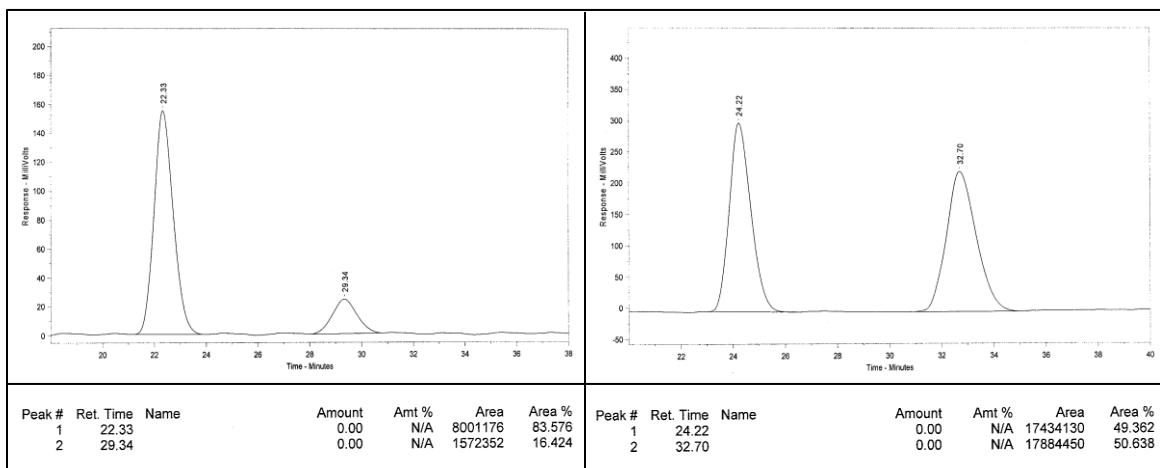


(1S,2R)-2-((tert-butyldimethylsilyl)oxy)-1,2-diphenylethanol

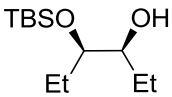

IR (neat, thin film): 3453 (br), 3032 (w), 2928 (m), 2856 (m), 1453 (w), 1252 (m), 1097 (s), 862 (m), 835 (s), 777 (s), 757 (m), 699 (s). **¹H NMR** (CDCl₃, 400 MHz); δ 7.26-7.19 (10 H, m), 4.66 (2 H, m), 2.21 (1 H, s), 0.77 (9 H, s), -0.26 (6 H, d, *J* = 22.0 Hz). **¹³C NMR** (CDCl₃, 400 MHz); 140.9, 140.7, 127.9, 127.7(5), 127.7(0), 127.5, 127.3(1), 127.2(9), 79.4, 78.8, 25.7, 18.0, -5.0, -5.5. **HRMS** (*m/z*): Calculated: 329.194; Found: 329.195.

Optical Rotation: $[\alpha]_D^{25}$ -12 (*c* = 1.0, CHCl₃).

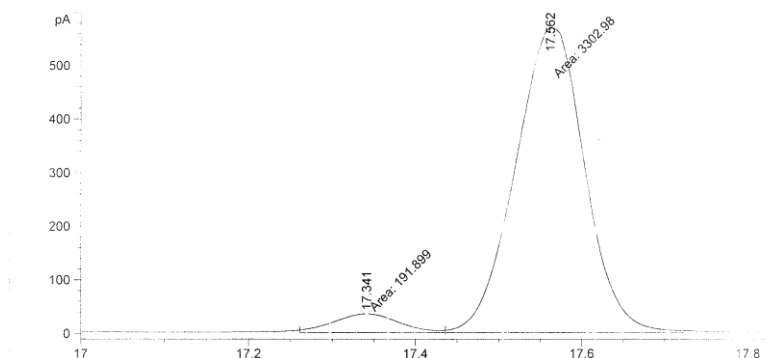
Optical purity was established by HPLC analysis (Chiralpak OD-C column (25 cm x 0.46 cm), 99/1 hexanes/*i*-PrOH, 0.5 mL/min, 220 nm); chromatograms are illustrated below for a 68 % ee sample:



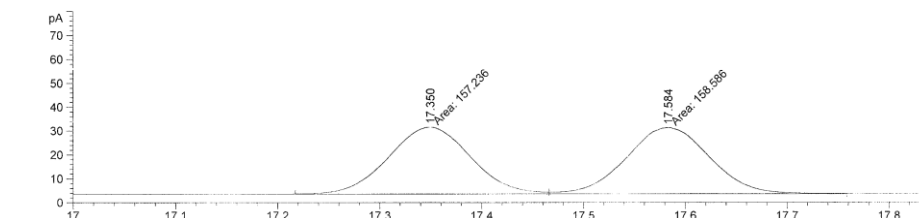
(3S,4R)-4-((tert-butyldimethylsilyl)oxy)hexan-3-ol


IR (neat, thin film): 3467 (br), 2958 (m), 2930 (m), 2882 (m), 2858 (m), 1463 (w), 1254 (m), 1100 (m), 1054 (m), 1004 (m), 834 (s), 774 (s). **¹H NMR** (CDCl₃, 400 MHz); δ 3.54-3.48 (2 H, m), 2.11 (1 H, s), 1.52-1.37 (4 H, m), 0.95 (3 H, t, *J* = 7.6 Hz), 0.87 (12 H, m), 0.06 (6 H, s). **¹³C NMR** (CDCl₃, 400 MHz); 76.3, 75.9, 25.8, 24.7, 23.4, 18.1, 10.5, 10.2, -4.5. **HRMS** (*m/z*): Calculated: 233.194; Found: 233.195. **Optical Rotation:** [α]_D²⁵ +10 (*c* = 1.0, CHCl₃).

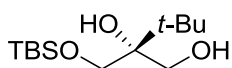
Optical purity was established by chiral GLC analysis (Supelco Beta Dex 120 (30 m x 0.15 mm x 0.25 μm), 80-140 °C at 2 °C/min, 25 psi.); chromatograms are illustrated below for a 90 % ee sample:



Peak #	RetTime [min]	Sig	Type	Area [pA*s]	Height [pA]	Area %
1	17.341	1	MF	191.89906	35.21371	5.49087
2	17.562	1	FM	3302.97510	570.38574	94.50913



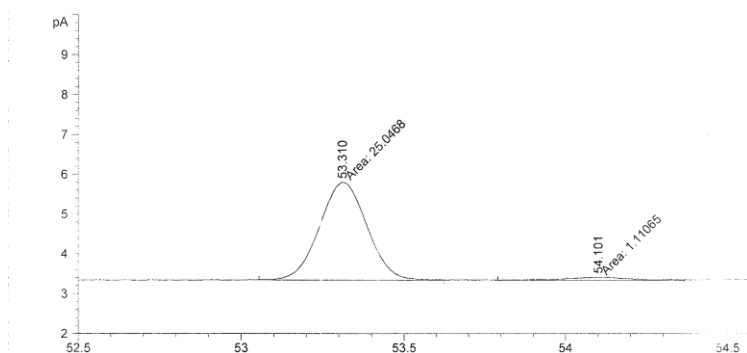
Peak #	RetTime [min]	Sig	Type	Area [pA*s]	Height [pA]	Area %
1	17.350	1	MF	157.23567	28.07186	49.78624
2	17.584	1	FM	158.58585	27.77370	50.21376

(R)-2-(((tert-butyldimethylsilyl)oxy)methyl)-3,3-dimethylbutane-1,2-diol

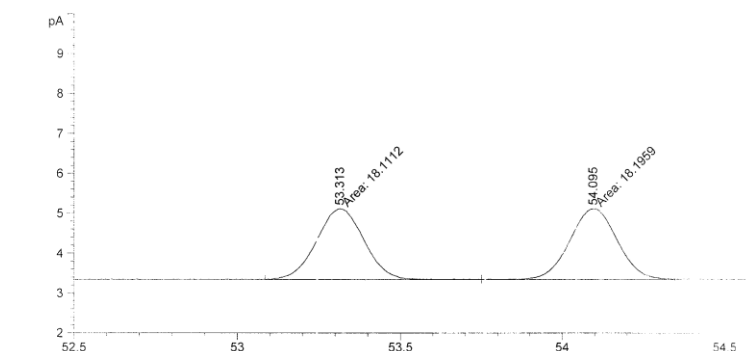
Optical Rotation: $[\alpha]_D^{25} -2.4$ ($c = 1.0$, CHCl_3). Optical purity was established by chiral GLC analysis after conversion to the corresponding

aldehyde (Supelco Beta Dex 120 (30 m x 0.15 mm x 0.25 μm), 80-140 $^\circ\text{C}$ at 1 $^\circ\text{C}$, 10 psi.);

chromatograms are illustrated below for a 92 % ee sample:



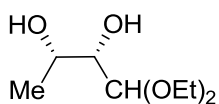
Peak #	RetTime [min]	Sig	Type	Area [pA*s]	Height [pA]	Area %
1	53.310	1	MM	25.04678	2.46897	95.75398
2	54.101	1	MM	1.11065	8.13223e-2	4.24602



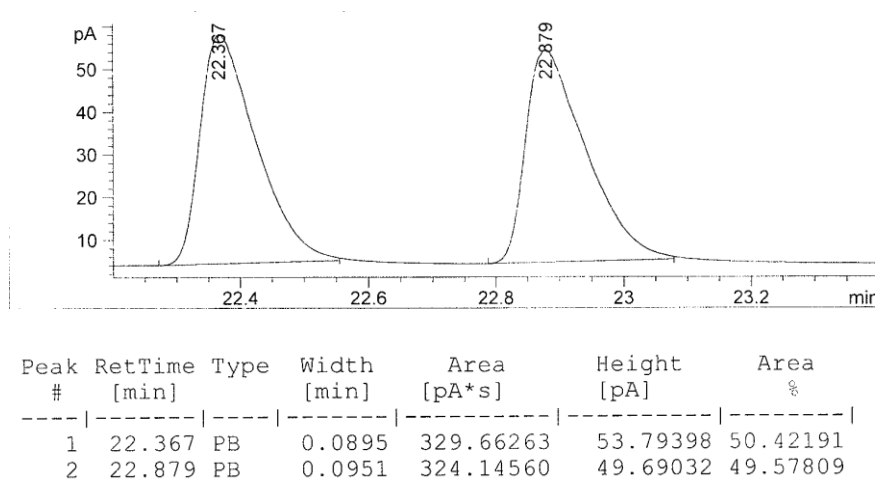
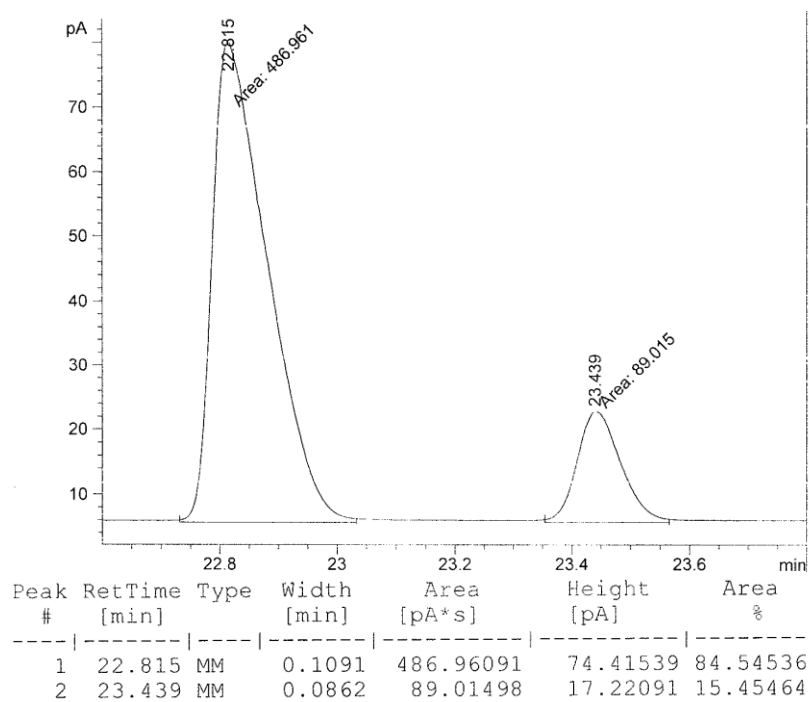
Peak #	RetTime [min]	Sig	Type	Area [pA*s]	Height [pA]	Area %
1	53.313	1	MF	18.11123	1.77404	49.88339
2	54.095	1	FM	18.19590	1.77425	50.11661

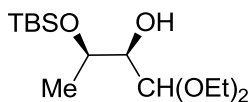
General procedure for the kinetic resolution of syn-diols by catalytic enantioselective silylation

The catalyst (18 mg, 0.060 mmol), 5-ethylthiotetrazole (2.9 mg, 0.023 mmol) and the diol substrate (0.30 mmol) were weighed into a 10 x 75 mm test tube. DIPEA (65 μ L, 0.38 mmol) was added with a Gilson Pipetman. The contents were dissolved in THF (240 μ L), the tube was capped with a rubber septum, and the mixture was cooled to -40 °C. In a separate test tube, TBSCl (57 mg, 0.38 mmol) was dissolved in THF (210 μ L), cooled to -40 °C, and added to the test tube with a Gilson Pipetman. The test tube was capped with a rubber septum, wrapped with Teflon tape, and the mixture was allowed to stir at -40 °C in a cryocool apparatus for the reported period of time. The reaction was quenched by the addition of DIPEA (52 μ L, 0.30 mmol) and methanol (25 μ L). The mixture was allowed to warm to 22 °C and directly purified by silica gel chromatography. The product and unreacted starting material were analyzed by chiral GLC or HPLC. The recovered catalyst was purified further by acid-base extraction and recrystallization.³¹

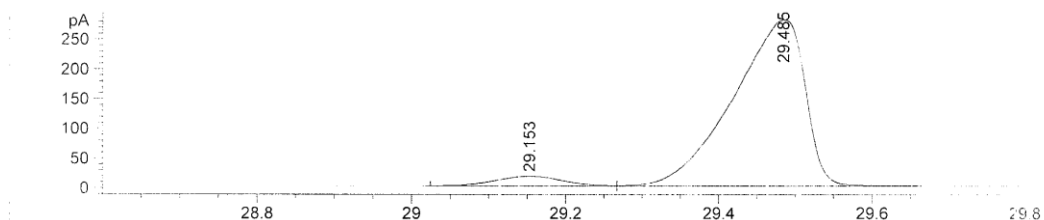
(S,3S)-1,1-diethoxybutane-2,3-diol

Optical Rotation: $[\alpha]_D^{25} -13$ ($c = 1.0$, CHCl_3). Optical purity was established by chiral GLC analysis (Supelco Beta Dex 120 (30 m x 0.15 mm x 0.25 μm), 80-140 $^\circ\text{C}$ at 2 $^\circ\text{C}/\text{min}$, 25 psi.); chromatograms are illustrated below for a 70 % ee sample:

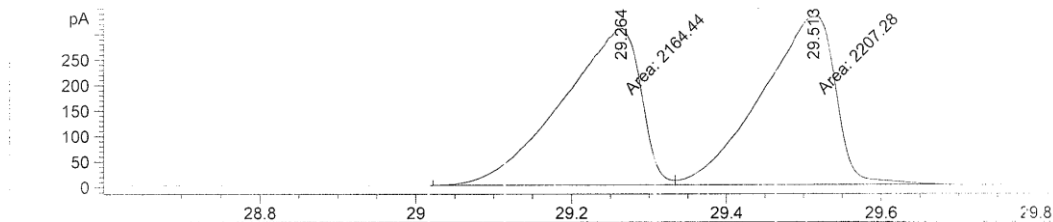


(2R,3R)-3-((tert-butyldimethylsilyl)oxy)-1,1-diethoxybutan-2-ol

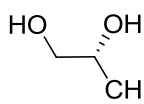
Optical Rotation: $[\alpha]_D^{25} -6.0$ ($c = 1.0$, CHCl_3). Optical purity was established by chiral GLC analysis (Supelco Beta Dex 120 (30 m x 0.15 mm x 0.25 μm), 80-140 $^\circ\text{C}$ at 2 $^\circ\text{C}/\text{min}$, 25 psi.); chromatograms are illustrated below for a 90 % ee sample:



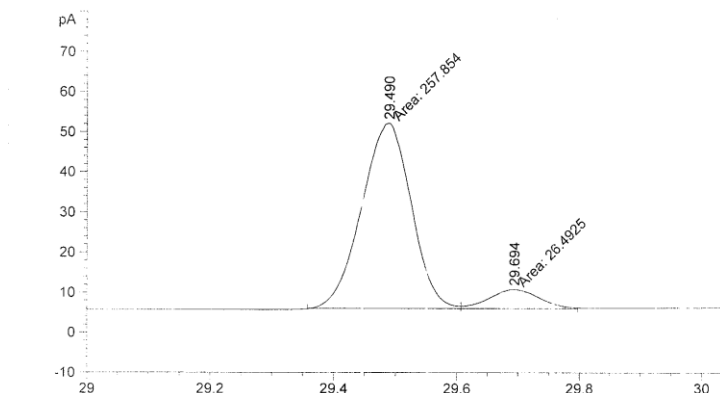
Peak #	RetTime [min]	Sig	Type	Area [pA*s]	Height [pA]	Area %
1	29.153	2	BV	97.17396	16.29460	5.07922
2	29.485	2	VB	1817.99316	278.62180	95.02532



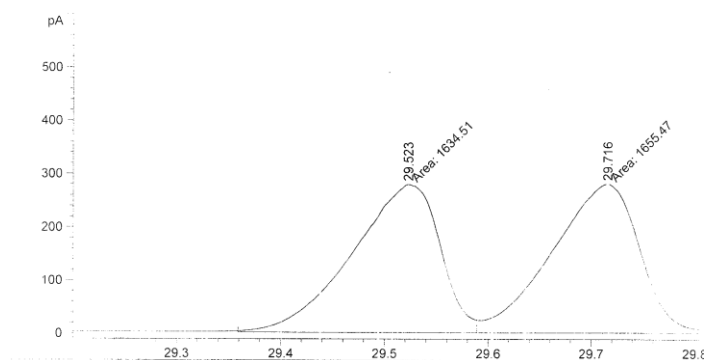
Peak #	RetTime [min]	Sig	Type	Area [pA*s]	Height [pA]	Area %
1	29.264	2	MF	2164.43872	306.92688	49.53270
2	29.513	2	FM	2207.27783	329.35089	50.51307

(S)-3,3-diethoxypropane-1,2-diol

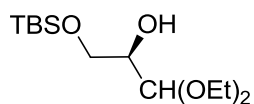
Optical Rotation: $[\alpha]_D^{25} -18$ ($c = 1.0$, CHCl_3). Optical purity was established by chiral GLC analysis after conversion to the corresponding mono-silylate (Supelco Beta Dex 120 (30 m x 0.15 mm x 0.25 μm), 80-140 $^\circ\text{C}$ at 2 $^\circ\text{C}/\text{min}$, 25 psi.); chromatograms are illustrated below for a 82 % ee sample:



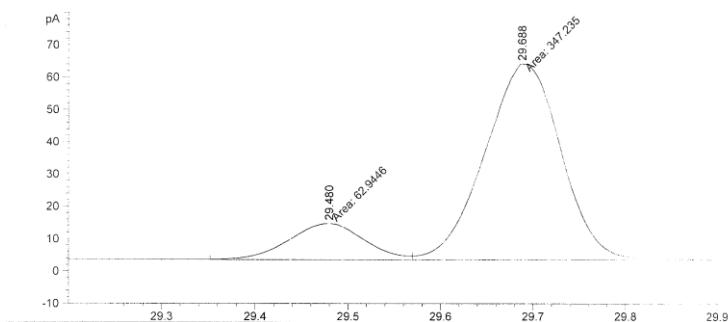
Peak #	RetTime [min]	Sig	Type	Area [pA*s]	Height [pA]	Area %
1	29.490	1	MF	257.85364	46.10937	90.68302
2	29.694	1	FM	26.49246	4.73290	9.31698



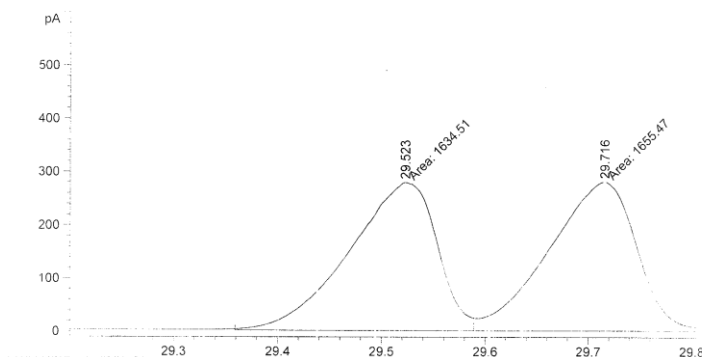
Peak #	RetTime [min]	Sig	Type	Area [pA*s]	Height [pA]	Area %
1	29.523	1	MF	1634.50525	278.16745	49.68144
2	29.716	1	FM	1655.46631	279.83167	50.31856

(R)-3-((tert-butyldimethylsilyloxy)-1,1-diethoxypropan-2-ol

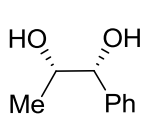
Optical Rotation: $[\alpha]_D^{25} +11$ ($c = 1.0$, CHCl_3). Optical purity was established by chiral GLC analysis (Supelco Beta Dex 120 (30 m x 0.15 mm x 0.25 μm), 80-140 $^\circ\text{C}$ at 2 $^\circ\text{C}/\text{min}$, 25 psi.); chromatograms are illustrated below for a 70 % ee sample:



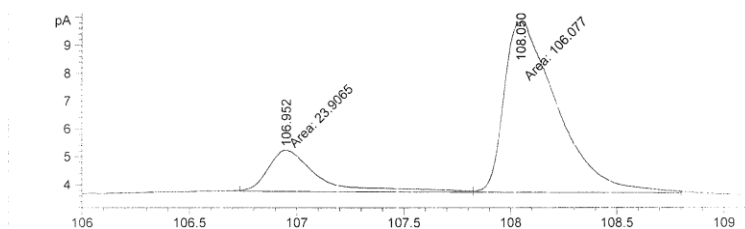
Peak #	RetTime [min]	Sig	Type	Area [pA*s]	Height [pA]	Area %
1	29.480	1	MF	62.94458	11.23658	15.34562
2	29.688	1	FM	347.23495	60.65051	84.65438



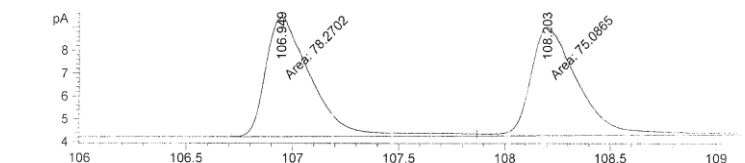
Peak #	RetTime [min]	Sig	Type	Area [pA*s]	Height [pA]	Area %
1	29.523	1	MF	1634.50525	278.16745	49.68144
2	29.716	1	FM	1655.46631	279.83167	50.31856

(1R,2S)-1-phenylpropane-1,2-diol

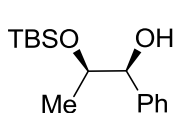
Optical Rotation: $[\alpha]_D^{25} -30$ ($c = 1.0$, CHCl_3). Optical purity was established by chiral GLC analysis (Supelco Beta Dex 120 (30 m x 0.15 mm x 0.25 μm), 100 °C for 98 min, 20 °C/min to 140 °C, hold for 30 min, 25 psi.); chromatograms are illustrated below for a 64 % ee sample:



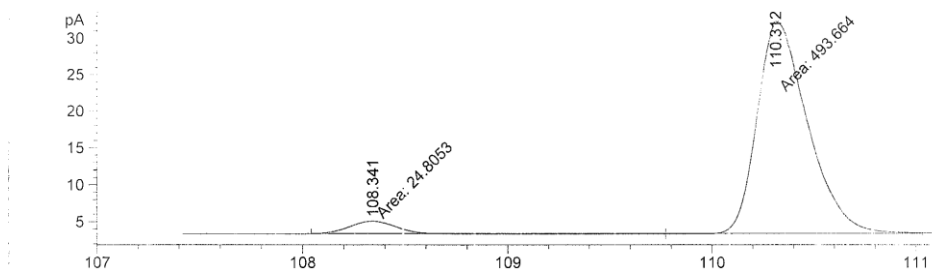
Peak #	RetTime [min]	Type	Width [min]	Area [pA*s]	Height [pA]	Area %
1	106.952	MF	0.2696	23.90651	1.47798	18.39191
2	108.050	FM	0.2888	106.07729	6.12208	81.60809



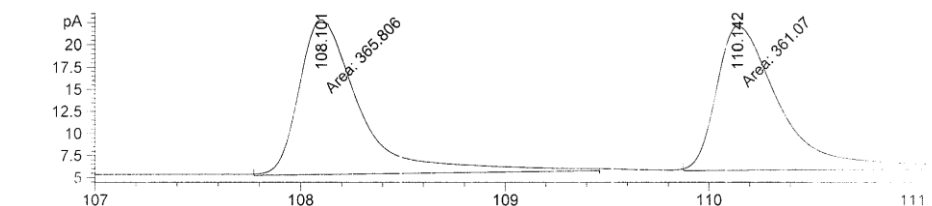
Peak #	RetTime [min]	Sig	Type	Area [pA*s]	Height [pA]	Area %
1	106.949	2	MF	78.27019	5.20102	51.71242
2	108.203	2	FM	75.08647	4.70248	49.60896

(1S,2R)-2-((tert-butyldimethylsilyl)oxy)-1-phenylpropan-1-ol

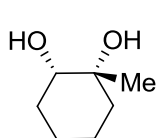
Optical Rotation: $[\alpha]_D^{25} -7.6$ ($c = 1.0$, CHCl_3). Optical purity was established by chiral GLC analysis (Supelco Beta Dex 120 (30 m x 0.15 mm x 0.25 μm), 100 °C for 98 min, 20 °C/min to 140 °C, hold for 30 min, 25 psi.); chromatograms are illustrated below for a 90 % ee sample:



Peak #	RetTime [min]	Type	Width [min]	Area [pA*s]	Height [pA]	Area %
1	108.341	MF	0.2504	24.80534	1.65082	4.78434
2	110.312	FM	0.2848	493.66446	28.88543	95.21566

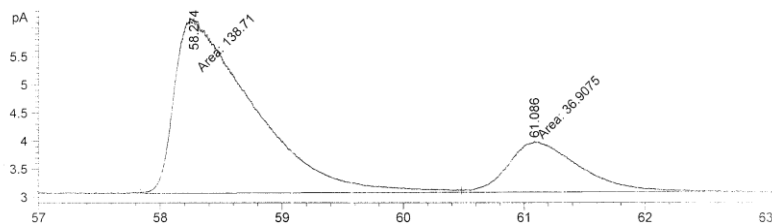


Peak #	RetTime [min]	Sig	Type	Area [pA*s]	Height [pA]	Area %
1	108.101	2	MM	365.80566	17.46052	50.46464
2	110.142	2	MM	361.06955	16.23478	49.81127

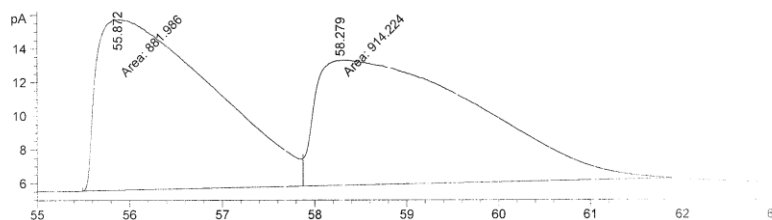
(1R,2S)-1-methylcyclohexane-1,2-diol

Optical Rotation: $[\alpha]_D^{25} +2.2$ ($c = 1.0$, CHCl_3). Optical purity was established by chiral GLC analysis (Supelco Beta Dex 120 (30 m x 0.15 mm x 0.25 μm), 90

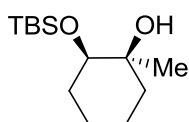
$^\circ\text{C}$ for 90 min, 25 psi.); chromatograms are illustrated below for a 58 % ee sample:



Peak #	RetTime [min]	Type	Width [min]	Area [pA*s]	Height [pA]	Area %
1	58.274	MF	0.7462	138.71016	3.09818	78.98416
2	61.086	FM	0.6782	36.90753	9.06975e-1	21.01584

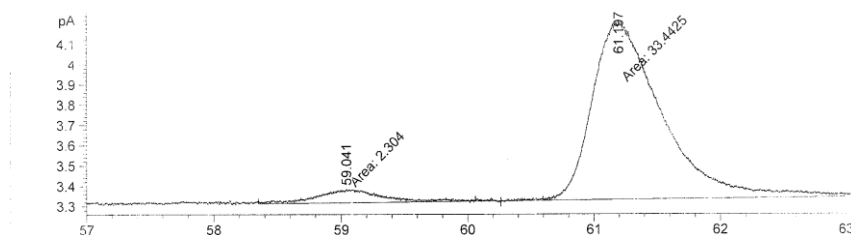


Peak #	RetTime [min]	Type	Width [min]	Area [pA*s]	Height [pA]	Area %
1	55.872	MF	1.4498	881.98572	10.13915	49.10260
2	58.279	FM	2.0471	914.22424	7.44329	50.89740

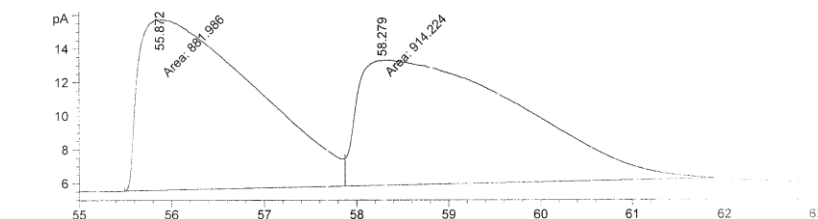
(1S,2R)-2-((tert-butyldimethylsilyl)oxy)-1-methylcyclohexanol

IR (neat, thin film): 2931 (s), 2858 (m), 1462 (w), 1252 (m), 1081 (s), 1056 (m), 886 (m), 836 (s), 776 (m). **¹H NMR** (CDCl₃, 400 MHz); δ 3.50 (1 H, dd, *J* = 6.4, 6.0 Hz), 2.25 (1 H, s), 1.77-1.20 (8 H, m), 1.13 (3 H, s), 0.89 (9 H, s), 0.06 (6 H, s). **¹³C NMR** (CDCl₃, 400 MHz); 81.0, 76.2, 41.5, 35.8, 32.0, 30.8, 28.2, 26.5, 23.0, 0.79, 0.00. **HRMS** (m/z): Calculated: 245.194; Found: 245.194. **Optical Rotation:** [α]_D²⁵ -20 (*c* = 0.50, CHCl₃).

Optical purity was established by chiral GLC analysis after conversion to the corresponding diol (Supelco Beta Dex 120 (30 m x 0.15 mm x 0.25 μm), 90 °C for 90 min, 25 psi.); chromatograms are illustrated below for a 88 % ee sample:

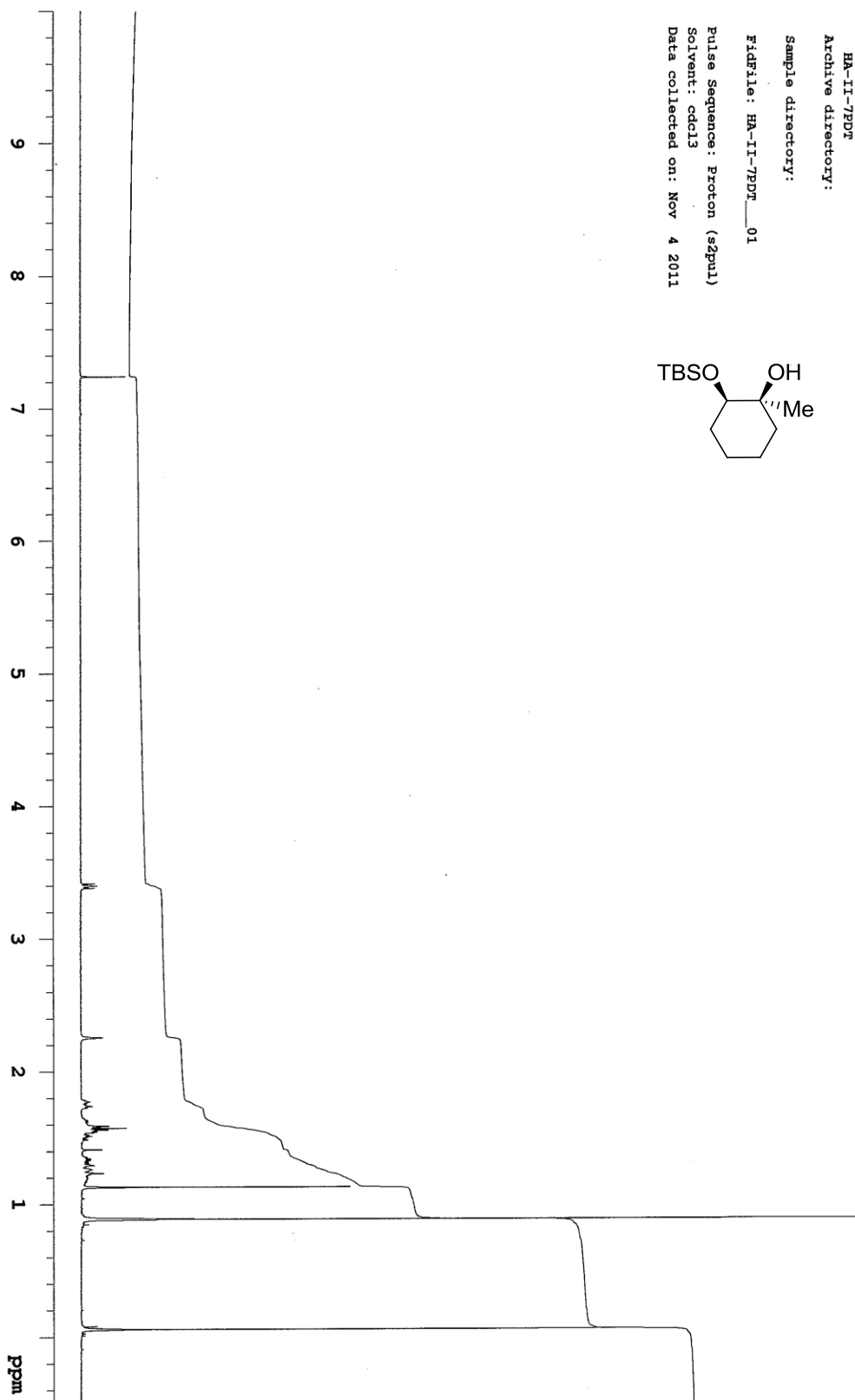
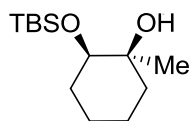


Peak #	RetTime [min]	Type	Width [min]	Area [pA*s]	Height [pA]	Area %
1	59.041	MF	0.5826	2.30400	6.59064e-2	6.44539
2	61.197	FM	0.6344	33.44248	8.78576e-1	93.55461

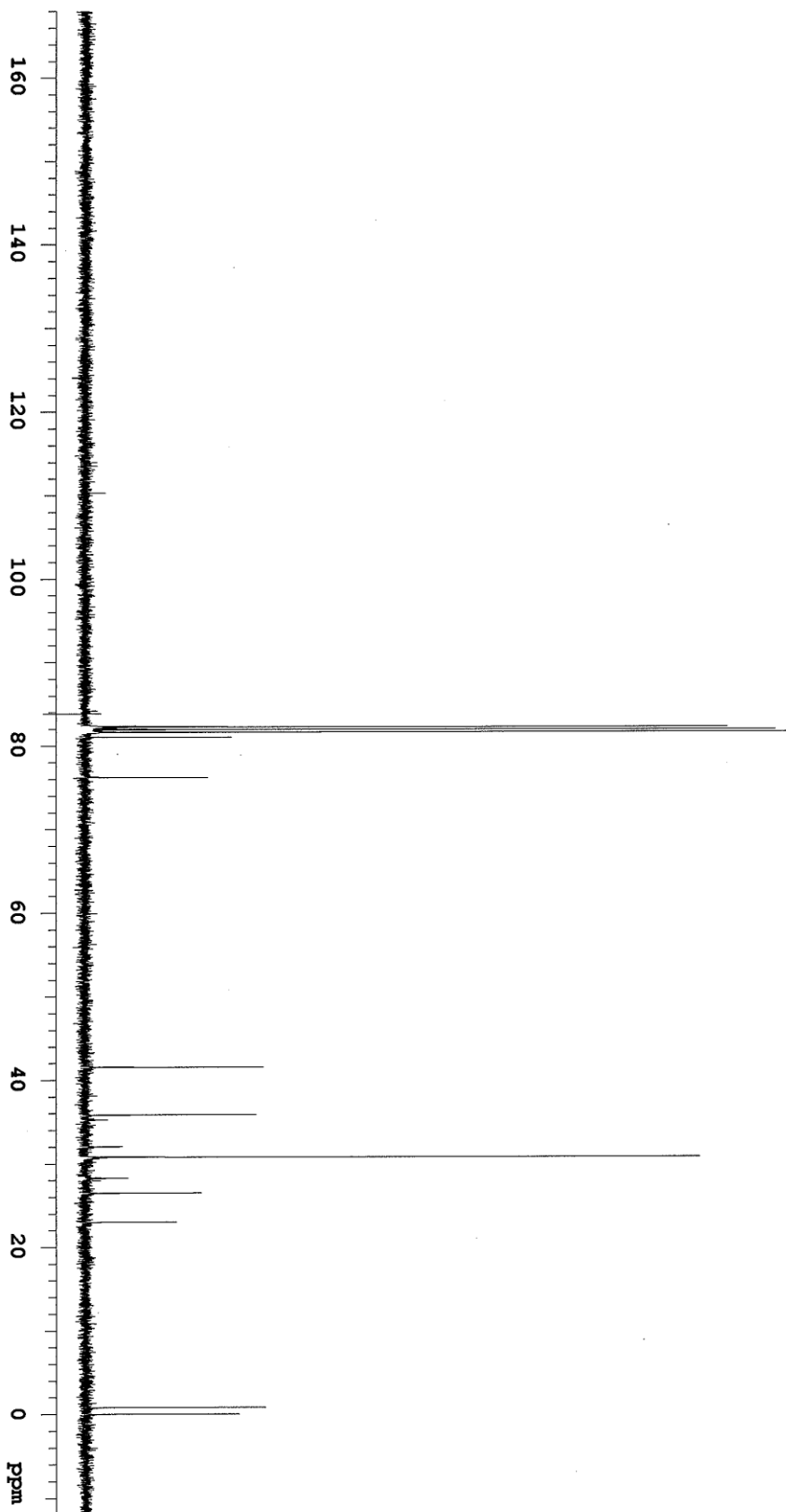
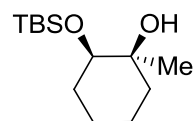


Peak #	RetTime [min]	Type	Width [min]	Area [pA*s]	Height [pA]	Area %
1	55.872	MF	1.4498	881.98572	10.13915	49.10260
2	58.279	FM	2.0471	914.22424	7.44329	50.89740

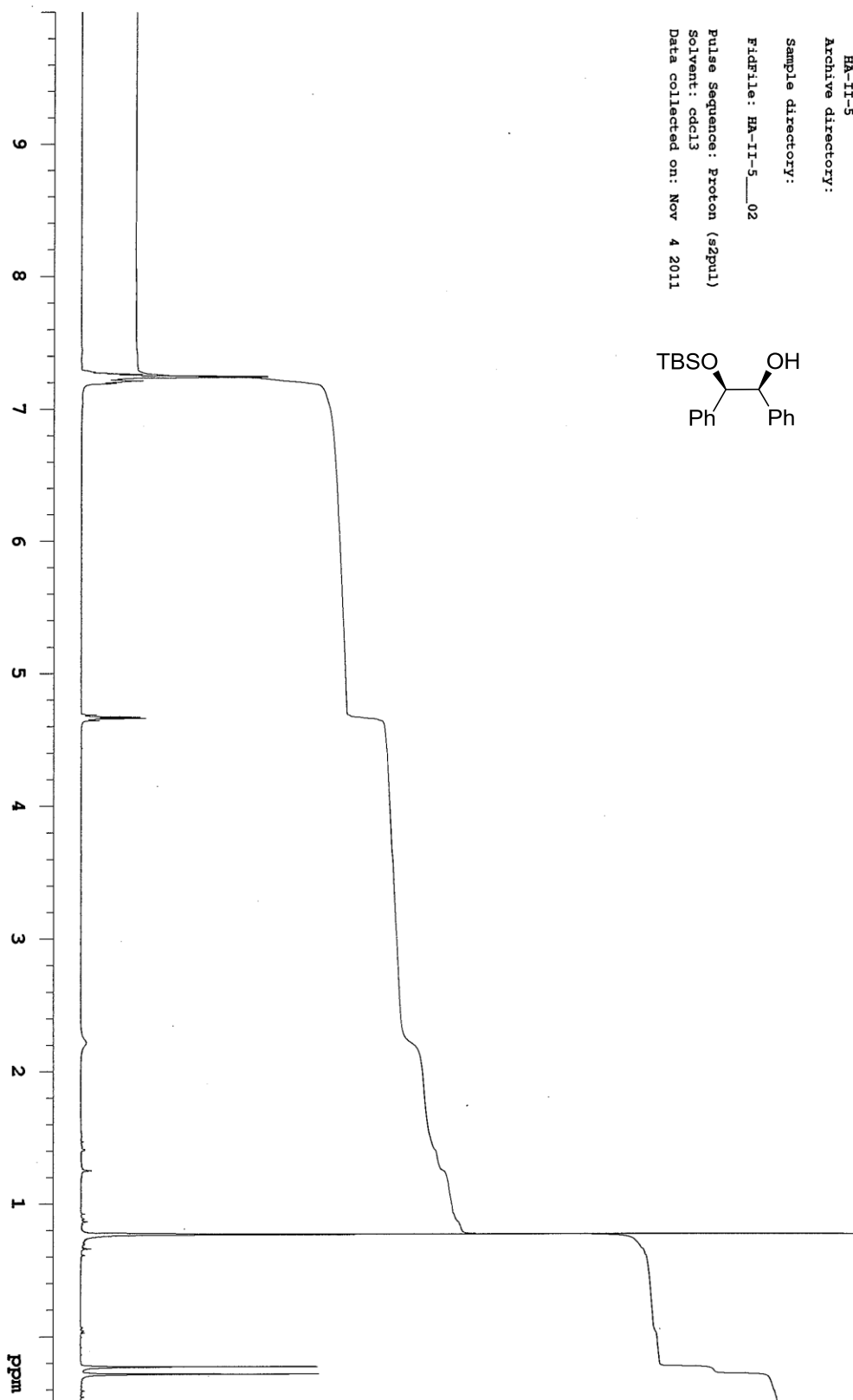
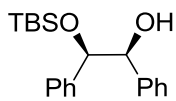
Sample Name:
HA-II-7PDT
Archive directory:
Sample directory:
FidFile: HA-II-7PDT_01
Pulse Sequence: Proton (s2pul)
Solvent: cdcl3
Data collected on: Nov 4 2011



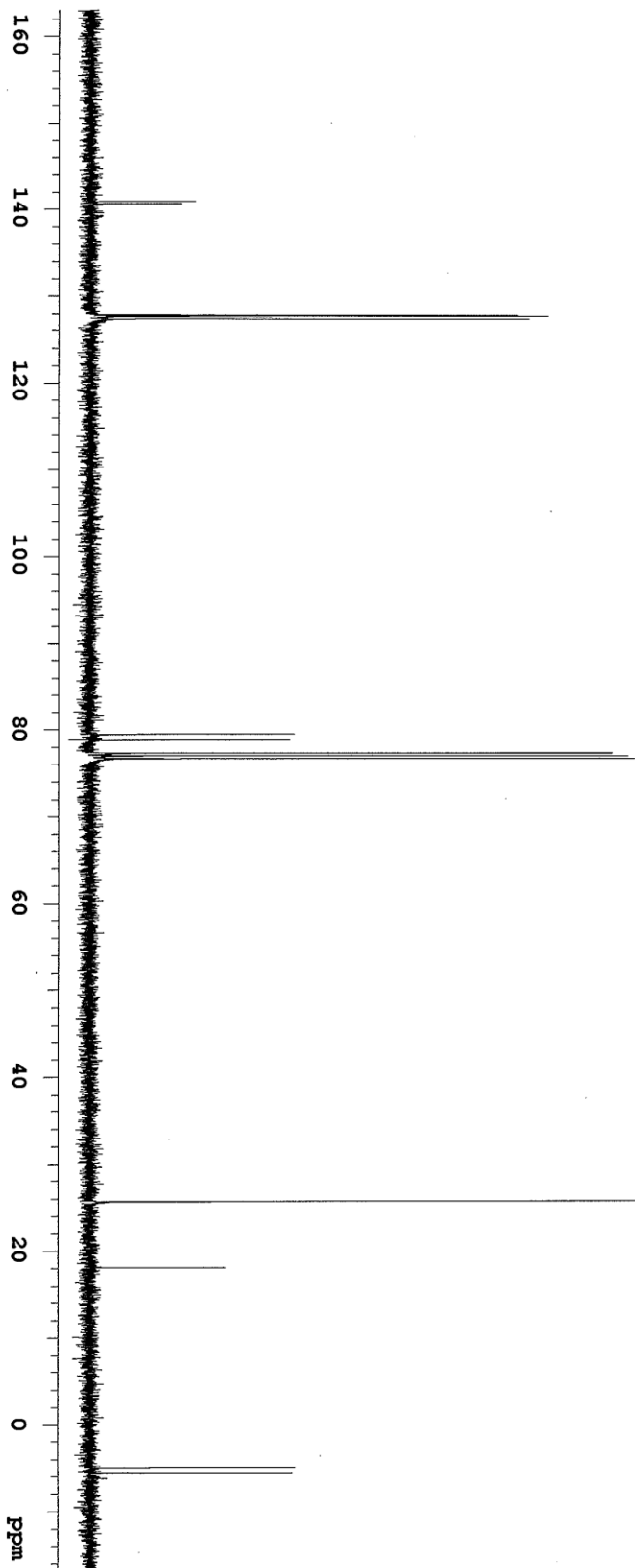
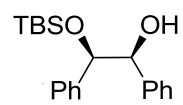
Sample Name :
HA-II-7PDR
Archive directory :
Sample directory :
FidFile: HA-II-7PDR__04
Pulse Sequence: Carbon (s2pul)
Solvent: cdcl3
Data collected on: Nov 4 2011



Sample Name:
HA-II-5
Archive directory:
Sample directory:
Fidfile: HA-II-5_02
Pulse Sequence: Proton (szpu1)
Solvent: cdcl3
Data collected on: Nov 4 2011



Sample Name :
HA-II-5
Archive directory:
Sample directory:
FidFile: HA-II-5__03
Pulse Sequence: Carbon (s2pu1)
Solvent: cdcl3
Data collected on: Nov 4 2011



Sample Name:
HA-II-10
Archive directory:

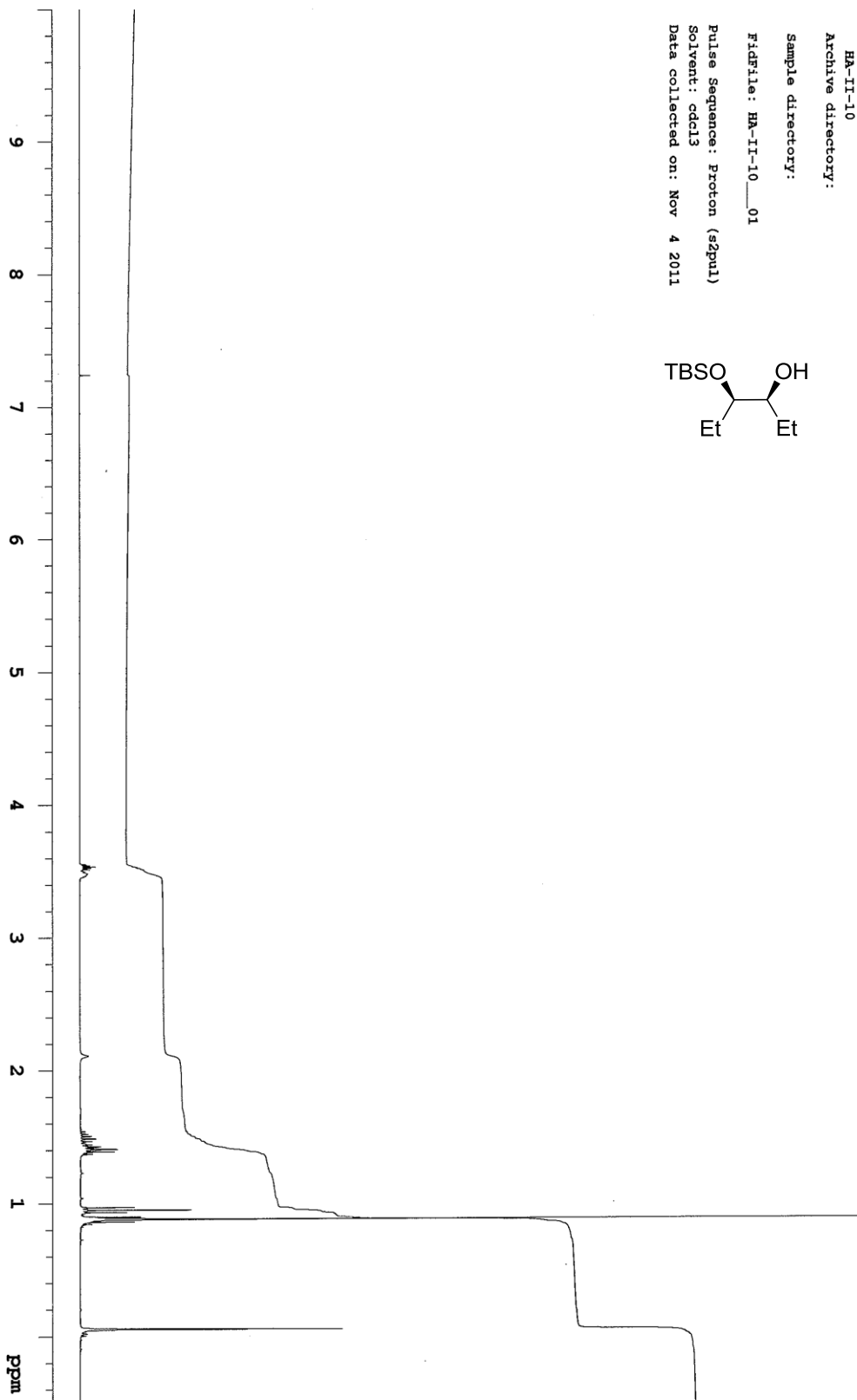
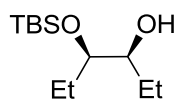
Sample directory:

FidFile: HA-II-10_01

Pulse Sequence: Proton (zgpg1)

Solvent: cdcl3

Data collected on: Nov 4 2011



Sample Name:
HA-II-10
Archive directory:
Sample directory:
FIDFile: HA-II-10__02
Pulse Sequence: Carbon (szpu1)
Solvent: cdcl3
Data collected on: Nov 4 2011

